INFORMATION TO USERS

This manuscript has been reproduced from the microfilm master. UMI films the text directly from the original or copy submitted. Thus, some thesis and dissertation copies are in typewriter face, while others may be from any type of computer printer.

The quality of this reproduction is dependent upon the quality of the copy submitted. Broken or indistinct print, colored or poor quality illustrations and photographs, print bleedthrough, substandard margins, and improper alignment can adversely affect reproduction.

In the unlikely event that the author did not send UMI a complete manuscript and there are missing pages, these will be noted. Also, if unauthorized copyright material had to be removed, a note will indicate the deletion.

Oversize materials (e.g., maps, drawings, charts) are reproduced by sectioning the original, beginning at the upper left-hand corner and continuing from left to right in equal sections with small overlaps.

Photographs included in the original manuscript have been reproduced xerographically in this copy. Higher quality 6" x 9" black and white photographic prints are available for any photographs or illustrations appearing in this copy for an additional charge. Contact UMI directly to order.

ProQuest Information and Learning
300 North Zeeb Road, Ann Arbor, MI 48106-1346 USA
800-521-0600

ANGIOGENESIS AND IMMUNE REGULATION IN TUMOR GENE THERAPY

By

STEVE FRANK GYORFFY

A Thesis

Submitted to the School of Graduate Studies

in Partial Fulfilment of the Requirements

for the Degree

Doctor of Philosophy

McMaster University

DOCTOR OF PHILOSOPHY (1999)
(Medical Sciences Department,
Molecular Immunology, Virology, and Inflammation)

McMaster University
Hamilton, Ontario

TITLE: Angiogenesis and Immune Regulation in Tumor Gene Therapy

AUTHOR: Steve Frank Gyorffy
B. Sc. (Hons) Biology (Trent University)
M.Sc. Microbiology (University of Guelph)

SUPERVISOR: Jack Gauldie, Ph. D.

Number of pages: 169

ABSTRACT

The coming millennium will usher in new therapies for cancer treatment. At the forefront, is the use of gene therapeutics which, as the name suggests, is the delivery of specific genes into tumor cells resulting in a genetic modification that will cause the tumor to regress. Adenoviruses, which have been modified so that they are incapable of reproducing and causing disease, represent ideal tools for delivery of genetic material. These viruses are highly infectious, they can produce large amounts of the therapeutic product and only persist for a short period of time. Prospective genes should induce a selective anti-tumor response that affects not only the primary tumor but also inhibits metastasis, prevents recurrence and will not be limited by the development of resistance. Angiogenesis inhibitor genes, which cut off the blood supply to the tumor, and cytokine genes, which produce hormones that stimulate the immune system to react against the tumor, have the potential to satisfy the criteria listed above.

Angiogenesis, the process of continued expansion of new blood vessels from pre-existing vasculature, is highly regulated and plays a role in many pathological functions. Angiogenesis is necessary for tissue growth, wound healing and female reproduction. However, uncontrolled angiogenesis is seen in many diseased states including retinal neovascularization, rheumatoid arthritis, hemangiomas and

psoriasis. The growth of new blood vessels is especially significant in tumor growth and metastasis.

Small tumors (less than 3 mm in diameter) are limited in their ability to progress without perfusion from the blood stream. Vascularization of the tumor creates a blood flow which increases the transport of oxygen and nutrients and removes toxic waste products. Genes that produce the positive and negative regulatory factors responsible for controlling the growth of blood vessels regulate the change from a non-vascularized tumor to a vascularized one. Angiostatin is a protein which has been shown to be a potent inhibitor of blood vessel growth that can inhibit primary and metastatic tumors.

The human immune system is designed to distinguish self-materials produced by our bodies from foreign materials produced by viruses and bacteria. Although tumors produce substances which are considered foreign, they are protected from the immune system because they developed from tissue that already existed in our bodies. The immune system is regulated by cytokine genes and it has been possible to suppress tumor growth by modulating the cytokines which are present within the tumor. Interleukin-12 (IL-12) is a cytokine that promotes the activation of killer white blood cells which can attack tumor cells. Interestingly, this cytokine can also activate genes that produce angiogenesis inhibitors.

In our studies, we have used adenoviruses containing the genes for Angiostatin (Ad-Angiostatin) and IL-12 (Ad-IL12) for tumor therapy. The biological activity of the Ad-Angiostatin has been characterized using an artificial matrix which promotes the growth of blood vessels (Matrigel). We observed suppression of vessel growth in the Matrigel following treatment with Ad-Angiostatin demonstrating the inibitory activity of this virus. Treatment of growing tumor in mice with either Ad-Angiostatin or Ad-IL12 resulted in modest delays in tumor growth compared to tumors treated with viruses which did not contain any genes. Ad-IL-12 treatment also causes tumors to regress in a small fraction of the treated animals (13%). However, when used in combination, treatment with Ad-Angiostatin and Ad-IL12 resulted in tumor regression in 54% of the cases, a strong anti-tumor response by killer white blood cells, and the cured animals were resistant to further outgrowth of tumor.

These results are the first to demonstrate the usefulness of combining angiogenesis inhibitors with cytokines using gene therapy. The rationale for this therapy is to limit the tumor size by attacking the vasculature with angiostatin, allowing the Interleukin-12 to activate killer white blood cells to respond against foreign products present in the tumor tissue. In this manner, the potential for the white blood cells to reject the tumor is increased as there is less tumor mass present.

ACKNOWLEDGEMENTS

I would like to express my sincere appreciation and gratitude to Dr. Jack Gauldie, my supervisor, for his wisdom, expert advice, generosity, and continual encouragement during this endeavour. I feel very fortunate and privileged to have had the opportunity to pursue this degree under his supervision. His careful attention to detail, both in the experimental and written aspects of my work, made him an outstanding, first-class supervisor.

I am thankful to members of my supervisory committee Dr. Carl Richards, and Dr. Gurmit Singh for their expert advice and useful discussion throughout the course of my research. I would also like to express my gratitude to Dr. Mark Hatton, Dr. Mary Richardson and Dr. Tom Podor for their inspiring insights into endothelial cell biology. I would like to thank Dr. Kao-Lee Liaw for invaluable instruction in the statistical analyses of my data.

I would also like to thank Dr. Mary Hitt for her patience and her help in allowing me understand the biology of adenoviruses. Thanks also to Dr. Jonathan Bramson for his critical review of the thesis.

Special thanks goes to my friends and colleagues Dr. Ronan Foley, Dr. Yonghong Wan, Duncan Chong, and Xueya Feng. (Dr. to be) Kay Palmer has been especially helpful with experimental animal studies, and has been a great coffee compatriot. It has been a pleasure working and socializing with them.

Finally, I am especially grateful to my beautiful wife, Dr. Patricia Liaw, and to my parents Karl and Eva, for their unconditional support and encouragement.

TABLE OF CONTENTS

LIST OF FIGURES

LIST OF TABLES

LIST OF ABBREVIATIONS

Ad5	human adenovirus type 5
Ad2	human adenovirus type 2
APC	antigen presenting cell
ATP	adenosine triphosphate
B7-1	T cell and NK cell co-stimulatory molecule 1
B7-2	T cell and NK cell co-stimulatory molecule 2
BAL	bronchial alveolar lavage
bFGF	basic fibroblast growth factor
CAM	chick chorioallantoic membrane
cDNA	complementary deoxyribonucleic acid
CHO	Chinese hamster ovary
conA	concanavalin A
CTL	cytotoxic T lymphocyte
CD28	T cell receptor for B7-1 and B7-2
DNA	deoxyribonucleic acid
dNTP	deoxynucleotide triphosphate
DTT	dithiothreitol
E1	early region 1
E2	early region 2

E3	early region 3
E. coli	*Escherichia coli*
ECM	extracellular matrix
FBS	fetal bovine serum
GSH	glutathione
H&E	hematoxylin and eosin
HUVEC	Human umbilical vein endothelial cell
ICE	interleukin 1β converting enzyme
IFNγ	interferon gamma
IgG	immunoglobulin G
IL-1	interleukin-1
IL-2	interleukin-2
IL-10	interleukin-10
IL-12	interleukin-12
IL-18	interleukin-18
i.n.	intranasal
IP-10	interferon-inducible protein 10
i.v.	Intravenous
JAK	Janus kinase
kb	kilobase

Kd	dissociation constant
kDa	kilodalton
LAK	lymphokine-activated killer cells
LLC	Lewis lung carcinoma
MEM	modified Eagle's medium
MMP	matrix metalloproteinase
mRNA	messenger ribonucleic acid
NK cells	natural killer cells
PAI-1	plasminogen activator inhibitor
PBS	phosphate buffered saline
PCR	polymerase chain reaction
pfu	plaque forming unit
PyMidT	polyoma middle T
RCC	renal cell carcinoma
RT	reverse transcription
STAT-3	signal transducers and activators of transcription 3
STAT-4	signal transducers and activators of transcription 4
s.c.	subcutaneous
TAA	tumor associated antigen
TCR	T cell receptor

TGFβ	transforming growth factor beta
T1	Type 1 helper lymphocyte ($CD4^+$)
T2	Type 2 helper lymphocyte ($CD4^+$)
TIL	tumor infiltrating lymphocytes
TIMP	tissue inhibitor of matrix metalloproteinase
TPA	tissue-type plasminogen activator
TNFα	tumor necrosis factor alpha
TSP-1	thrombospondin-1
uPA	urokinase-type plasminogen activator
VEGF	vascular endothelial growth factor
vWF	von Willebrand factor

CHAPTER 1-INTRODUCTION

1.0 Tumor Biology: The Transformed Cell

Cancer is a genetic disease that arises from an accumulation of somatic mutations of the cellular DNA leading to clonal selection of cells that exhibit loss of differentiation, acquire aggressive uncontrolled growth and are more invasive. While 1% of all cancers are inherited through familial germ line mutations, the majority develop as a result of unknown and elusive mechanisms (Fearon, 1997). The relationship between carcinogenesis and mutagenesis is well established and can be induced by at least three mechanisms: chemical carcinogens, ionizing radiation, and viruses. However, it is estimated that spontaneous mutations, as a result of normal cellular replication and limited by the DNA replication and repair machinery, can account for 10^{10} mutations over the course of an individuals lifetime (Alberts et al., 1994). From such a large number of mutations, it would be expected that cancer would occur with high frequency, but this is not the case. Rather, it is the succession of numerous mutational changes within a cell, estimated to be six to seven for the development of carcinoma, which increases as a function of age and results in spontaneous tumor development (Klein and Klein, 1985).

1.1 Oncogenes, Tumor Suppressor Genes and Cell Cycle

Cells are constantly being replaced in the human body. It is estimated that 10^{12} cells die everyday and are replaced by the same number of new cells (Baserga, 1993). Cell division is tightly controlled to maintain this balance between new cell development and cell death. Oncogenes and tumor suppressor genes are responsible for the maintenance of controlled cell proliferation. Oncogenes were first described as retroviral genes that could induce tumors in infected animals, but it was subsequently shown that it was the viruses that acquired dominant mutated forms of genes involved in growth control, called proto-oncogenes, from the host cell (Cantley et al., 1991). The oncogenes encode for proteins that include: growth factors, growth factor receptors, signal transduction proteins, and transcription factors. Overexpression of the oncogene results in uncontrolled cell growth that allows the cell to escape from normal proliferative control mechanisms and enhances the cell's ability to survive (Steele et al., 1998).

In contrast, tumor suppressor genes encode for proteins that inhibit unnecessary cell proliferation and are therefore anti-tumorgenic. Mutations to these tumor suppressor genes results in loss of protein function allowing for unchecked cellular proliferation. One of the most studied tumor suppressor genes encodes for p53, a 53 kDa protein which is a transcription factor that is activated in response to cellular stresses, and induces either cell growth arrest or programmed cell death (Prives and Hall, 1999). p53, has been found to be mutated

in about 50% of all cancers, and was initially thought to be an oncogene, until the wild type protein was isolated in 1989 (reviewed in Steele et al., 1998). The human p53 protein consists of 393 amino acids and has three functional domains: a 42 amino acid-N-terminal transcriptional activation domain; a protease resistant, zinc ion containing central DNA binding domain; and a C-terminal homo-oligomerization domain (Oren, 1997;Levine, 1997). The majority of mutations that inactivate p53 are missense mutations of amino acids in the DNA binding region resulting in the inability of p53 to bind DNA and to act as a transcription factor (Levine, 1997). Transcriptional activity by p53 is crucial in regulating downstream genes that are involved in the cell cycle or apoptotic pathways.(Oren, 1997).

The cell cycle refers to the complex series of events that regulates cell division and ensures that the DNA is correctly replicated. The cell cycle initiates from the G_1 phase, during which time a cell commits towards mitosis based on signals transduced from membrane bound receptors and signalling pathways. Alternatively, if conditions do not warrant cell division, the cell may become quiescent or differentiate and remain in a resting state known as G_0 (Sherr, 1996). If the correct stimulus has been received, the cell then proceeds to the S, or synthesis phase where DNA is replicated. The transition point in late G_1 to S phase is termed the restriction or "R point", and is controlled by a protein family of D cyclins, which in turn bind cyclin-dependent protein kinases (CDK) for activation (Sherr, 1996). At this point, the cell no longer requires stimulus from extracellular

receptors and is committed to DNA replication. However, it is at the G_1 to S phase checkpoint that oncogenic events culminate and exert their greatest effects towards the development of uncontrolled cellular proliferation (Bartek et al., 1999; Hunter and Pines, 1994). Mutations leading to the over expression of Cyclin-D, acting as a proto-oncogene, have been found in a number of cancers including breast cancer (Levine, 1997; Winslow-Saslow et al., 1995). The late G_1 phase Cyclin-E has been shown to be critical in the transition to S phase. Cyclin-E, along with its catalytic subunit CDK2, are regulated by the tumor suppressor p27. Mutations in cyclin-E, or reduced expression of p27 have been associated with enhanced tumor growth in both breast and colon cancers (Porter et al., 1997).

These complex interactions in the cell cycle are not limited to the G_1 to S phase. Following DNA replication in the S phase, the G_2 to M checkpoint is also critical but is not well understood. DNA damage at this point triggers p53 activation, and the inhibition of B-cyclin, such that mitosis does not occur. Defects in this checkpoint allow tumor cells to enter the mitotic M phase of the cell cycle with damaged or incompletely replicated DNA (Hunter and Pines, 1994; Paulovich et al., 1997).

Cancer is a generic term used to describe many different types of neoplasia or malignancy. From a pathological basis, tumors are designated based upon embryonic tissue origins, such that a tumor of the mysenchymal origin is a sarcoma and those derived from epithelial cell origins are carcinomas (Cotran et al., 1996).

While these cancers generally form solid masses, it must be kept in mind that neoplasia of hematopoietic origin such as leukemia and myeloma are important cancers of the white blood cells.

1.2 Breast Cancer

Breast cancer can be expected to develop in 10% of the female population in North America. According to 1991 statistics, in the United States 182,000 new cases were diagnosed and 46,000 women died from this disease (Yang and Lippman, 1999). Heredity accounts for 5-10% of breast cancers, while the remaining cases represent spontaneous neoplasia (Yang and Lippman, 1999; Morrison, 1994).

Carcinomas of the breast are classified as being of either ductal or of lobular origin with reference to the structures found in the normal breast tissue (van Diest, 1999). The ducts, lined with epithelial cells, connect the nipple to the terminal lobules within the breast which are themselves lined with secretory cells responsible for lactation. These cells proliferate in response to hormonal changes during the menstrual cycle and during pregnancy (Cotran et al., 1996). Ductal carcinoma *in situ* (DCIS) and lobular carcinoma *in situ* are pathologically defined as non-invasive neoplastic cells of epithelial origin which have not invaded the basement membrane into the surrounding stroma (Hartmann, 1984). In contrast, infiltrating ductal carcinomas account for up to 80% of breast lesions and are

characterized by extensive fibrous tissue and calcification giving a stony appearance. These tumors invade the surrounding stroma and have a high metastatic potential which correlates with a poor outcome (Cotran et al., 1996).

The molecular biology behind the development of neoplasia in breast tissue has been the subject of significant advances in recent years. Hereditary breast cancer has been linked to two genes, BRCA1 and BRCA2 (Zhang et al., 1998). Mutations in these genes increase the risk of breast cancer development by 15 to 20 times over those individuals who do not carry the mutation (Zhang et al., 1998; Yang and Lippman, 1999). BRCA 1 is a tumor suppressor gene which is involved in cell cycle regulation and DNA repair (Yang and Lippman, 1999). BRCA2, a 3418 amino acid protein that shares no homology to BRCA1, has also been found to be involved in the repair of damaged DNA (Zhang et al., 1998).

Mutations in the p53 gene occur in about 50% of spontaneous breast cancers (Morrison, 1994). Many cancer treatments exert their effects by damaging DNA, in turn inducing apoptosis through a p53 mediated pathway. Thus, inactivating mutations in p53 abrogate the effectiveness of the treatment (Elledge and Allred, 1998). The human homologue of the *neu* oncogene, HER2/*erb*B-2 is related to the epidermal growth factor receptor (EGF) and is overexpressed in 30% of human breast cancers (Morrison, 1994;Norton, 1999). The expression of this receptor, which possesses endogenous tyrosine kinase activity and which may interact with the signalling pathway of the estrogen receptor, is correlated with a

poor prognosis (Norton, 1999; Pegram et al., 1998).

Models of breast cancer have been developed in transgenic mice which mimic the progression and pathology found in human tumors. The Polyoma middle T (PyMidT) model, expresses the transforming capability of the middle T antigen of the polyoma virus specifically within the mammary epithelium. This is accomplished using the mammary epithelium specific mouse mammary tumor virus (MMTV) transcriptional promoter to drive the expression of the PyMidT (Guy et al., 1992). PyMidT possesses potent constitutive tyrosine kinase activity which activates members of the Src family of tyrosine kinases as well as the phosphatidylinositol-3' kinase signalling pathway (Guy et al., 1994). The mice expressing PyMidT rapidly develop tumors along the entire mammary epithelium that can metastasize to the lungs (Webster and Muller, 1994).

The *neu* transgenic model, more closely resembles the development of tumors seen in human breast tissue overexpressing Her2. A point mutation in the *neu* gene arising in the transmembrane domain of the protein leads to constitutive tyrosine kinase activity and Src activation (Guy et al., 1996). Mice overexpressing this activated *neu* under the control of the MMTV promoter also develop rapid mammary epithelium transformation (Guy et al., 1996). The NDL mouse model derived from studies with wild-type catalytically inactivated neu demonstrate tumor development after a long latency period. These tumors arise due to alterations in the extracellular domain of Neu that allow for the formation of intermolecular

disulfide bonds and increased receptor homodimerization (Siegel et al., 1994).

1.2.1 Current Breast Cancer Therapies

The current treatment regimes for breast cancer include surgery, radiation therapy and chemotherapy. The surgical techniques developed for breast cancer are over 100 years old. The technique of radical mastectomy involves removing the entire breast tissue and the underlying muscle (Harris et al., 1993). Although surgery may remove the primary tumor it is ineffective against the disseminated metastatic disease. Radiation therapy is limited by toxicity to the patient, and the development of radio-resistant cells that has been correlated to mutation and subsequent loss of function of p53 in breast cancer patients (Bergh et al., 1995).

Chemotherapy drugs target the rapidly dividing cancerous cells, but do not discriminate between healthy replicating cells such as those found in the bone marrow resulting in dose limiting hematopoietic toxicity. In addition to side effects related to toxicity, many tumors return after an initial successful response because of acquired drug resistance (Kerbel, 1997). Multidrug resistance (MDR) is a result of the over expression of P-glycoprotein transmembrane pumps on the surface of the tumor cells which remove the chemotherapeutic agent from the cell cytoplasm in an energy dependent manner (Ruetz and Gros, 1994). The expression of the MDR in breast cancer is also associated with a poor prognosis (Bargou et al., 1997). The convoluted blood supply and poor perfusion within solid tumors limits

the ability of a chemotherapeutic agent to adequately diffuse throughout the tumor mass (Jain, 1994). In addition, acidic pH levels as a result of poor perfusion and tumor hypoxia results in the inactivation of many anti-cancer agents (Helmlinger et al., 1997).

1.3 The Role of the Vascular System in Tumor Growth and Metastasis

Solid tumors are a heterogenous population of cells that require new blood vessel invasion to supply nutrition and oxygen to the tumor as well as providing a route by which the tumor can spread and metastasize (Leek et al., 1994). A solid tumor may only reach a size of 2 to 3 mm in diameter before requiring neovascularization, otherwise, it is suggested that the rate of tumor cell proliferation and death reaches an equilibrium (Folkman, 1995). Blood vessels in their rudimentary state are tubes of endothelial cells that form by two processes: vasculogenesis, the development of new, *de novo* blood vessels, and angiogenesis, the sprouting of new blood vessels from existing vasculature (Hanahan and Folkman, 1996).

1.3.1 Endothelial cells

Endothelial cells line the blood vessels in every organ and are responsible

for maintaining the fluidity of blood, the transport of oxygen and nutrients and for the production of numerous growth factors (Cines et al., 1998). The endothelium in an adult covers a surface area equivalent to 7 m^2 and is composed of 1-6 $X10^{13}$ cells (Cines et al., 1998). Endothelial cells are one of the longest lived cells in the human body and normally exist in a quiescent state with only 0.01% of cells undergoing mitosis at any given time (Hanahan and Folkman, 1996).

Derived from angioblasts, endothelial cells develop from the embryonic mesoderm along with the hematopoietic stem cells that give rise to the blood (Cines et al., 1998). Maturation from the angioblast, to the endothelial cell requires the presence of a series of growth and differentiation factors, including basic fibroblast growth factor (bFGF) as well as vascular endothelial growth factor (VEGF) (Folkman and D'Amore, 1996). The process of endothelial cell differentiation and maturation was thought to be limited only to embryonic development. However, angioblasts have been isolated from the peripheral blood of adult humans (Asahara et al., 1997). These progenitor endothelial cells were isolated based on double selection using CD34 antibodies combined with an antibody specific for the VEGF receptor, VEGF-R2. Following culture on fibronectin coated plates, these cells developed the spindle shaped endothelial cell phenotype and expressed endothelial cell markers including, CD31, factor VIII and E-selectin (Asahara et al., 1997).

1.3.2 Vasculogenesis

Vasculogenesis establishes the formation of capillary tubes within the embryo. VEGF binding to the VEGF-R1 receptor initiates endothelial cell migration and assembly into capillary structures (Hanahan, 1997). Subsequent to the actions of VEGF, angiopoieten-1, a 70 kDa glycoprotein binds to the Tie-2 receptor found exclusively on endothelial cells (Davis et al., 1996). This initiates the recruitment of mesenchymal cells including, pericytes, smooth muscle cells, and myocardiocytes around the developing tube, and stabilizes the formation of the developing vessels (Davis et al., 1996;Suri et al., 1996). It is believed that angiopoietin-1 secreted by pericytes binds to Tie-2 causing the release of other stimulatory factors from the endothelial cell which are chemotactic for additional cells of mesenchymal origin (Folkman and D'Amore, 1996). Knockout mice deficient in either angiopoieten-1 or Tie-2 genes die early in development. These mice have loosely formed vessels consisting of rounded endothelial cells that are not well connected to the extracellular matrix and lack association with supporting cells (Suri et al., 1996). Angiopoietin-2 is the natural agonist for angiopoietin-1, and also binds to the Tie-2 receptor (Maisonpierre et al., 1997). This ligand interferes with capillary integrity making the endothelial cells more responsive to growth factors initiating new cell proliferation and migration for the assembly of additional capillaries (Hanahan, 1997). Tie-2 expression in the adult is limited to regions undergoing vascular remodelling, and is involved in the process of angiogenesis

(Maisonpierre et al., 1997). Final differentiation of the blood vessels into veins and arteries is control by the ephrin family of tyrosine kinase ligand/receptors. The ephrin-B2 ligand, a transmembrane protein, is only expressed on endothelial cells in the artery, whereas the receptor Eph-B4 is found on those endothelial cells which line veins (Yancopoulos et al., 1998). Both membrane bound ligand/receptors interact at the cell to cell junction in the transition point of the vessel as it changes from artery to vein (Yancopoulos et al., 1998).

1.3.3 Extracellular Matrix

The extracellular matrix, a complex mixture of proteins and polysaccharides secreted by cells, forms the framework to which the cells bind, and regulates many cell functions. In addition, the extracellular matrix is a storage depot for growth factors, stabilizing and protecting them from degradation (Benezra et al., 1993). Endothelial cells, smooth muscle cells and fibroblasts secrete transforming growth factor β (TGFβ), which acts in an autocrine manner upon the endothelial cell stimulating the production of extracellular matrix components (Gerritsen, 1996). The composition of this matrix includes: the collagens, glycosaminoglycans such as heparin and dermatan sulfate, hyaluronic acid, fibronectin, proteoglycans and laminin. Endothelial cells bind to a sheet-like basement membrane containing type IV collagen, laminin, and proteoglycans (Yurchenco and Schittny, 1990). Attachment to the basement membrane is mediated by integrins, which are

transmembrane receptors that physically link the cell cytoskeleton to the collagen. Integrin binding can initiate gene expression, and influences cellular elongation, alignment and migration (Vernon and Sage, 1995). Apoptosis, or programmed cell death, occurs if the endothelial cell becomes unattached from the extracellular matrix. This is known as anchorage dependence (Ruoslahti and Reed, 1994). Anchorage independent growth is a hallmark of transformation and tumorigenicity. Sethi and co-workers, have recently demonstrated that small cell lung cancers promote extracellular matrix production in the lung and that integrin mediated binding to fibronectin, laminin and type IV collagen protects the tumor cells from chemotherapeutic induction of apoptosis in a MDR independent manner (Sethi et al., 1999).

1.3.4 The Plasminogen Activating System and Metalloproteinases

Whereas the maintenance of blood vessels requires basement membrane and extracellular matrix for structural integrity, this also poses a mechanical barrier to the migration of endothelial cells and their ability to form new vessels from the existing vasculature by the process known as angiogenesis. The localized degradation of the extracellular matrix involves two groups of proteolytic enzymes: plasminogen activators/plasmin, and the matrix metalloproteinases (MMP) (Vassalli and Pepper, 1994).

Plasminogen activators (PA) are serine proteases that cleave plasminogen

from an inactive zymogen state, into the biologically active enzyme plasmin, which itself is a serine protease (Vassalli et al., 1991; Plow et al., 1995). The physiological role of the plasminogen activators/plasmin pathway in the body is to: a) dissolve fibrin blood clots and b) degrade the extracellular matrix and allow cell migration (Plow et al., 1995). Two distinct PAs have been identified; urokinase-type PA (uPA), and tissue-type PA (tPA). tPA is a 530 amino acid, double kringle containing enzyme with a molecular weight of 68 kDa. The enzyme is secreted from the endothelial cell in an active single chain form, and can be cleaved by plasmin at amino acid residue 278 generating a two chain active isoform that is connected by a disulfide bridge (Bachmann et al., 1984). uPA , which contains only one kringle domain, is released in a pro-form and requires activation by plasmin, kallikrein, Factor VIII or cathepsin B. This converts the single chain 52 kDa pro-enzyme into the biologically active disulfide linked 36 kDa two chain form (Vassalli et al., 1991;Stephens et al., 1998). tPA and uPA share structural homology within the kringle domains and in the serine protease domain. In addition, uPA contains a growth factor domain that allows it to bind to the uPA receptor on cells (Vassalli et al., 1991). Normal resting endothelial cells do not produce PAs and require the stimulus of bFGF, TGFβ, or tumor necrosis factor (TNFα), among others, for protein production (Gerritsen, 1996). Physiologically, the function of tPA is mainly related to fibrinolysis and the degradation of fibrin clots, whereas uPA plays a more dominant role in wound healing, tumor metastasis and angiogenesis (deVries et al.,

1996).

Plasminogen is a 790 amino acid plasma protein produced by the liver and found in concentrations of 1-2 μM in the blood (Miyashita et al., 1988). As described earlier, plasminogen is a zymogen, of the serine protease plasmin. Plasminogen structure is well conserved in all mammalian species, and exists in two glycosylated forms (Degen et al., 1990). In humans, form 1 is N-glycosylated at $Asparagine_{288}$, and O-glycosylated at $Threonine_{345}$, while form 2 is only mono-glycosylated at $Threonine_{345}$ (Miyashita et al., 1988; Flamme and Risau, 1992). The reduced carbohydrate content in the second form, increases the binding affinity of plasminogen to fibrin (Miyashita et al., 1988). Plasminogen binds to various proteins in the extracellular matrix including: fibronectin, laminin, and type IV collagen (deVries et al., 1996). Binding to proteins is facilitated by five disulfide bonded kringle structures within plasminogen that possess affinity for lysine residues (Miyashita et al., 1988).

Activated plasmin is generated by cleavage of whole length native Glutamic $acid_1$ plasminogen at $Arginine_{561}$ -$Valine_{562}$ by tPA or uPA. This form of plasmin then undergoes autocatalysis, and cleaves off the first 76 amino acids at $Lysine_{76}$-$Lysine_{77}$ generating a two chain molecule that is connected by two disulfide bonds (Castellino, 1984; Miyashita et al., 1988). Plasmin generation occurs most efficiently when plasminogen is bound to receptors on the cell surface. An endothelial cell possesses 1.4 -210 X 10^5 plasminogen receptors (Plow et al.,

1995). In addition, uPa in the active two chain form is also bound to the cell surface via the uPA receptor. The active uPA and plasminogen are thus in close proximity to one another on the cell surface enhancing the generation of plasmin (Plow et al., 1995;deVries et al., 1996).

Plasmin is a broad spectrum protease that can directly degrade many extracellular matrix components including: vitronectin, fibronectin and laminin(Plow et al., 1995). In addition, plasmin can activate matrix metalloproteinase zymogens from their latent state (Vassalli and Pepper, 1994). MMPs are a family of Zn^{2+} dependent enzymes that are important for the degradation of the extracellular matrix and include: MMP-1, a collagenase that degrades collagen types I to III; MMP-2 or gelatinase, digests collagen types IV and V; MMP-3, stromelysin dissolves proteoglycans; MMP-9 also dissolves collagen types IV and V (Xie et al., 1994). The MMPs are produced by active endothelial cells. Endothelial derived inhibitors of the enzymes, tissue inhibitors of matrix metalloproteinases (TIMP1,2) are released to regulate MMP activity (Gerritsen, 1996).

1.3.5 Angiogenesis

As described earlier, angiogenesis is the formation of new capillary blood vessels from existing vessels. Angiogenesis is a carefully controlled, fundamental process necessary in the body for reproduction, development, and wound repair. However, in many diseases unregulated angiogenesis contributes to the pathology.

Rheumatoid arthritis, characterized by pannus development and erosion within the synovium of the joints, and neovascularization of the retina leading to blindness are two pathological conditions where angiogenesis is a key factor (Storgard et al., 1999; Alon et al., 1995). Angiogenesis is important for solid tumor growth and metastasis. Neovascularization increases the perfusion of the solid tumor allowing more nutrients and oxygen to enter while simultaneously enhancing the removal of catabolites (Folkman, 1995). In addition, new blood vessels provide an enhanced route for the tumor cells to escape into the circulation and metastasize to distant regions in the body (Folkman and Shing, 1992).

In the process of wound healing, new blood vessels are necessary for the removal of debris from the granulation tissue and for bringing in cells and nutrients. Angiogenesis is stimulated by the inflammatory process with the release of angiogenic cytokines and growth factors from infiltrating macrophages, and granulocytes (Seljelid and Busund, 1994). Wound repair entails collagen secretion from infiltrating fibroblasts and degradation by secreted MMPs. Fibrin, a mesh work of thrombin activated fibrinogen, is also deposited within wounds and in blood clots. Excess fibrin is removed from the wound by plasmin and the PA system (Romer et al., 1996). These mechanisms of extracellular matrix build-up, degradation and angiogenic development hold true for tumor growth as well.

The process of angiogenesis occurs in a complex, multi-step manner. Endothelial cells within a capillary or post capillary venule receive stimuli in a

paracrine manner from surrounding cells in the stroma or released growth factors from the extracellular matrix pool. Growth factors which induce a positive angiogenic response by the endothelial cell include: bFGF, VEGF, platelet-derived growth factor (PDGF), interleukin-8, prostaglandins, and angiogenin (Leek et al., 1994) In addition, the endothelial cells must overcome the effects of negative angiogenic regulating factors (O'Reilly et al., 1994).

Degradation of the basement membrane by plasmin/PA and MMPs follows endothelial cell activation. Many tumor types overexpress uPA and tPA thereby accelerating ECM degradation, enhancing angiogenesis and metastasis (deVries et al., 1996;Stephens et al., 1998). Endothelial cell migration towards the positive stimuli ensues with the development of sprouts from the leading edge of the preexisting blood vessel (Jain et al., 1997). Normally quiescent endothelial cells trailing behind the migrating cells, rapidly proliferate with a mean turnover time of five days, replacing the migrated cells (Folkman, 1995; Jain et al., 1997). The sprouting endothelial cells form tubes and connect to other blood vessels permitting blood to flow, a process known as anastomoses (Jain et al., 1997). These primordial capillaries do not yet have supporting pericytes, but begin to express the formation of the basement membrane. Angiopoietin-1/Tie2 receptor activation initiates endothelial quiescence, vessel maturation, basement membrane formation and endothelial cell adhesions to supporting cells (Hanahan, 1997). Unlike normal tissue, the vasculature of the tumor develops with a tortuous architecture resulting

in irregular blood flow (Jain, 1994). In addition, the tumor vessels may not have accompanying pericytes or smooth muscle cells, which inhibit endothelial cell proliferation within normal tissue (Torry and Rongish, 1992). The endothelial cells within vessels of a solid tumor have been found to overexpress Angiopoieten-2, a signal for vessel disruption and dissociation. This is accompanied by a subsequent rise in VEGF production, that leads to robust angiogenesis, especially at the tumor periphery. This self sustaining cycle of vessel growth and vessel disassembly enables the tumor to maintain angiogenesis (Holash et al., 1999).

1.3.6 The Angiogenic Phenotype

A solid tumor may remain small in a poorly vascularized state for extended periods of time as a carcinoma *in situ*. For the tumor to enlarge, an angiogenic switch is thought to occur within a population of the tumor cells initiating neovascularization that is not simply a result of the overexpression of an angiogenic factor (Folkman and Shing, 1992; Folkman, 1995). Although tumor cells may release VEGF and bFGF early in tumorigenesis, lowered expression of negative regulators and inhibitors of angiogenesis, some of which are under the control of tumor suppressor genes is thought to contribute to angiogenic phenotype. Negative regulators of angiogenesis include: thrombospondin-1 (TSP-1), platelet factor 4, Interleukin-12 (IL-12), interferon alpha (IFNα), TGFβ, tumor necrosis factor alpha (TNFα), angiostatin, endostatin among others (Folkman, 1995;Dameron et

al., 1994; Coughlin et al., 1998; O'Reilly et al., 1997; O'Reilly et al., 1994). An example of tumor suppressor involvement is illustrated in p53 mutated cells from patients with Li-Fraumeni syndrome. Isolated late passage fibroblasts were shown to have decreased mRNA levels of TSP-1, a potent matrix glycoprotein that is an inhibitor of angiogenesis. Culture supernatants from these fibroblasts could not inhibit neovascularization in a bFGF induced cornea model, whereas supernatants from early passage cells retaining a single wild type p53 allele could produce TSP-1 and inhibit angiogenesis (Dameron et al., 1994). p53 regulates the promotor of the TSP-1 gene, and restoration of the mutated protein restored TSP-1 levels (Dameron et al., 1994).

1.4 Angiogenesis and Breast Cancer

A number of factors have been associated with a poor prognosis in breast cancer including: (1) the overexpression of *erb*-B-2, (2) lymph node status and, (3) tumor size. More recently, microvessel counting has been demonstrated to be an independent and accurate indicator of the clinical outcome in breast cancer patients (Hayes, 1994). Microvessel counting was shown to more accurately reflect disease progression, metastatic potential and long term survival than other prognostic indicators (Hayes, 1994;Weidner, 1995b). Weidner, demonstrated that antibodies against factor VIII, an endothelial cell protein involved in coagulation, can be used to stain individual or clusters of endothelial cells from paraffin embedded breast

tumor sections (Weidner, 1995a). In a blinded study, counts of over 100 vessels per field of view correlated with metastatic disease and a 100% chance of tumor recurrence, whereas only 5% of patients with less than 33 microvessels per field had tumor recurrence (Weidner, 1995a).

Given that solid tumors require new blood vessels for growth and metastasis, and that the vascularity of a breast tumor is a prognostic indicator of patient outcome, therapies designed to inhibit angiogenesis would be an attractive and effective treatment for primary tumors and their metastasis. Strategies aimed at the endothelial cell, homogenous throughout the body and genetically stable would be able to disrupt the tumor blood supply and effectively starve the cancer (Kerbel, 1997).

1.5 Anti-Angiogenesis Therapy

A variety of novel strategies have been developed in an attempt to specifically inhibit angiogenesis within a solid tumor. In doing so, it is hoped that the primary tumor and any metastasis can be starved of blood curtailing growth, or at least preventing additional tumor burden. The use of antibodies against the integrin $\alpha_v\beta_3$, was shown by Brooks and co-workers (1994) to effectively inhibit bFGF induced angiogenesis in a chick chorioallantoic (CAM) assay. This monoclonal antibody, LM609, inhibits the $\alpha_v\beta_3$ integrin which is expressed on the endothelial cell surface and is a receptor for von Willebrand factor (vWF),

fibrinogen and fibronectin (Brooks et al., 1994a;Brooks et al., 1994b). Blocking the association of this integrin with the ECM substrates by LM609 initiates apoptosis of the endothelial cells (Brooks et al., 1994b). Systemically delivered LM609 could also inhibit the growth of a human breast cancer xenograft, and the antibody treated tumors were four times less vascular than control treated tumors (Brooks et al., 1995).

In a mouse skin carcinoma model, VEGF-R2 was found to be overexpressed in endothelial cells in malignant, but not in benign keratinocytes lesions. Anti-VEGF-R2 antibodies delivered systemically for 4 weeks inhibited angiogenesis, and decreased invasion by the malignant cells into the surrounding stromal tissue (Skobe et al., 1997). Whereas the two previous examples used monoclonal antibodies which interfered with the function of an endothelial cell associated receptor, Huang and co-workers (1997) used an antibody fused to a coagulation cascade protein to induce thrombosis specifically within the tumor. Using a tumor model in which the cells overexpress interferon gamma (IFNγ), endothelial cells within the tumor, but not healthy tissue, upregulated major histocompatibility complex class II (MHC II). Antibodies against MHC II fused to the active truncated form of tissue factor (TF), bound to tumor endothelial cells and induced the coagulation cascade on the endothelial surface thereby generating thrombin. Clots formed 30 minutes after the injection of the antibody conjugate. This was followed by rapid necrosis of the tumor (Huang et al., 1997).

Other novel therapeutic approaches include the use of matrix metalloproteinase inhibitors, such as the compounds batimastat (BB 94), and marimastat to block endothelial and tumor cell migration (Barinaga, 1997;Bergers et al., 1999). A similar concept has been proposed to inhibit the recently cloned and purified enzyme heparanase (Vlodavsky et al., 1999;Hulett et al., 1999). This membrane bound glycosidic enzyme, found on highly metastatic tumors, cleaves the carbohydrate heparan in the ECM allowing tumors cells to migrate. In addition, heparanase releases heparan bound bFGF and is a pro-angiogenic molecule (Vlodavsky et al., 1999). The heparanase inhibitor PI-88, a sulfated oligosaccharide phosphomannopentaose compound, has been reported to significantly inhibit primary and metastatic breast cancer in a rat model (Hulett et al., 1999). The compound fumagillin (TNP-470, AGM 1470) isolated from the fungus *Aspergillus fumigatus*, has also shown potential in inhibiting angiogenesis in the late stages of pancreatic islet carcinoma growing in a transgenic mouse model (Bergers et al., 1999).

1.5.1 Angiostatin

Concomitant tumor resistance refers to the ability of some primary tumors to hold the grow of metastases. Surgical removal of a primary tumor was often followed by rapid growth of the metastasis (O'Reilly et al., 1994a). Though studies in animals demonstrated that the primary tumor could inhibit the metastatic growth,

it could not control the number of micro-metastasis that developed (O'Reilly et al., 1994a). A report in 1994 described the isolation of a novel protein produced by Lewis lung carcinoma (LLC) tumors in mice, which could inhibit the growth of LLC metastasis (O'Reilly et al., 1994a;O'Reilly et al., 1994b). Removal of the primary subcutaneously implanted tumor resulted in angiogenesis and growth of distant metastasis in the lungs. The compound isolated from the serum and urine of mice bearing the primary tumors could inhibit metastatic growth when injected into mice which had the primary lesion removed (O'Reilly et al., 1994a). Moreover, inhibition of angiogenesis and metastatic growth could be repeated in SCID mice indicating that the phenomenon was not induced by the immune system. The isolated compound could also inhibit the growth of cultured endothelial cells (O'Reilly et al., 1994a).

Purification and amino acid sequencing revealed that the compound, termed "Angiostatin", was a 38kDa polypeptide which corresponded to the first four kringle domains of the plasma protein plasminogen encompassing amino acids 78-440 (O'Reilly et al., 1994a). Digestion of human plasminogen by elastase produced three polypeptides encompassing kringles 1-3 and 1-4 which retained anti-angiogenic activity when injected into mice and inhibited endothelial cell proliferation *in vitro* (O'Reilly et al., 1994a). Angiostatin's inhibitory activity could be detected for up to five days, indicating the protein has a relatively long half-life.

A mechanism for generating angiostatin within the tumor environment has

been suggested from *in vitro* studies using cultured tumor cells lines, including PC-3 prostate, Chinese hamster ovary (CHO), and HT1080 fibrosarcoma cells (Gately et al., 1997;Gately et al., 1996;Stathakis et al., 1997). First, plasminogen is converted to plasmin. Plasmin is then reduced by an as yet unpurified plasmin reductase enzyme which reduces the disulfide bonds at amino acids $Cysteine_{461}$-$Cysteine_{540}$ and $Cysteine_{511}$-$Cysteine_{535}$ within kringle 5 in the presence of a cofactor believed to be glutathione (GSH) (Stathakis et al., 1997;Stathakis et al., 1999). The reduced plasmin is then enzymatically cleaved by serine proteases, possibly involving plasmin itself, in generating bio-active angiostatin (Gately et al., 1997;Gately et al., 1996;Stathakis et al., 1999). The formation of angiostatin from plasminogen, but not from exogenous plasmin, could be inhibited by plasminogen activator inhibitor-1 (PAI-1). In contrast, the less specific serine protease inhibitor aprotinin, could inhibit the formation of angiostatin from both plasminogen and plasmin (Stathakis et al., 1997). While this is one possible mechanism, others have described the conversion of plasminogen to angiostatin by macrophage derived metalloelastase within a LLC tumor environment (Dong et al., 1997).

Though angiostatin is generally considered to be kringles 1-4 of plasminogen, kringles 1-3 and 1 to part of kringle 5 also retain anti-endothelial cell proliferative activities (Cao et al., 1996;Stathakis et al., 1999). In addition, individual kringles derived by recombinant methods or by proteolytic digestion of plasminogen also retain some degree of anti-proliferative activity (Cao et al.,

1996;Ji et al., 1998). The mechanism of endothelial cell growth inhibition by kringle domains does not appear to depend on abilities of the kringles to bind lysine. Competitive inhibitors for lysine binding do not reduce the bio-activity of either individual kringles, or kringles 1-3 (Cao et al., 1996). However, disruption of the kringle structure by reducing agents abrogates biological activity (Cao et al., 1996). The inhibition of endothelial cell proliferation is a function of kringles 1-3, whereas kringle 4 is required to inhibit cell migration (Ji et al., 1998).

Endothelial cells treated with angiostatin undergo apoptosis by an unknown molecular mechanism(s) (Claesson-Welsh et al., 1998; Lucas et al., 1998). Angiostatin activates tyrosine kinases associated with integrin signalling pathways, but this activity cannot be competitively inhibited with the addition of RGD peptides (Claesson-Welsh et al., 1998). However, angiostatin does not activate Src phosphorylation, a protein known to accumulate at focal adhesions. Thus, angiostatin may inappropriately activate focal adhesion kinases, perturbing normal cell adhesion and signal transduction, in the favour of those pathways leading to apoptosis (Claesson-Welsh et al., 1998).

While Claesson and co-workers did not establish direct binding of angoistatin to any endothelial cell integrin, Moser *et al*, (1999) identified the α and β subunits of the ATP synthase complex on the surface of human umbilical cord vein endothelial cells (HUVEC) as capable of binding angiostatin, but not plasminogen (Moser et al., 1999). The binding of angiostatin to the 55 kDa cell

surface complex could not be inhibited with ε-amino caproic acid, a competitor for lysine binding sites, in agreement with previous reports that the binding of angiostatin is not a lysine dependent process. Scatchard analysis indicated angiostatin bound with a dissociation constant (K_d) of 158nM and that there were 38,000 angiostatin binding sites per HUVEC cell. This binding could be inhibited with antibodies specific for the α subunit and could block the anti-proliferative effect of angiostatin on cultured HUVEC cells (Moser et al., 1999). From these experiments, Moser and co-workers put forth a hypothesis that endothelial cells within the hypoxic tumor environment elevate ATP synthase on the cell surface in order to maintain high levels of ATP. Angiostatin inhibits ATP production by binding to the ATP synthase complex resulting in endothelial cell death and blood vessel disruption (Moser et al., 1999). While this may explain ATP synthase expression on the surface of endothelial cells within the hypoxic tumor, this does not explain why HUVEC cells express such a high number ATP synthase complexes *in vitro*. Moreover, the study did not examine if angiostatin has any ability to inhibit mitochondrial ATP synthase complexes.

Recombinant human and murine versions of angiostatin encompassing plasminogen kringles 1-4, have been expressed from the yeast *Pichia pastoris* (Sim et al., 1997;Wu et al., 1997). The recombinant proteins retain the biological activity of angiostatin derived from elastase digestion of plasminogen but have slightly altered glycosylation patterns or are unglycosylated (Sim et al., 1997). Human

recombinant angiostatin injected daily subcutaneously into mice bearing primary LLC tumors was shown to inhibit tumor growth at a dose of 100 mg/kg/day (2mg/mouse/day) (Sim et al., 1997). In contrast, murine recombinant angiostatin required a dose of only 6 mg/kg/day to inhibit the growth of the same tumor model (Wu et al., 1997). While angiostatin does not appear to be species specific, the murine analogue has a longer half life of 2 days, compared to only 4 hours for the human form in the mouse (Sim et al., 1997). Immunohistochemical staining with anti-vWF antibodies showed that LLC metastasis in the lungs of mice treated with angiostatin had decreased neovascularization as compared to control mice (Sim et al., 1997). Primary tumor growth was only suppressed during the course of angiostatin treatment, and once the therapy was discontinued, tumor growth resumed (Sim et al., 1997). The administration of angiostatin was not associated with any gross side effects or bleeding disorders (Sim et al., 1997).

1.6 The Immune System

The immune system protects the host from infection by invading pathogens including viruses, bacteria and parasites. Developed from stem cells in the bone marrow, the cellular component of the immune system is composed of the white blood cells: T lymphocytes, B cells, macrophages, neutrophils, eosinophils, dendritic cells and natural killer (NK) cells. Within the immune system, two pathways exist to deal with infectious agents: innate or natural immunity, and

acquired or adaptive immunity. The innate system provides rapid and incomplete defence through the use of cell surface or soluble receptors until specific immunity can develop (Fearon and Locksley, 1996). These receptor proteins usually recognize carbohydrate antigens such as those expressed on the surface of bacteria. Activation of such receptors on macrophages or neutrophils causes the release of cytokines, polypeptide hormone mediators of the immune system, that promote the development and expansion of helper T cells in the acquired immune system.

T and B cells of the acquired immune system can rearrange genetic elements encoding for the T cell receptor (TCR) or for immunoglobulins such that 10^{11} different T or B cell clones may be generated, each specific for a different antigen (Fearon and Locksley, 1996). The B cell immunoglobulins can bind protein, carbohydrate or even chemical groups, whereas the TCR on the T cell only recognizes peptides that are bound to the cell surface protein, major histocompatibility complex (MHC) class I and class II on antigen presenting cells. Thus the acquired immune system can be divided two sections: 1) the cell mediated response, which acts against intracellular pathogens and tumors generating CD8+ cytotoxic T lymphocytes (CTL); 2) the antibody based humoral response which is directed against extracellular pathogens, and in the case of parasitic infections may play a role in the pathology of allergy (Timmerman and Levy, 1999;Seder and Paul, 1994).

Naive T cells when stimulated can develop into at least two unique T cell subsets, T1 and T2, that are characterized by their ability to secrete cytokines (Mossman et al., 1986; Seder and Paul, 1994; Cherwinski et al., 1987). The T1cells promote a cellular immune response and secrete primarily IFNγ, lymphotoxin, interleukin-2 (IL-2) and TNFα. IL-12 induces the differentiation of naive T cells to the T1 phenotype through the production of IFNγ and the down regulation of interleukin-4 (IL-4). T2 cells are characterized by the production of interleukins 4, 5, 6, 10 and 13 and are pivotal in the development of humoral immunity (Seder and Paul, 1994).

The CTL response is characterized by CD8+ cells which recognize antigen bound to MHC class I molecules on the surface of infected or tumor cells leading to direct cytolytic killing of the cell. CTL cells first become trained to recognize foreign antigen by professional antigen presenting cells (APC), which include dendritic cells (Timmerman and Levy, 1999). In addition CD4+, T1 helper cells will bind MHC class II on APC and secrete cytokines like IL-2 and IFNγ that promote the expansion and activation of the CD8+ cells (Timmerman and Levy, 1999). Optimal T cell activation requires not only engagement of the TCR receptor, but costimulatory molecules expressed on the surface of the cell presenting the antigen. The CD28 molecule is present on T cells and binds B7-1 or B7-2 on the APC providing the second activation signal following TCR/MHC engagement. TCR engagement in the absence of this second signal leads to T cell anergy or non-

responsiveness (Timmerman and Levy, 1999;Guinan et al., 1994).

1.6.1 Tumor Immunotherapy

As discussed earlier, the development of cancer involves mutations of genes within the normal cell environment. Thus, the protein products from such mutation events can serve as potential targets for recognition by the immune system. Numerous tumor associated antigens (TAA) including: MART-1, gp100,and tyrosinase expressed in melanoma; neu, and CA125 found in breast and ovarian cancers; and β-catenin expressed by colon tumors have been identified (Rosenberg, 1997). In the 18th century, it had been noted that cancer could spontaneously regress in patients following a bacterial infection. Based on these observations, Dr. William Coley treated cancer patients with preparations that included bacterial fragments in hopes of stimulating the immune system to non-specifically attack the tumor (reviewed in Trinchieri and Scott, 1994).

In the 1980's nonspecific active immunotherapy was first attempted after the isolation and cloning of the cytokines IFNγ and IL-2. IFNγ, originally identified based on its anti-viral activity, stimulates antigen presentation through the increased expression of MHC class I and II receptors, increases the production of T1 type cytokines, and mediates leukocyte-endothelial cell interactions (Boehm et al., 1997). IL-2, stimulates the growth and activity of T cells, NK cells, monocytes and B cells. In addition, IL-2 enhances the production of IFNγ and TNFα

(Oppenheim and Lotze, 1994). Systemic IL-2 therapy has been shown to have beneficial effects in 10-30% of patients with melanoma (Shu et al., 1997). However the required high dosages leads to toxicity manifesting as vascular leak and multiple organ failure limiting the practical use of IL-2 (Oppenheim & Lotze 1994)..

Another approach, passive adoptive immunotherapy, involves isolation of lymphokine activated killer (LAK), or tumor infiltrating lymphocytes (TIL) from the tumor of a patient. This is followed by *in vitro* expansion in the presence if IL-2, and infusion of the activated cells back into the patient (Shu et al., 1997). While studies using this treatment approach did show some benefits for melanoma patients, results with other cancers were disappointing (Sussman et al., 1994).

It is established that T cells can mount an anti-tumor response. It is also apparent that many tumors can escape immunosurveillance. Evasion from the immune system has been linked to many possible mechanisms including: down regulation of MHC class I on the tumor, the lack of costimulatory molecules on the tumor cell surface, immunoselection of tumor cells that are weakly antigenic, immunotolerance to tumor antigens, the secretion of immunosuppressing cytokines by the tumor, generation of suppressor T cells and the enhanced expression of Fas ligand on the tumor cell triggering apoptosis on T cells expressing Fas (O'Connell et al., 1999; Shu et al., 1997).

Active immunization or vaccination protocols with tumor antigens attempts to induce a T cell specific anti-tumor immune response, overcoming the immune

privilege of the tumor environment while maintaining limited toxicity. One approach has been to genetically modify autologous tumor cells or tumor infiltrating lymphocytes (TIL) to secrete cytokines, and then return them to the patient in the hopes of increasing the tumors immunogenicity (Rosenberg, 1997; Rosenberg et al., 1990). Other strategies have employed the use of immunodominant peptides of tumor antigens presented on MHC, alone or in combination with peptide pulsed APC (Rosenberg, 1997). The use of intracellular bacteria including *Listeria monocytogenes* and *Salmonella sp* to express antigenic genes from within the tumor has also been explored (Pan et al., 1995; Low et al., 1999). Gene therapeutics, the delivery of genes directly into the tumor may hold great potential for immunotherapy of cancer. Studies have demonstrated that adenoviral viral vectors expressing cytokines, alone or in combination with costimulatory molecules can be directly injected into a tumor *in vivo*. The expression of the transgene product by the tumor can elicit a potent T cell mediated anti-tumor response (Addison et al., 1995;Putzer et al., 1997). The biology and utilization of these adenoviral vectors as it pertains to cancer therapy will be discussed in more detail at the end of this chapter.

1.7 Interleukin-12

The cytokine, IL-12 was originally identified on the basis of its ability to potentiate IFN-γ, secretion from NK cells lymphokine-activated killer cells (LAK) and

cytotoxic T lymphocytes (CTL). IL-12 plays an important role in the functional shift in the immune system towards the T1 T cell phenotype resulting in $CD8^+$ cellular immunity (Germann et al., 1993; Hendrzak and Brunda, 1995). In addition to being a key immunoregulatory cytokine, IL-12 also promotes anti-angiogenic events. Inhibition of angiogenesis is a result of the induction of IFNγ triggering the release of the CXC chemokine interferon-inducible protein 10 (IP-10) and Mig from the endothelium (Angiolollo et al., 1995; Yao et al., 1999; Coughlin et al., 1998).

Produced mainly by professional antigen presenting cells including, monocytes/macrophages and dendritic cells, IL-12 is a unique heterodimeric 70 kDa cytokine composed of two disulfide linked subunits (Storkus et al., 1998). The 40 kDa heavy chain designated p40 is composed of 306 amino acids and contains 10 cysteine residues, whereas the 35 kDa (p35) light chain contains 197 amino acids and 7 cysteine residues. The genes for the two subunits are encoded on separate chromosomes (Brunda and Gately, 1995). Murine IL-12, is structurally similar to the human analogue and shares 70% and 60% amino acid homology with respect to the p40 and p35 subunits. The p35 subunit determines species specificity. While murine IL-12 is fully functional on human T cells, human IL-12 is inactive on murine lymphocytes (Hendrzak and Brunda, 1995). Approximately 100 to 1000 high affinity and 1000-5000 low affinity IL-12 receptors are found per activated NK or T cells. The two receptor chains β1 and β2, are type I transmembrane receptors which have molecular weights of 100 and 130 kDa

respectively and belong to gp130 superfamily of cytokine receptors (Lamont and Adorini, 1996). Signal transduction is mediated through the large cytokine family of Janus kinases (JAK), and signal transducers and activators of transcription 3 (STAT3), STAT4 pathways (Lamont and Adorini, 1996). Mice deficient is STAT4 are unresponsive to IL-12 and have impaired T1 profiles including disrupted NK cell function (Thierfelder, 1996).

The potent cytotoxic immune stimulating effects of IL-12 has made it an ideal cytokine for cancer immunotherapy. IL-12 has been shown to have powerful anti-tumor activity in numerous animal models including carcinomas and melanomas (Trinchieri and Scott, 1994; Brunda and Gately, 1995). Recombinant IL-12 injected systemically or intratumorally has been able to reduce or totally eliminate primary lesions and their metastasis. Moreover, cured animals were shown to have long-term T cell specific memory against tumor re-challenge (Brunda and Gately, 1995). However, serious toxicities have been observed following the systemic delivery of IL-12 in mice and in clinical trials of patients with various tumor types. Daily injections of 1 µg/day of IL-12 for 7 days in non-tumor bearing mice resulted in hepatotoxicity, skeletal muscle degradation, anemia, neutropenia, lymphopenia, and thromocytopenia (Hendrzak and Brunda, 1995). In a Phase I clinical trial, patients with renal cell carcinoma (RCC) reflected similar side effects when treated with a daily bolus injection of IL-12 at 3-1000 ng/kg (Storkus et al., 1998). Of the six patients treated, four had stabilization of the disease. A more recent Phase I

trial involving 40 patients also noted lymphopenia 24 hours after IL-12 injection and this is thought to be a reflection of the *in vivo* activation of lymphocytes with their subsequent margination into tissue (Robertson et al., 1999). However in a Phase II study, 15 of 17 patients had severe toxicity associated with intravenous administration of IL 12 with two mortalities (Lamont and Adorini, 1996;Storkus et al., 1998).

To limit the toxicity of systemic IL-12, while retaining the immune stimulating benefits, numerous groups have devised methods to target IL-12 locally to the tumor environment. This has included administration of autologous fibroblasts transfected with IL-12 genes into the tumors of patients with breast carcinoma (Zitvogel et al., 1995). Other gene therapeutic strategies have involved intramuscular injection of DNA plasmids encoding for both subunits of IL-12 which inhibited metastasis in a B16F10 melanoma in mice (Schultz et al., 1999). Viral vectors expressing IL-12 have been reported by several groups (Zitvogel et al., 1994; Puisieux et al., 1998; Bramson et al., 1996). Bramson and co-workers (1996) delivered an adenovirus deliver expressing IL-12 into a murine breast cancer model and observed significant regressions in tumor growth. Moreover mice that had total tumor regressions demonstrated the presence of CTL against tumor antigen and immunity against tumor re-challenge.

1.8 Interleukin-18

Interleukin-18 (IL-18) is a recently identified cytokine isolated from the serum of mice suffering from septic shock (Okamura et al., 1998). The production of high levels of IFNγ from NK and T cells following lipopolysaccharide (LPS) exposure was observed in these mice and the molecule was originally termed interferon gamma inducing factor (IGIF) (Okamura et al., 1998). Purification and subsequent cloning revealed murine IL-18 to be a 18-19 kDa polypeptide composed of 157 amino acids that could promote IFNγ secretion from activated cultured T cells (Okamura et al., 1995). The gene for IL-18 encodes for 192 amino acid biologically inactive precursor molecule which lacks a conventional signal sequence (Okamura et al., 1995). The precursor cytokine, pro-IL-18, is cleaved at Aspartic $acid_{35}$ by the interleukin 1β converting enzyme (ICE) also known as caspase 1, generating the biologically active mature IL-18 (Ghayur et al., 1997; Gu et al., 1997). Human IL-18 was subsequently cloned and found to be a 193 amino acid pro-IL-18, which is also cleaved by ICE at Aspartic $acid_{35}$ generating the 158 amino acid biologically active molecule (Ushio et al., 1996; Akita et al., 1997). Human and murine IL-18 share 65% amino acid homology, possess no N-linked glycosylation sites and have four free cysteine residues (Okamura et al., 1995; Ushio et al., 1996). Interestingly, IL-18 shares structural, activation and receptor binding homologies to the interleukin-1 family of cytokines (Dinarello et al., 1998; Kohno and Kurimoto, 1998).

The original excitement over IL-18 was due to the ability of the cytokine to induce IFNγ from T cells and NK cells. This biological activity mirrors that of IL-12,

and as such IL-18 is regarded as a T1 type cytokine. IL-18 combined with IL-12 was shown to produce higher levels of IFNγ from CD3 activated T cells or T cell clones than was possible with either cytokine individually (Okamura et al., 1995;Ushio et al., 1996;Kohno et al., 1997). IL-18, but not IL-12, can up regulate the expression of IL-2 from T and NK cells which is thought to be responsible for IL-18's ability to induce T cell proliferation (Ushio et al., 1996;Tomura et al., 1998). Further, human IL-18 can decrease the production of the T2 cytokine IL-10 but has no effect on IL-4 secretion from stimulated T cells (Ushio et al., 1996). In contrast, murine IL-18 cannot augment IL-10 or IL-4 production from stimulated peripheral blood mononuclear cells(PBMC) or from T2 T cell clones (Kohno et al., 1997). Unlike IL-12, IL-18 by itself does not have the capacity to drive naive T cells into development of the T1 phenotype (Robinson et al., 1997). The signal transduction pathways of the two cytokines converge on the promotor region of IFNγ gene resulting in synergy of IFNγ protein expression and enhancing T1 development (Robinson et al., 1997). Signalling of IL-18 initiates from a receptor complex that is known to be composed of the IL-1 receptor-related-protein (IL-1Rrp) and travels via the IL-1 receptor-associated kinase (IRAK) activating nuclear factor κB (Robinson et al., 1997;Kojima et al., 1998;Matsumoto et al., 1997).

As with IL-12, the properties of IL-18 including IFNγ production, T cell and NK cell activation has potential anti-tumor therapeutic benefits. Studies using mice bearing Meth A sarcomas, demonstrated that daily injections of 1 μg recombinant

IL-18 could totally inhibit tumor growth and that mice developed tumor specific immunity (Micallef et al., 1997). This study also demonstrated no toxicity or side effects with IL-18 at the dosages used. Osaki and co-workers(1998), using a similar model found that NK and CD4, but not CD8 cells infiltrated the tumors following IL-18 administration, and that these cells were responsible for tumor regressions. This study, which included IFNγ knockout mice, demonstrated that IL-18 could still retain some anti-tumor effects independent of IFNγ (Osaki et al., 1998). Using an IL-18 gene transfected breast cancer model, Coughlin and colleagues,(1998) demonstrated that IL-18, like IL-12, exhibits anti-angiogenic properties that are mediated through the production of IFNγ and that IFNγ antibodies could abrogate this effect.

1.9 Gene Therapy

The advent of molecular medicine has advanced our understanding of many pathological conditions at the genetic level. Yet even as the human genome is being sequenced and unravelled, the ability to effectively treat many of these conditions remains a challenge. Gene therapy represents a unique therapeutic approach for treating disease that is based on the introduction of a gene into the somatic cells of the patient in the hopes of correcting the defect or modifying the cellular environment. The delivery of therapeutic genes has been attempted using a variety of different methods including, naked DNA injections, liposome mediated

transfer, and viral based systems. Each method has potential advantages as well as drawbacks.

Adenoviruses are at the forefront in many gene therapy applications, including the *in vivo* therapy of cancer. Replication deficient adenoviruses have numerous advantages for gene delivery, including: the ability to infect both replicating and non-replicating cells, high level transient gene expression, no integration into the host genome, no association with human malignancy and ease of production of high titre virus (Bramson et al., 1995). A major limitation of the adenovirus system is that multiple administrations would be required for the treatment of disease like cystic fibrosis, due to the transient nature of gene expression (Friedmann, 1997). Of greater significance, the host cellular and humoral immune response that develops after the initial vector administration precludes re-administration of the adenovirus. (Douglas and Curiel, 1997). However, for active immunization against cancer, the transient expression of a therapeutic cytokine from the adenovirus may in fact be beneficial as prolonged expression and immune activation may lead to unwanted severe systemic side effects.

1.9.1 Adenovirus

Adenoviruses are nonenveloped, linear double stranded DNA viruses in which the 36 kb genome is contained within an icosahedral capsid composed of

fiber proteins, 12 penton bases and hexon proteins (Douglas and Curiel, 1997). The adenovirus has a lytic life cycle and is taken up by cells through an unknown receptor that binds the knob at the end of the fiber protein. Secondary binding and internalization is mediated by the integrins $\alpha_v\beta_3$ and $\alpha_v\beta_5$. Once inside the cell, the capsid protein is dissolved inside an endosome and the viral DNA migrates to the nucleus where expression of the viral genes occurs without integration into the host chromosome (Douglas and Curiel, 1997). The first genes expressed before DNA replication occurs are the early genes, E1a, E1b, E2, E3 and E4 which encode mainly for regulatory proteins required for DNA replication (Hitt et al., 1998). The late genes code for the structural proteins that make up the viral capsid.

Of the more than 40 human adenoviral serotypes, the types 2 (Ad2) and 5 (Ad5) are the most commonly used as gene therapy vectors. Recombinant Ad5 vectors have deletions of the E1 region, rendering the virus replication deficient. When combined with a deletion of the E3 region, which is non-essential for virus growth, the first generation adenovirus vector can accommodate approximately 8 kb of exogenous DNA (Bett et al., 1994). The generation of the recombinant adenovirus occurs in transformed 293 human kidney embryonic cells that express the E1 protein in trans (Graham et al., 1977). Homologous recombination, following cotransfection in the 293 cell between a shuttle plasmid, composed of the left end of the viral genome and a rescue plasmid composed of the circularized viral genome missing the E1 and E3 regions, results in the formation of a functional virus

(Bett et al., 1994; Hitt et al., 1998). Therapeutic genes of interest can be cloned into either the E1 or E3 regions under the control of any promoter, including the highly efficient cytomegalovirus promoter.

The success of adenovirus mediated gene therapy for the treatment of cancer has been well documented by our group and as well as by others. Using a mouse mammary adenocarcinoma model, Addison and colleagues (1995) demonstrated that the direct injection of a tumor with Ad-5 expressing human IL-2 lead to a significant delay in the tumor growth, and complete regressions in many instances. This study also showed that cured mice were resistant to tumor re-challenge suggesting that a specific anti-tumor immune response had been generated. Bramson and co-workers (1996) showed that the direct injection of an adenovirus expressing murine IL-12 could also regress tumors and elicit a strong anti-tumor CTL response. Whereas these successes demonstrated the effectiveness in using adenoviral vectors expressing cytokines in the generation of a specific CTL mediated anti-tumor response, Emtage and colleagues (1998), described the of co-expression of IL-2 with the B7-1 costimulatory molecule from the same adenovirus in their tumor model (Emtage et al., 1998). Adenovirus has also been used to deliver tumor antigens directly into cultured dendritic cells. Bone marrow derived dendritic cells transduced with an adenovirus expressing a viral tumor antigen, were shown to completely vaccinate mice against the development of tumor growth while at the same time generating no toxic side effects (Wan et al.,

1997).

1.10 Objectives

Based on the principles of anti-angiogenesis and immunotherapies, the goal of this thesis work was to examine the effectiveness of such treatments in a murine adenocarcinoma model. The first objective was to construct a type 5 adenovirus which expressed murine angiostatin. This virus was characterized *in vivo* using a matrigel angiogenesis assay in mice. The adenovirus, which is tropic for the lung epithelium was delivered into the lungs of mice bearing breast tumor nodules to demonstrate the effectiveness of such treatment in reducing metastatic burden. The vector was also directly injected into the tumor to see if long term expression could regress tumor growth by inhibiting angiogenesis.

While the use of anti-angiogenic therapy is promising, in some circumstances it would require that the patient be maintained on a long term treatment regime so that relapse does not occur. A second line of attack involving immunotherapy would ensure total vaccination against tumor reoccurrence through a CTL mediated response. The injection of adenovirus expressing a cytokine has been shown to be beneficial in inducing this type of a treatment. However, the ability of the immune system to overcome a larger tumor burden may be limited by factors including the immunosuppresive nature of the tumor as well as the immunocompetance of the patient.

The second objective of this work was to combine the effectiveness of Ad-angiostatin with the potent immunotherapeutic properties of an adenovirus expressing IL-12 in the mammary breast tumor model. As stated above, the rationale for such therapy is to effectively shrink the tumor mass through anti-angiogenic mechanisms, with the concomitant tumor specific immunity.

The third objective of this study was to construct an adenovirus expressing the newly discovered T1 type cytokine IL-18. This novel cytokine was of interest because of the properties it shares with IL-12, namely the induction of IFNγ expression from activated T cells. A comparison of the anti-tumorgenic features of IL-18 and IL-12 in the tumor model was performed alone or in combination with angiostatin.

CHAPTER 2-EXPERIMENTAL PROCEDURES

2.0 Materials

Oligonucleotides were synthesized by the Institute for Molecular Biology and Biotechnology (MOBIX), McMaster University. All plasmids described containing cDNA PCR products for angiostatin, mIL-18 and hIL-18 were sequenced at MOBIX. Six to eight week old C57BL/6 and FVB/n female mice were obtained from Charles River (Troy, NY) and housed in a specific pathogen free environment until use

The bacterial expression plasmid pET32b and the competent host *Escherichia coli* Ad494 was purchased from Novagen (Madison, WI). Competent DH5α E. coli cells used for subcloning were purchased from Gibco BRL (Gaithersburg, MD). The shuttle plasmid pACCMV containing the human CMV promotor was obtained from Dr. Bruce Beutler, University of Texas Southwestern (Dallas, TX). The rescue plasmid pJM17 was provided by Dr. Frank Graham, McMaster University.

Adenoviruses were propagated in 293 (Ad5 E1-transformed) human embryonic kidney cells maintained in Eagle's medium (MEM) F-11 supplemented with 10% fetal bovine serum (FBS) and 100 µg/ml penicillin and 100 U/ml streptomycin (Hitt et al., 1998). Viruses were purified by double cesium chloride gradient centrifugation following growth in suspension 293 N3S cells, using Joklik's

medium and 10% FBS (Hitt et al., 1998). A549 human lung carcinoma cells (ATCC# CCL-185) were maintained in MEM with 10% FBS. Polyoma middle T tumor explants were grown as single cell monolayer in complete MEM F-11 (Guy et al., 1992). Human umbilical cord endothelial cells (HUVEC) were isolated from fresh umbilical cords by gentle mechanical disruption with 2% collagenase in Hanks buffered saline. HUVECs were maintained in monolayer on culture dishes pre-coated with 2% collagen in PBS, M199 media supplemented with 10 ng/ml endothelial cell growth factor (ICN, Montreal, P.Q.) and 10% FBS (Battista and Soderland, 1998).

All cell culture media and reagents including: αMEM, αMEM F-11, M-199, RPMI, HANKS, DMEM, FBS and penicillin/streptomycin were products of Gibco BRL. Basic fibroblast growth factor (bFGF) was purchased from Gibco BRL. Endothelial cell growth factor was from ICN Chemicals (Montreal, P.Q). Tissue culture plasticware was bought from Corning (Corning, NY).

Restriction enzymes, as well as Vent DNA polymerase were obtained from New England Biolabs (Beverly, MA). Matrigel was purchased from Becton Dickinson Labware, (Bedford, MA) and was stored at -20°C until use. Construction and characterization of the murine IL12.1 containing the p35 subunit in E1 and the p40 in E3 has been described earlier (Bramson et al., 1996). 293 cell culture supernatant containing human IL-12 was obtained from Mary Hitt (McMaster University). A cDNA probe for human interleukin-1 converting enzyme (ICE) was

obtained from Dr. Brian Leber (McMaster, University). Polyclonal goat anti mouse antibodies to murine IL-18 (mIL-18) and mouse anti-human IL-18 (hIL-18) monoclonal antibodies were purchased from R&D Systems (Minneapolis,MN). Donkey anti goat alkaline phosphatase conjugated secondary polyclonal antibody was purchased from Sigma (St. Louis, Mo). A goat anti-mouse alkaline phosphatase conjugated polyclonal antibody was purchased from Biorad (Mississauga, ON). Alkaline phosphatase substrate, NBT/BCIP was purchased from Biorad. ConA was purchased from Sigma. All DNA manipulations were carried out using standard cloning techniques (Sambrook et al., 1989)

2.1.0 RNA extraction and Reverse Transcription-PCR (RT-PCR) of Murine Angiostatin

Total cellular RNA was extracted from quick frozen livers of C57BL/6 mice using Trizol reagent (Gibco, Gaithersburg, MD). Reverse transcription (RT) reactions were carried out with 0.5,1.0, 3.0, and 5.0 pg of total RNA in a 20 µl final volume using oligo dT primers supplied with the SuperScript RT reaction kit (Gibco). RNA and oligo dT primers were heated to 70°C for 10 min and then placed on ice. 10X RT buffer, $MgCl_2$ dNTPs and DTT were added to the reaction which was subsequently heated to 42°C for 5 min after which 1 µl of Superscript reverse transcriptase enzyme was added and the reaction incubated for another 50

min. The reaction was stopped by heating to 70°C for 10 min and then treated with RNase for 20 min at 37°C.

PCR reactions were carried out in a Perkin Elmer 9600 thermocycler in a final volume of 100 µl using Vent polymerase (NEB, Mississsauga, ON). The angiostatin cDNA is based on the corresponding amino acids 1-32 and 98-458 of the native murine plasminogen (Degen et al., 1990) and the protein sequence of angiostatin derived by enzyme proteolysis (Wu et al., 1997; O'Reilly et al., 1994a). Two PCR reactions were carried out, one to form the sequence for amino acids 1-32 which also contained the native plasminogen signal sequence and a second reaction which adds the bioactive four kringle region of angiostatin. The following primer pairs were used in the first PCR reaction: forward primer, (A) 5'TGGGGAATTCTTGTTGGCCAGTCCCAACATGGACCATAAGGAAT3', reverse primer (B) 5'ACCACTCGAGAAGAAGCCCCTTGTGTGCTTATGTAGCCATCCAT3', which contained an EcoR1 and Xho1 restriction enzyme site respectively. The second PCR reaction used the following primer pairs: (C) 5'CTTCTTCTCGAGTGTATCTGTCAGAATGTAAG3', reverse primer, (D) 5'CCGAAGCTTTTATCATCCTGTCTCTGAGCTCCGCTTCAG3' which contained a stop codon. Primers C and D contained Xho1 and HindIII restriction enzyme sites respectively. Cycling conditions for the first section were: denaturation at 94°C, 3 min; 94°C, 1 min; annealing at 55°C, 1 min; extension at 72°C , 1 min for 35 cycles. The cycling conditions for the second segment was identical, except that the

extension time was increased to 1 minute and 30 seconds. The PCR fragments were run on 1% agarose gels, excised, and isolated using QIAex II gel purification (Qiagen, Chatsworth, CA). The PCR fragments were restriction enzyme digested, re-purified, and ligated into the EcoR1 and HindIII polylinker region of the adenovirus shuttle plasmid pACCMV forming a 1170 bp open reading frame which codes for murine angiostatin. The shuttle plasmid pACCMV-Angiostatin was cotransfected into 293 cells with pJM17 using calcium phosphate coprecipitation (Ghosh-Choudhury et al., 1986). Ad-Angiostatin was isolated from a single plaque, expanded in 293 cells and purified by cesium chloride centrifugation (Ghosh-Choudhury et al., 1986;Hitt et al., 1998).

2.1.1 Northern Blotting

Total RNA was isolated from 293 and A549 cells infected with Ad-dl70-3 or Ad-Angiostatin at a MOI of 100 using Trizol (Gibco). 20 µg of RNA was loaded per lane, and electrophoresed through a 1% agarose formaldehyde denaturing gel at 20V. The RNA was transferred overnight by capillary action using 10X SSC to Nytran membranes (ICN). Membranes were hybridized overnight at 55°C with α^{32} P-dCTP with the random primed (Pharmacia, Upsula, Sweden) 662 bp mouse angiostatin cDNA PCR product.

2.1.2 Western Blotting

Supernatants from HUVEC cells infected 5 days earlier withAd-Angiostatin or Ad-dl70-3 at MOI 100, were incubated overnight at 4°C with 250 µl of lysine-Sepharose (Pharmacia, Uppsula, Sweden) per ml of supernatant. The slurry was collected by centrifugation and washed with 50 mM sodium phosphate buffer, pH 7.4. A 20 µl aliquot was loaded onto a 15% SDS-PAGE gel under non-reducing conditions, and transferred to Immobulon-P membranes (Millipore, Mississauga, ON). The membranes were probed with a 1/500 diluted chicken-anti-rabbit plasminogen IgY antibody (kind gift by Dr. Mark Hatton, McMaster University, Hamilton, ON), followed by a secondary rabbit anti-chicken alkaline phosphatase conjugated antibody (Zymed, San Francisco, CA). A positive control, partially purified rabbit angiostatin derived from bovine elastase digested rabbit plasminogen was used as a positive control (kind gift by Dr. Mark Hatton).

2.1.3 *In vivo* Matrigel assay

Matrigel at 4°C was mixed with 100 ng/ml bFGF (Gibco) alone or in combination with Ad-dl70-3 (1 X 10^9 pfu), Ad-Angiostatin (1 X 10^9 pfu) or recombinant murine IL-18 (1µg) in a final volume of 0.5 ml. The matrigel mixture was then injected s.q. into the abdominal midline of C57BL/6 mice, where it polymerized to form a plug. The plug was removed on day seven, fixed in Sodium

phosphate (0.075M, pH 7.4-7.6) buffered 4% formaldehyde buffered formalin solution (Fisher Chemicals, Ottawa) for 24 hours and then embedded in paraffin. All tissues were sectioned (5 µm thickness), mounted onto slides and stained with Masson's trichrome using standard techniques. Total cell invasion was determined by image analysis of stained sections using a Sony CCD camera and Vidas (Kontron,UK) software. The amount of cell migration was determined by calculating the percent area occupied by the endothelial cells which stained red, versus the total area of the matrigel which stained blue/green.

2.1.4 *In vitro* Biological Assay

120,000 HUVEC cells per well were plated in 6 well plates pre-coated with 2% gelatin in 3 ml of complete M199 media. Cells were infected with Ad-dl70, or Ad-Angiostatin at a MOI of 100 and were allowed to proliferate for seven days. Two ml of fresh complete M-199 media was added every other day to maintain cell viability. On day seven, the cells were removed with 0.5X trypsin, and total cells including those floating in the media were counted using trypan blue (Gibco) exclusion staining to determine total numbers and viability.

2.1.5 Electron Microscopy

Portions of paraffin embedded matrigel plugs from the bFGF and bFGF plus

Ad-Angiostatin treatments were extricated. The samples chosen were based on regions of the trichrome stained sections that exhibited cellular morphological changes indicating endothelial infiltration, capillary development, or apoptosis.

The matrigel was removed from the paraffin by heating and then dissolving the sample in xylene. This was followed by re-hydration using 50% ethanol/xylene, 70% ethanol/xylene, 100% ethanol, 90% ethanol and finally 70% ethanol. The sample was then placed in 0.1M sodium cacodylate (NaCac) pH 7.4, followed by fixation in 2% glutaraldehyde buffered in 0.1M NaCac, pH7.4. All procedures were carried out at room temperature. Treatment with 1% OsO_4 in 0.1M NaCac at 4°C for one hour ensued. The samples were dehydrated using a gradient of ethanol washes ranging from 50% to 100%, followed by propylene oxide treatment. The samples were then embedded in 100% Spurr's Resin, heated overnight at 65°C and sectioned to a thickness of 1 µm. Sections were placed on copper grids and examined using a JEOL 1200 EX Biosystem electron microscope at 80 kV.

2.1.6 Expression of Angiostatin in the Lungs and Effects on Metastatic Murine Breast Cancer

Ad-Angiostatin or control virus Ad-dl70-3 were introduced into the lungs of FVB/n mice by intranasal delivery (i.n.). Briefly, 1 X 10^9 pfu virus in a total volume of 30 µl PBS was inserted into the nostrils of anaesthetized mice in 15 µl aliquots

using a p10 Pipetteman and tip. Seven days post infection, the lungs were removed, and bronchial alveolar lavage (BAL) fluid was obtained. The anaesthetized mice were sacrificed by cutting the abdominal aorta and the entire lung with the attached trachea was removed from the chest cavity. A small diameter section of Tygon tubing attached to a 26 gauge needle and 1 ml syringe was inserted into the lungs through the trachea. BAL fluid was collected from the the lungs by twice filling with 150 µl of PBS, which was then aspirated. Lungs were fixed for 24 hours in 10% neutral buffered formalin and paraffin embedded. 5 µm sections were Hematoxylin and Eosin (H&E) stained using standard techniques.

300,000 PyMid-T murine breast adenocarcinoma cells in a volume of 200µl PBS, were injected as a single cell suspension i.v into the tail vein of FVB/n mice. Sixteen days post tumor injection, Ad-Angiostatin, and Ad-dl70-3 (1×10^9 pfu) were delivered i.n.. Lungs were removed on day 24, weighed, and two representative lungs from each treatment group were lavaged. The lungs were then formalin fixed for 24 hours and the total number of surface lung metastases were counted under a stereo microscope on six times power. Following paraffin embedding, 5 µm sections were cut and H&E stained to observe tumor vasculature and lung pathology.

2.1.7 Polyoma Middle T Tumor Studies

Tumor bearing PyMid T transgenic mouse strain MT640, which undergoes

the transformation of the mammary epithelium were sacrificed. The tumors were removed and processed to a single cell suspension with mechanical disruption in the presence of 25 mg collagenase (Gibco) carried out in phosphate buffered saline (PBS). The cells were then placed in complete F-11 media and cultured for 48 hours.

The PyMidT tumor cells were harvested, and 5×10^5 cells were injected s.c. in a volume of 200 µl PBS into the right flank of a syngeneic female FVB/n host. Approximately 18-21 days later a palpable tumor (approximately 150 mm^3) had developed in all mice that were injected. The tumors were injected with control virus Ad-dl70-3 (1×10^9 pfu/ml), Ad-Angiostatin (5×10^8 pfu/ml), Ad-IL12.1 (5×10^8 pfu/ml), recombinant murine IL-18 (1 µg every two days for 1 week), combination Ad-Angiostatin plus Ad-IL12.1 ($2 \times 5 \times 10^8$ pfu/ml) and combination Ad-Angiostatin (5×10^8 pfu/ml) plus recombinant murine IL-18. Total viral load was made up to 1×10^9 pfu/ml with the addition Ad-dl70-3 to compensate the effect of the anti-adenoviral immune response and the total volume of the injected was 50 µl.

Tumors were measured in millimetres (mm) using vernier calipers at the time of virus injection and at weekly intervals. Tumor volumes were calculated from the longest diameter and average width, assuming a prolate spheroid (Addison et al., 1995). Those mice which underwent a total tumor regression on the right flank were re-challenged with a similar tumor dose in the left flank eight weeks later. Failure of this re-challenge to grow was deemed a total cure. Mice were sacrificed

when any single or two measurements of a tumor exceeded 20 mm.

2.1.8 CTL assay

A single cell suspension from the spleens of mice that were cured by co-injection of angiostatin and IL-12 were removed aseptically and homogenized into a single cell suspension. The splenocytes were separated from red blood cells using a Ficoll gradient (Pharmacia, Upsula, Sweden) and co-cultured with irradiated (5000 rad) 516MT3 cells expressing the PyMidT antigen, at an effector to target of 50:1, and co-cultured for five days. Five days later, the activated cytotoxic lymphocytes were harvested and tested for activity against ^{51}Cr (100 µCi) labelled 516MT3 or control PTO516 cells. The assay was carried out in a volume of 50 µl using a 250 µl V bottomed 96 well plates at effector to target ratios of 90:1, 30:1 and 10:1 for three hours. Maximum release and spontaneous release was determined by adding 1N HCl or media alone to the target cells. The supernatants were placed in a gamma counter, and the percent specific lysis was calculated as follows: 100 X (experimental cpm-spontaneous release cpm)/(maximal cpm-spontaneous cpm)

2.1.9 Anti CD31 Immunostaining of Tumor Vasculature

Palpable PyMidT tumors in the right flanks of FVB/n mice were treated with

adenovirus in an identical manner as described in section 2.1.7. One week following vector administration, the tumors were removed, embedded in OCT compound, and frozen rapidly in isopentane, which was pre-cooled in liquid nitrogen to -180 °C. The samples were wrapped in aluminum foil and stored at -70 °C to prevent thawing.

The frozen tumors were cryosectioned at -20 °C to 5 µm, placed on glass slides, and were allowed at air dry overnight. The slides were fixed in cold acetone for 10 minutes, air dried for 30 minutes, and were treated with 1% H_2O_2 for 10 minutes at room temperature to remove endogenous peroxidases. Slides were rinsed three times for 5 minutes with PBS, and nonspecific binding was blocked using Powerblock (Biogenex, San Ramon, CA) for 6 minutes, followed by another PBS wash cycle. The sections were then incubated with anti-CD31 antibody (Pharmingen, San Diego, CA) at a 1:800 dilution in antibody diluting fluid (Dako, Sweden) for 1 hour. Following three washes in PBS, the secondary biotinylated anti-rat IgG (Vector Laboratories, Burlington, CA) was added at a 1:400 dilution for 1 hour. The slides were washed in PBS, and incubated in a 1:60 dilution of ABC, aviden-biotinylated enzyme complex (Vector Laboratories) for 1 hour followed again by three washes with PBS. The substrate chromogen AEC (3-amino-9-ethylcarbazole)(Vector Laboratories) was added to the sections for 30 minutes. The sections were counterstained in 50% Mayer's hemotoxylin, and a cover slip was added using glycerin gelatin.

2.1.10 Anti-CD31 Vessel Quantification

Vessel quantification of CD31 stained tumor sections was carried out using a Leica Laborlux microscope equipped with a Sony CCD digital camera. Five medium power fields (200X) were examined per section in a blinded manner. Vessels were counted using Northern Exposure V2.9 imaging software (Empix Imagine Inc).

2.2.0 Cloning and Production of Adenovirus Expressing Murine or Human IL-18

Total RNA was extracted from the livers of C57BL/6 mice using trizol. RT-reactions were carried out under identical conditions as described above. PCR was carried out in a Perkin Elmer 9600 thermocycler in 100 µl final volume using Vent polymerase (NEB, Mississauga, ON). The following primer pairs were used: the forward primer contained a nested EcoR1 site, (A) 5'GGGGAATTCGCCTCAAACCTTCCAAATCACTTCCTCUG 3', the reverse primer contained a nested Xba1 site, (B) 5'CCCTCTAGAGCATGTGTGCTAATCATCTTTCTGG3', which produced a 662 bp product. Cycling conditions were denaturation at 94°C, 1 min; annealing at 55°C 1 min; extension at 72°C, 1 min for 35 cycles.

Human total RNA was extracted from confluent HepG2 cells using the

RNeasy kit (Qiagen, Chatsworth, CA). Reverse transcription was carried out as described above. PCR procedures were identical to those used above with the exception of the primer pairs: forward primer, (C) 5' GGGGAATTCGCTTCCTCTCGCAACAAACTATTTGTCGCA 3'reverse primer, (D) 5'GGGTCTAGATTACAGGCCTGAGCCACTGCCCCCGGCATG3', which produced a 663 bp fragment. Primers C and D carried nested EcoR1 and Xba1 sites respectively.

PCR products were separated by electrophoresis on a 1% agarose gel. Bands were excised and purified using QIAex II gel extraction (Qiagen). Primers for the murine and human IL-18 homologues were based on sequences from the NCBI, accession no. D49949 and D49950 respectively.

The cDNA for both murine and human IL-18 were ligated into the Eco R1/Xba1 site in the polylinker region of the shuttle plasmid pACCMV using T4 ligase (New England Biolabs) to create pACCMV-mIL-18 or pACCMV-hIL-18. Plasmids were transformed into *E. coli* DH5α competent cells (Gibco) using protocols supplied by the manufacturer and plated onto LB agar plates containing 100 µg/ml ampicillin. DH5α transformed cells were grown in large scale in 1 L volumes under conditions listed above. The plasmids were isolated using alkaline lysis and cesium chloride density gradient. The rescue plasmid pJM-17 was grown and purified in an identical manner. The shuttle plasmids and rescue plasmid were cotransfected into 293 cells using identical procedures described earlier. Ad mIL-

18 and Ad hIL-18 were isolated from single plaques, expanded in 293 cells and purified by cesium chloride centrifugation.

Total RNA was extracted from A549 or 293 cells infected for 48 hours with purified Ad-mIL-18 or Ad-hIL-18 at MOI of 100 using the Trizol method. Northern blotting using probes generated from the full length mIL-18 or hIL-18 cDNA PCR products was carried out as described above. IL-18 protein production was characterized from infected cell pellets and culture supernatants by 15% SDS-PAGE under denaturing and reducing conditions at 200V. Gels were transferred to Immobulon P membranes, blocked and probed with goat anti-murine IL-18 polyclonal antibody or mouse anti human IL-18 monoclonal antibody. Membranes were developed using the alkaline phosphatase conjugated secondary antibodies listed above and BCIP/NBT substrates.

2.2.1 Production of Escherichia coli Derived Recombinant Murine IL-18

Biologically active IL-18 is produced in a cell when the enzyme ICE, cleaves the pro-IL-18 (inactive) removing the initial 35 amino acids. PCR of the coding region for only the mature bioactive murine IL-18 required for the generation of the recombinant protein was carried out using nested primers internal to the original full length PCR product. In addition a Nco1 site and a Xho1 were placed into the

forward and reverse primers respectively. The primer pairs were as follows: forward primer, (E) 5'GGGGCCATGGGGMCTTTGGCCGACUCACTGTACA3', reverse primer, (F) 5'GGGCTCGAGCTAACTTTGATGTMGTTAGTGAGAGTGMCAUAC3[1]. Murine IL-18 cDNA from above was used as template generating a 493bp fragment under identical PCR conditions listed previously.

The cDNA encoding the mature mIL-18 protein was ligated into the Nco1 - Xho1 site of the pET32b (Novagen, Madison, WI) expression vector under the control of the *T7lac* promoter and transformed into *E. coli* BL2I (DE3) (Novagen).

E. coli BL2I (DE3) carrying pET32b-mIL-18 was grown in LB media supplemented with 100 µg/ml of ampicillin to an $O.D_{600}$ of 1.0. Cells were induced with 1 mM isopropyl-1-thio-D-galactopyranoside (IPTG) (Gibco) and grown for an additional three hours. The cells were harvested by centrifugation at 5 000 x g, and frozen at -70°C overnight.

The cells were thawed in 10 ml of binding buffer (5 mM imidazole, 0.5 M NaCl, 2O mM Tris-HCl), plus 1.0% Triton X100,1 mg of lysozyme, and 1 mM PMSF (Sigma, St.Louis, MO) pH 7.9. Cells were lysed by sonification using five, one minute bursts at 100W, and the cellular debris was removed by centrifugation at 12000 x g.

The recombinant mIL-18 was separated from the other cytoplasmic proteins using a Ni^{2+} charged Sepharose chelating column (Pharmacia, Upsala Sweden) which has affinity for a 6 histidine residue repeat in the fusion protein.

Recombinant protein was loaded onto the column in binding buffer. Contaminating proteins were washed from the column using 10 bed volumes of wash buffer (60 mM imidazole, 0.5 M NaCl, 20 mM Tris-HCl). The mIL-18 was eluted in 3 bed volumes of elution buffer (1 M imidazole, 0.25 M NaCl, 10 mM Tris-HCl). All fractions were collected and analysed by denaturing 15% SDS-PAGE.(Laemmli, 1970) The elution fraction containing the pure recombinant mIL-18 was dialysed against 10 mM PBS and subsequently lyophilized.

2.2.2 *In vitro* IL-18 bioassay

The spleens from C57BL/6 mice were removed, and minced in Hanks buffered saline (HBS) pH 7.2. Splenocytes were collected by centrifugation at 1000 x g, and erythrocytes were disrupted by osmotic shock using sterile deionized water. The cells were washed twice in complete RPMI media, placed in T-75 tissue culture flasks and incubated in complete RPMI media two hours to remove adherant monocytes and macrophages. Non-adherent cells (mainly T and B cells), were collected again by centrifugation, washed, and counted using trypan blue dye to determine viability.

3×10^5, Con A stimulated (1µg/ml) splenocytes were added to 96 well tissue culture plates in a total volume of 100 µl of complete RPMI media. To one series of wells, 100, 200 and 1000 ng/ml recombinant mIL-18 was added. A parallel set of wells containing 10, 50 and 100 µl of conditioned A549 culture supernatant which

had been infected with Ad-mIL-18 was added to a similar number of cells. To a third series of wells, 50 and 100 µl of Ad mIL-12.1, conditioned A549 media was also added as a positive control. Ad-dl70-3 infected A549 conditioned media, and Con A stimulated splenocytes alone were used to measure background production of IFNγ. Viral supernatants were exposed to U.V light for 15 minutes before being added to cells. The final volume in each 96 cell plate was adjusted to 250 µl with complete RPMI. The plates were then incubated for 48 h after which cell free culture supernatants were harvested and assayed for murine IFNγ production by ELISA (R&D Systems, Minneapolis,MN).

The bioassay for the Ad-hIL-18 was carried out using the principles from the murine assay, with the exception of some changes. Instead of using murine spleenocytes, peripheral blood mononuclear cells (PBMC) were isolated from my blood. Blood was extracted using venous puncture and collected into EDTA tubes. Mononuclear cells were separated from red blood cells using a Ficoll gradient. Blood was layered onto Ficoll and centrifuged at 1200 x g to separate the blood cells. The PBMC cells were washed three times in PBS and placed in T-75 flasks containing complete RPMI media to remove adherent cells. 3×10^5 cells (mainly T and B cells) stimulated with Con A were added to 96 well plates in volume of 100 µl RPMI. 10, 50 and 100 µl volumes of conditioned A549 Ad-hIL-18 or Ad-hIL12 infected supernatants were added to wells. Control virus and Con A stimulated cells alone were used to measure background IFNγ. The cells were incubated for

48 hours, and the cell free culture supernatants were measured for human IFNγ production by ELISA (Amersham, Mississauga, ON).

CHAPTER 3-CHARACTERIZATION OF AD-ANGIOSTATIN

3.0 RNA Expression and Protein Production From Ad-Angiostatin

The homologous recombination between the shuttle plasmid pACCMV, carrying the open reading frame for murine angiostatin, and the rescue plasmid pJM17 generated the adenovirus, Ad-Angiostatin (Figure 1). Northern blot analysis of RNA from 293 and A549 cells infected with Ad-Angiostatin revealed a single band at approximately 1.2 kb, consistent with the expected mRNA message of murine angiostatin cDNA [Figure 2, (Lane 2,3)]. No angiostatin mRNA could be found in the mock infected A549 cells (Lane 1).

Angiostatin protein production from HUVEC cells infected with Ad-Angiostatin at MOI 100 is shown in figure 3. Cell culture supernatants were harvested 5 days after infection and mixed with lysine- Sepharose to concentrate angiostatin from the media. A large single band is present in lane 3 that has an approximate molecular weight of 50 kDa. This single band may represent two angiostatin isoforms mixed together, as the unconcentrated culture supernatant (Lane 2) gives rise to two distinct bands between 50 and 60 kDa. This doublet may indicate differences in glycosylation. The chicken anti-rabbit plasminogen IgY antibody detected rabbit angiostatin (Lane 1), derived from the proteolytic digestion of rabbit plasminogen, as well as plasminogen from the culture media at 90 kDa.

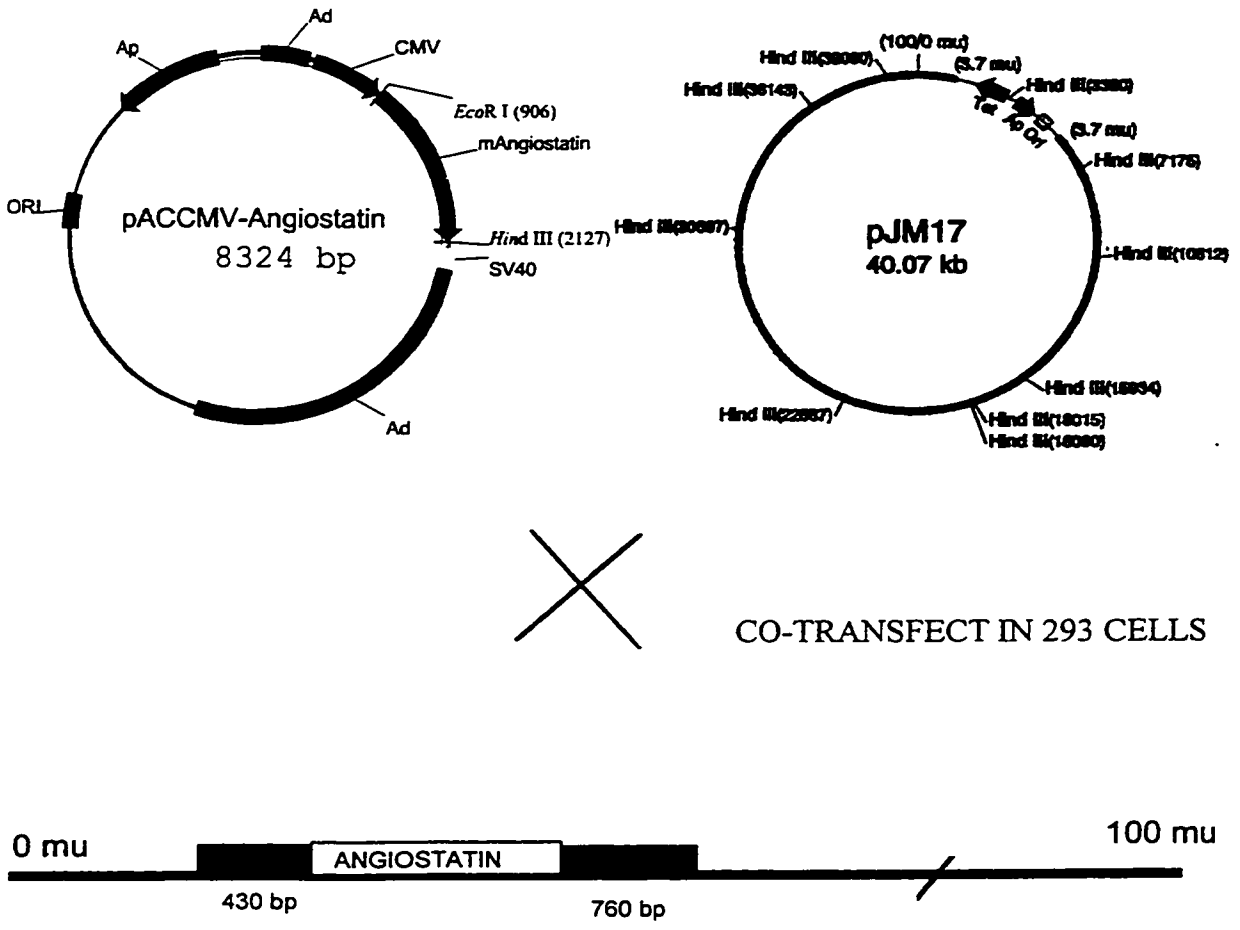

Figure 1. Construction of Ad-Angiostatin. The cDNA for murine angiostatin was ligated into the EcoRI and HindIII sites of the shuttle plasmid pACCMV under the control of the CMV promotor. Co-transfection of 293 cells with pACCMV-Angiostatin and pJM17 generated the recombinant virus.

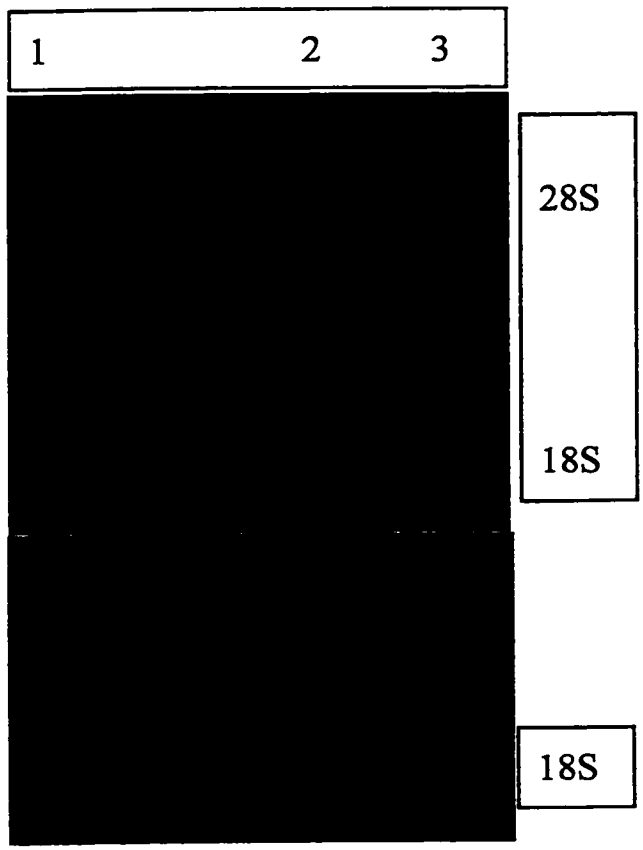

Figure 2. Murine angiostatin expression from Ad-Angiostatin infected 293 and A549 cells. Total RNA, 20 µg per lane was loaded onto a 1% agarose denaturing gel (18S and 28S ribosomal RNA evident), transferred to Nytran membranes and hybridized to ^{32}P labelled murine angiostatin cDNA. No expression of angiostatin was observed from Ad-dl70-3 infected A549 cells (Lane1). Infection of 293 cells with crude viral culture supernatant containing Ad-Angiostatin (Lane 2), or A549 cells at MOI 100 banded virus (Lane 3), resulted in a message of approximately 1.2 kb consistent with the expected size of the angiostatin message.

Figure 3. Western blot of HUVEC culture supernatants infected at MOI 100 with Ad-Angiostatin or control virus Ad-dl70-3. Culture supernatants were harvested five days post infection. A 20 µl aliquot of supernatant was run per lane under non-reducing conditions on a 15% SDS PAGE denaturing gel and transferred to Immobulon-P membranes. The membrane was blotted with 1/500 chicken (IgY) anti-rabbit plasminogen antibody followed by a goat anti-chicken alkaline phosphatase conjugated secondary antibody. Rabbit angiostatin derived from elastase digested rabbit plasminogen (Lane 1); culture supernatant from Ad-Angiostatin infected HUVEC, arrows indicate bands in the range of 50 to 57 kDa thought to be different glycoforms of angiostatin (Lane 2); lysine-Sepharose concentrated supernatant from Ad-Angiostatin infected HUVEC, arrow indicates large angiostatin band at approximately 42 kDa (Lane 3) and; lysine-Sepharose concentrated supernatant from control Ad-dl70-3 infected HUVEC (Lane 4). Prestained molecular weight markers are in kDa and are representative (Gibco).

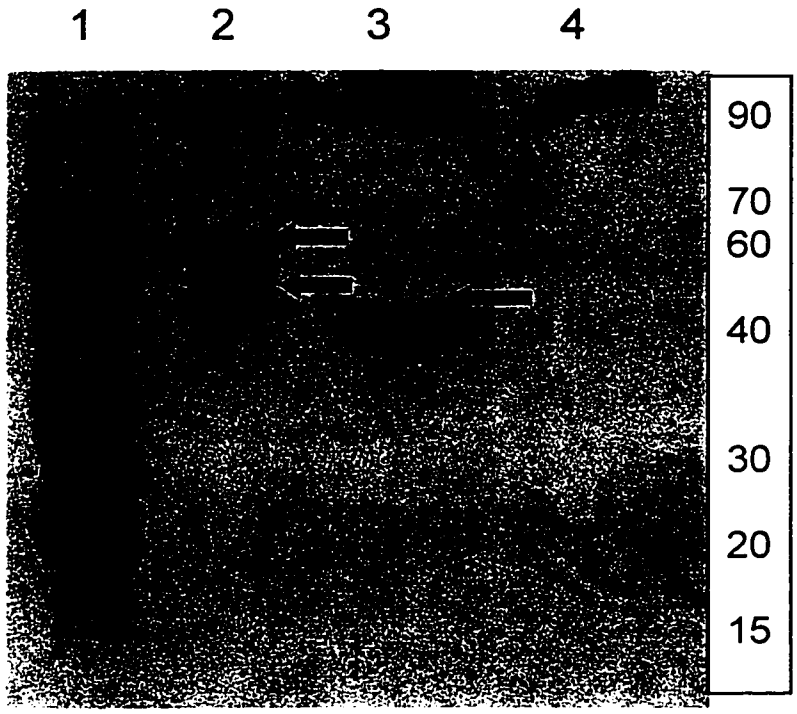
1
2
3
4
90
70
60
40
30
20
15

However, no bands were detected in the 50-60 kDa range in the mock transfected (Lanes 4) sample indicating that the bands appearing in the Ad-Angiostatin lanes were not simply the result of degradation of serum-derived plasminogen.

3.1 Biological activity *in vivo*

Matrigel, an extracellular matrix preparation from Englebreth-Holm-Swarm (EHS) murine sarcoma, is a liquid at 4°C but solidifies at 37°C (Baatout, 1997). This solid matrix when combined with angiogenic factors such as bFGF initiates endothelial cell migration and capillary tube formation into the matrix and is an excellent assay for angiogenesis studies *in vivo* (Jain et al., 1997;Baatout, 1997).

To assess the biological activity of angiostatin derived from the adenoviral vector, mice were injected s.q. with matrigel alone, matrigel mixed with bFGF (100 ng/ml), or matrigel plus bFGF plus control virus Ad-dl70-3 or Ad-Angiostatin (1 X 10^9 pfu).

Histological sections of the matrigel plugs stained with Masson's trichrome are shown in figure 4. Seven days post-infection, the matrigel alone revealed only a few endothelial cells invading from the tissue into the edge of the matrigel in the absence of any angiogenic factor (Figure 4, panel 1). In contrast, the addition of bFGF to the matrigel caused a large increase in endothelial cell infiltration, and the development of capillary tubes containing red blood cells is evident (Figure 4, panels 2-4). Morphologically, the endothelial cells appear long and tapered with

Figure 4. Photomicrographs of Masson's trichrome stained sections of matrigel plugs demonstrating *in vivo* neovascularization seven days post implantation into the abdominal midline of C57BL/6 mice.

Panel

1-No endothelial cell invasion is evident in the matrigel alone.

2-4-The addition of 100 ng/ml bFGF induces a large infiltration of mainly endothelial cells. Capillary formation and primordial vessel development is evident.

5-6-The addition of Ad-dl70-3 (1 X 10^9 pfu) does not diminish endothelial cell invasion or capillary tube formation induced by bFGF.

7-Ad-Angiostatin (1 X 10^9 pfu/ml) inhibits bFGF induced endothelial cell invasion into the matrigel. Endothelial cell morphology is changed from the long spindle shaped phenotype to a rounded cell with a pronounced nucleus.

8-Cell death occurs along a sharp line of demarcation near the outer edge of the matrigel. Cell nuclei appear dark and dense suggesting apoptosis.

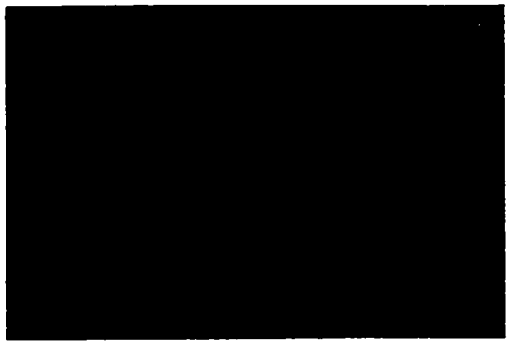

(1) MATRIGEL100X

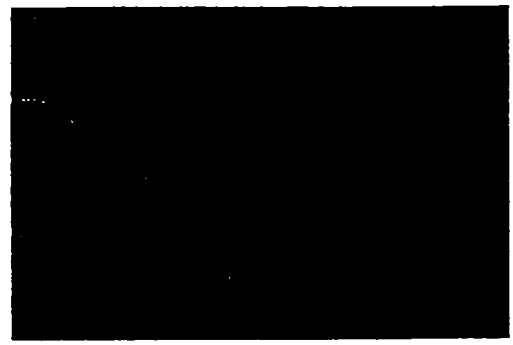

(2) bFGF200X

(3) bFGF100X

(4) bFGF 200X

(5) Ad-dl70100X

(6) Ad-dl70 200X

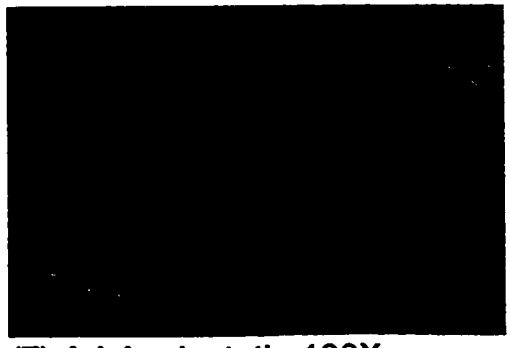

(7) Ad-Angiostatin 100X

(8) Ad-Angiostatin 400X

no distinct nuclear staining. Addition of the control adenovirus does not affect the process of endothelial cell invasion or capillary tube formation within the bFGF impregnated matrigel as seen in panels 5-6. In sharp contrast, the Ad-Angiostatin vector inhibited endothelial cell migration into the centre of the matrigel. The cellular invasion was limited to a sharp line of demarcation near the outer edge of the plug and no primordial vessel formation is evident (Figure 4, panels 7-8). Moreover, the endothelial cell morphology is distinct, changing from a long tapered phenotype, to a rounded cell with a large picnotic nucleus that exhibits intense nuclear staining suggesting apoptosis.

Electron microscopy of the bFGF and bFGF plus Ad-Angiostatin matrigel sections confirmed the observations made with light microscopy alone. The most astonishing feature of both treatment groups is that the vast majority of the cells infiltrating into the matrigel are endothelial cells (Figure 5, panel 1). This was confirmed by the presence of the von Willebrand factor (vWf) storage granule, Weibel Palade bodies that are unique to endothelial cells and co-localize to the cell's secretory machinery (Gerritsen, 1996). These longitudinal tubule structures formed by multimeric vWF are visible at high magnifications (Figure 5, panel 2). Interestingly, fibroblasts are not predominant within the matrigel sections, even though 100 ng/ml of bFGF was added to the matrigel. A small number of granulocytes, mainly eosinophils were observed in both treatment groups but there was no sign of an inflammatory process.

The electron micrographs unequivocally demonstrate apoptosis of the endothelial cells within the Ad-Angiostatin treated matrigel. The classic characteristics of apoptosis, including cell shrinkage and rounding, condensation of the chromatin, fragmentation of the nucleus, and membrane bound blebbing of the cytoplasmic contents, are shown in figure 6 (Wyllie et al., 1980). Weibel Palade bodies are not as pronounced suggesting release of the vWf into the matrigel. This is consistent with the release elicited during pathological processes in response to cytokines, histamine or thrombin (Gerritsen, 1996). Granulocytes are not affected by the angiostatin and appear normal and unstimulated with their enzyme storage granules intact.

Image analysis of the Masson's trichrome stained matrigel sections revealed however that the accumulation of the endothelial cells was 22% for the bFGF, Ad-dl70-3, and Ad-Angiostatin treatments. Thus if the amount of endothelial cells is the same for each treatment, the mechanism of vector derived angiostatin must work in a delayed fashion, whereby endothelial cells must first respond to the angiogenic stimuli of bFGF, and migrate into the matrigel by the process of intussusception (Jain et al., 1997). Upon entry into the matrix, some cells encounter the vector, integrate the virus particle and then produce and secrete the angiostatin transgene product. This in turn feeds back upon the infected or adjacent non-infected cells, inducing apoptosis.

Figure 5. Electron micrographs of bFGF (100 ng/ml) treated matrigel plugs removed from C57BL/6 mice seven days after injection. Photos illustrate predominant endothelial cell invasion, and capillary development.

Panel

1-Migrating endothelial cell. Weibel Palade bodies (WP), markers of endothelial cells, are visible. Ribosome rich endoplasmic reticulum (ER) is very predominant. Nucleus is intact and chromatin appears normal. Magnification 7000X

2-Weibel Palade bodies showing tubule structures of multimeric vWF. Magnification 42,000X

3- Longitudinal view through a young capillary lined by endothelial cells (E). Red blood cells (R), appear in the lumen indicating blood flow and connection to the mouse's blood supply. Magnification 8000X

4-Cross section through a capillary lined by three endothelial cells (E), Note granulocyte (G), at the 11 o'clock position. Magnification 5000X

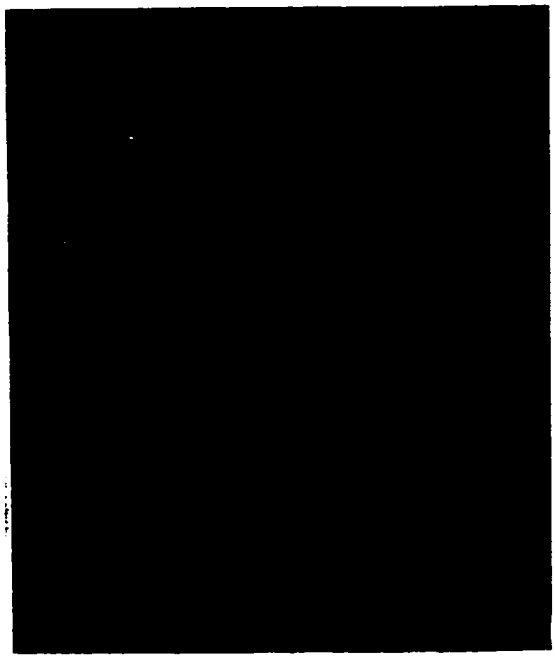

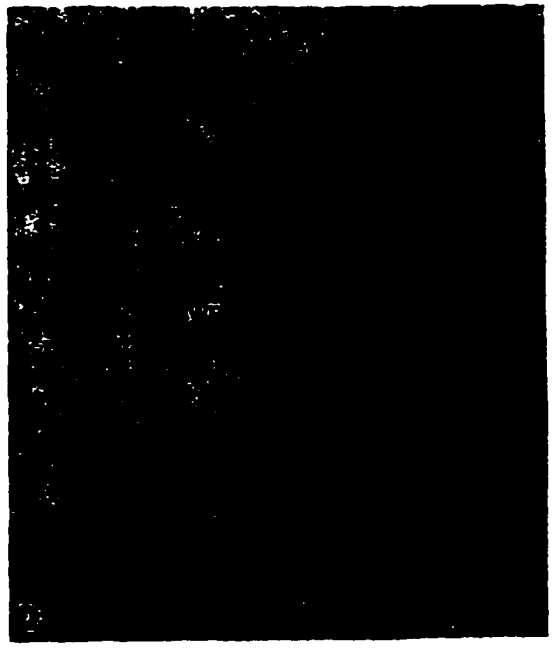

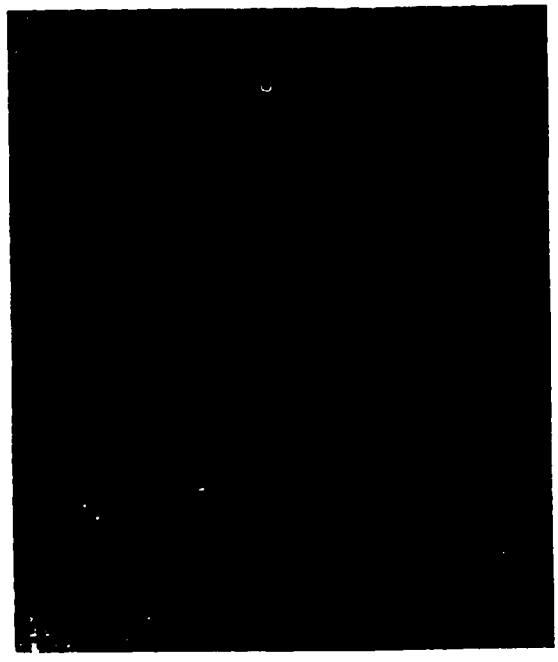

Figure 6. Electron micrographs of Ad-Angiostatin treated matrigel removed from mice seven days after injection show massive apoptosis to endothelial cells and no primordial vessel development.

Panel

1- Endothelial cell undergoing apoptosis. Cytoplasm is fragmented and contains translucent cytoplasmic vacuoles (V). Cytoplasmic blebbing is evident. Magnification 5000X

2,3- Cell nuclei show dark chromatin and are fragmented. Cells have no observable endoplasmic reticulum. Magnification 11,000X

4- Eosinophils are not effected by the actions of angiostatin. Enzyme granules (S) containing dense crystalloid (C) are retained by the cell demonstrating an inactive state. Magnification 20,000X

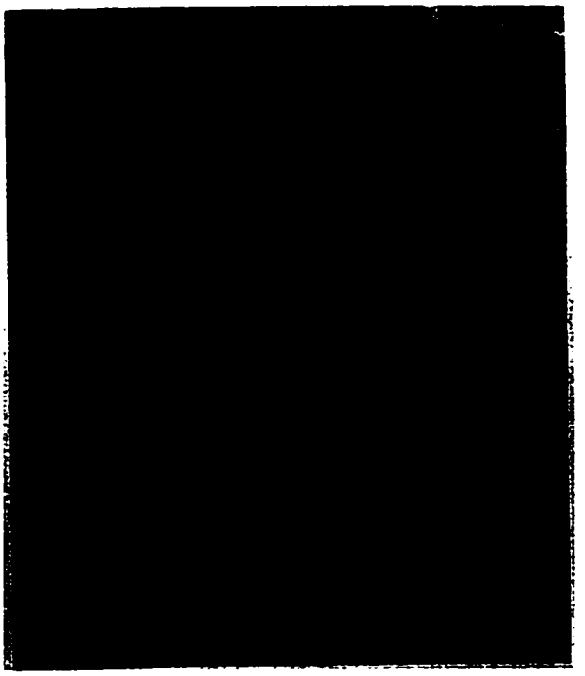

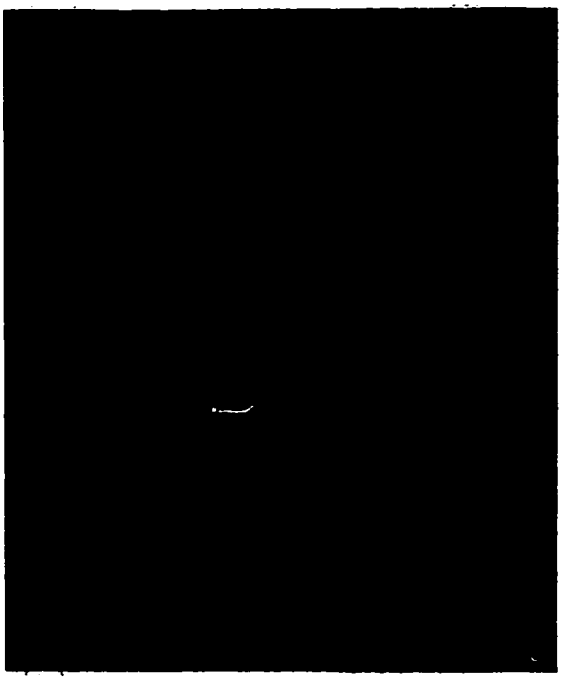

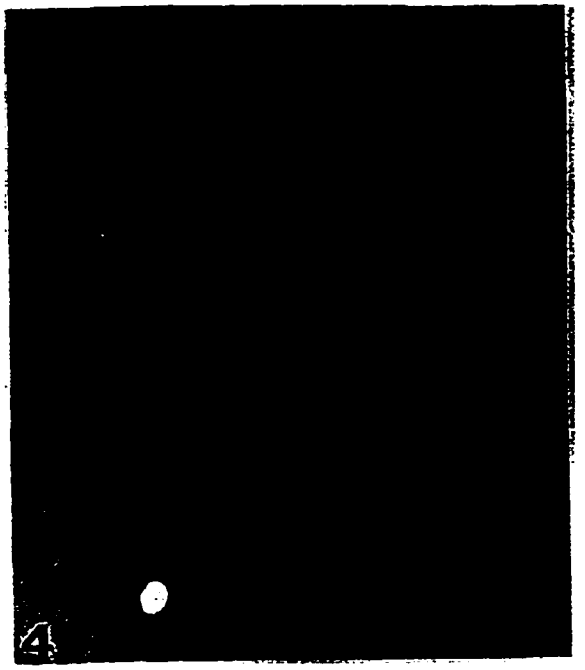

3.2 Biological activity *in vitro*

Angiostatin biological activity was determined *in vitro* using direct viral transduction of HUVEC cells (MOI of 100), plated at a density of 120,000 cells per well. The control wells were either uninfected, or infected with Ad-dl70-3, for comparison to Ad-Angiostatin. The HUVEC cells were photographed on a Zeiss inverted microscope to document cell density and morphology prior to viral infection. Seven days post infection, the cells were gently removed and counted using trypan blue exclusion staining. Direct transduction of sub-confluent HUVEC cells by Ad-Angiostatin led to a 38% decrease in the number of viable cells seven days after infection. In contrast, uninfected, and dl70-3 infected cells increased in cell numbers by 276%, and 240% respectively during the same period (Figure 7). As shown in figure 8A, cultured HUVEC cells whether uninfected, or infected with control virus proliferated to a confluent state with the cells exhibiting the normal endothelial phenotype. In contrast, those cells infected with Ad-Angiostatin are sparse, rounded and detached (Figure 8B). Further, these results demonstrate that murine angiostatin is not species specific and possesses biological activity against human endothelial cells.

3.3 Expression of Angiostatin in the Lung

The expression of Ad-Angiostatin in the lungs of mice did not induce any

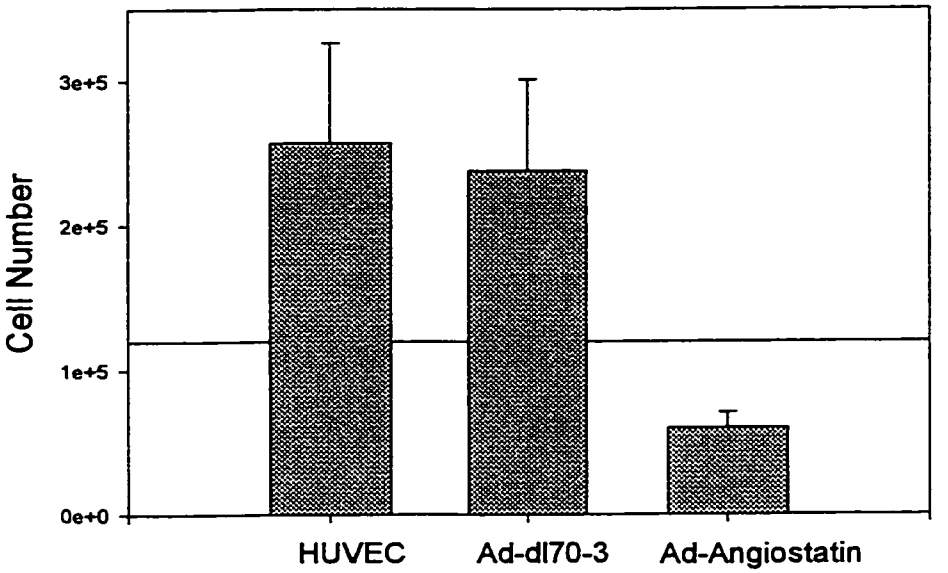

Figure 7. Ad-Angiostatin reduces HUVEC cell number in an *in vitro* bioassay. 120,000 HUVEC cells (line) were plated onto collagen coated plates and were uninfected or infected with Ad-dl70-3, or Ad-Angiostatin at MOI 100. Columns represent the mean number of viable cells per well (n=6 wells) seven days after infection. ($P<0.005$ as compared to control uninfected HUVEC).

Figure 8. Cultured HUVEC cells plated at 120,000 cells per well proliferate and become confluent within seven days in the presence or absence of control vector Ad-dl70-3 (A). The cells maintain the long spindle shape characteristic to endothelial cells. In contrast, infection with adenovirus expressing murine angiostatin at MOI 100 inhibits cell proliferation during the same time period (B). The cells appear rounded and are detached from the culture plate, consistent with the development of apoptosis seen in the matrigel.

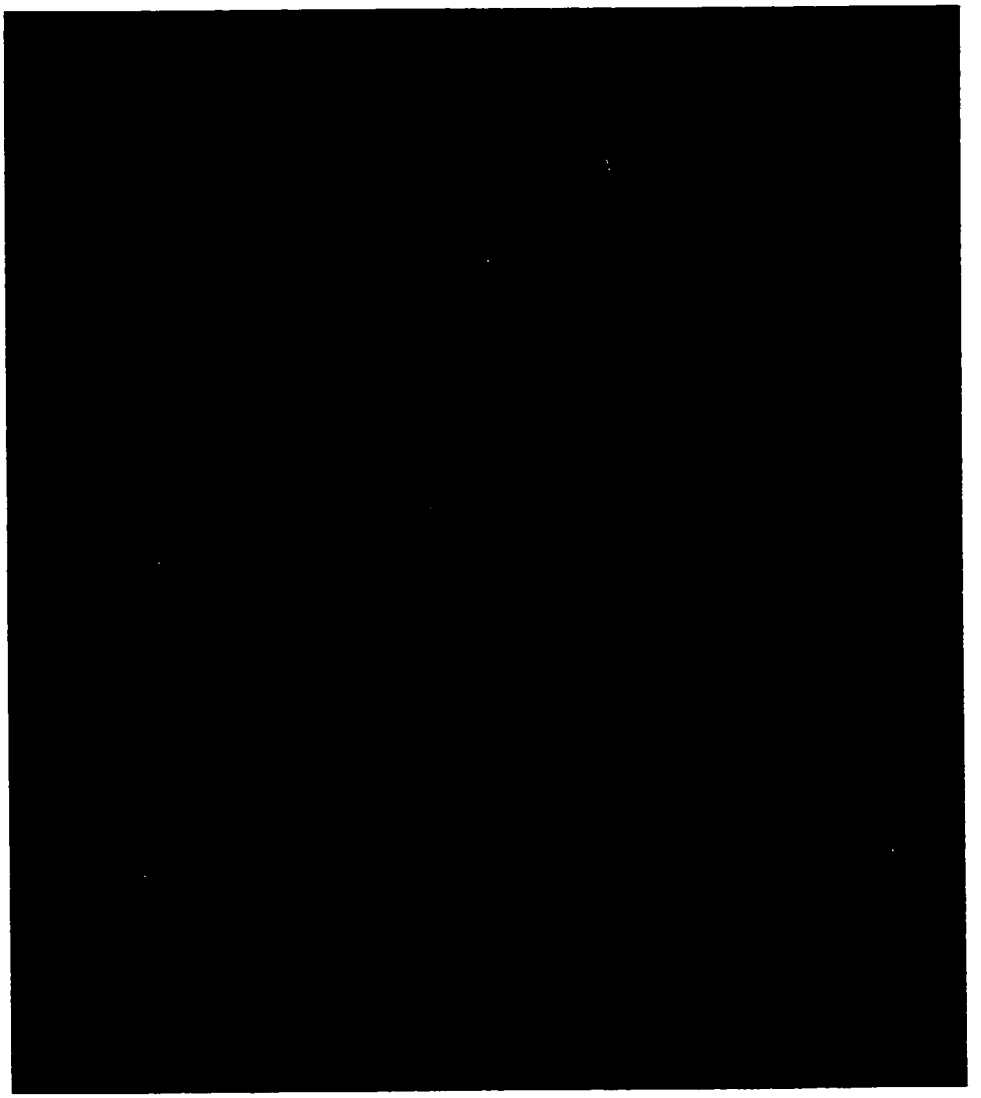

apparent abnormal pathology (Figure 9). Inflammation was limited to the extent of the control vector and no signs of fibrosis were evident at seven days. Examination of the BAL fluid contents revealed similar amounts of infiltrating lymphocytes (Table 1) in both angiostatin and control vector treated lungs in FVB/n mice. Endothelial cells lining the veins and arteries appear intact and are not thrombosed. No necrosis or apoptosis of the lung tissue due to insufficient blood perfusion is observed.

Table 1. *In vivo* biological activity in the lung of control and Ad-Angiostatin treated FVB/n mice, at day 7.

Treatment	Mean Cells/ml in BAL
no adenovirus	530,000 $\pm$50,000 n=2
Ad-dl70 1X10^9 pfu	580,000 $\pm$18,700 n=4
Ad-Angiostatin 1X10^9 pfu	581,000 $\pm$67,600 n=9

3.4 Inhibition of Metastatic Breast Cancer in the Lung by Direct Intranasal Delivery of Ad-Angiostatin

A model of breast cancer metastasis to the lung was established in FVB/n mice. Mice were injected i.v. with 3 X 10^5 PyMidT primary tumor cells and evidence of nodules on the lung surface appeared 14-15 days post injection. On day 16, 1 X 10^9 pfu control Ad-dl70-3 or Ad-Angiostatin was administered by intranasal

Figure 9. Angiostatin has no effects on the lungs of mice. Control virus Ad-dl70-3 (top panel; magnification left 100X, right 400X), or Ad-Angiostatin (bottom panel; magnification left 100X, right 200X) were delivered intranasal to the lungs of C57BL/6 mice. Seven days post infection, the lungs were removed, BAL fluid was collected and the sections were H& E stained. No abnormal pathology was observed, the lymphocytic infiltration present is due to the presence of virus. The endothelium lining the vessels appeared to be intact and red blood cells can be observed in the vessels. No thrombosis or fibrosis was evident in the lungs.

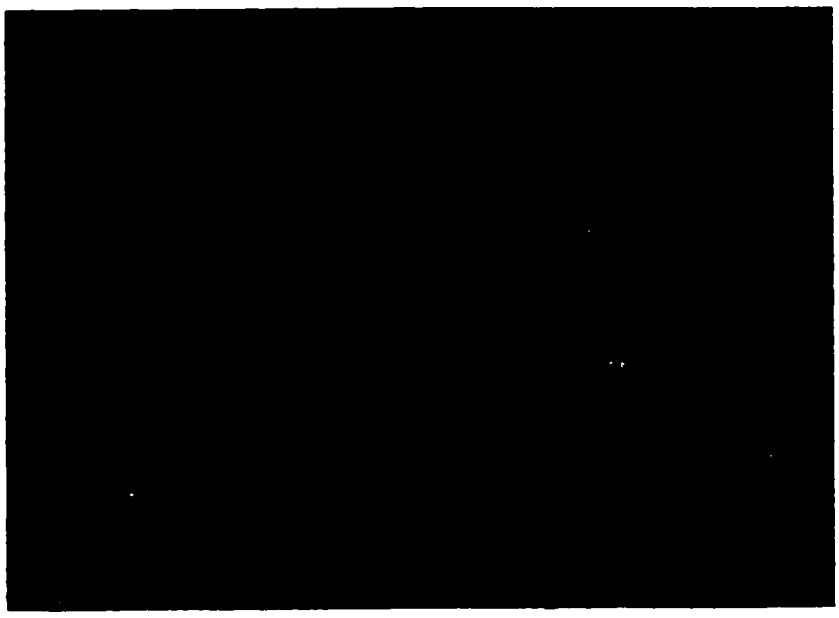

delivery. The mice were subsequently sacrificed one week later at which time the lungs were weighed, BAL fluid was collected, and the surface metastases counted.

Adenoviral mediated gene transfer of angiostatin to the lung inhibited the growth of metastatic tumors as quantified by scoring of surface metastases. Gross examination of the lungs revealed hard yellowish tumor nodules on the surface of both treatment groups (Figure 10). However, the animals in the control treated group had significantly more surface nodules (98 $\pm$37; n=7; Figure 11) than those mice which had received Ad-Angiostatin (18 $\pm$13; n=10;P<.0005). The average weight of the lungs treated with control vector alone was 0.72 $\pm$0.24 g, whereas the angiostatin treated animals had a mean lung weight of 0.44 $\pm$0.05 g (Figure 12). This difference was also highly significant (P<.005). BAL fluid sampled from the lungs of control treated mice contained 2.3 X 10^6 $\pm$2.1 X 10^5 cells/ml which appeared to be mainly macrophages, compared to only 6.4 X 10^5 $\pm$4.2 X 10^4 cells/ml in the angiostatin treated lungs. This value closely reflects the numbers obtained from normal non-tumor laden lungs and confirms our earlier findings that angiostatin does not appear to contribute to any inflammation or lung pathology.

H&E stained sections of the lungs of all mice show metastatic nodules in all treatment groups which were not limited to the lung surface. Mice which received the control vector had extensive tumor growth throughout the entire lung. This vast amount of growth severely diminished the area occupied by the alveolar sacs required for gas exchange in the normal lung (Figure 13, panel 1-2). Examination

Figure 10. Inhibition of breast metastases in the lung by Ad-Angiostatin. A) Examples of lungs of mice at day 23. The mice had been previously treated with 1 X 10^9 pfu Ad-Angiostatin or control virus administered by intranasal delivery 16 days after the establishment of breast tumor metastases. Lungs appeared normal and pink and had few tumor nodules. B) Lungs of control treated Ad-dl70-3 mice at day 23. Lung surface was covered with metastatic nodules.

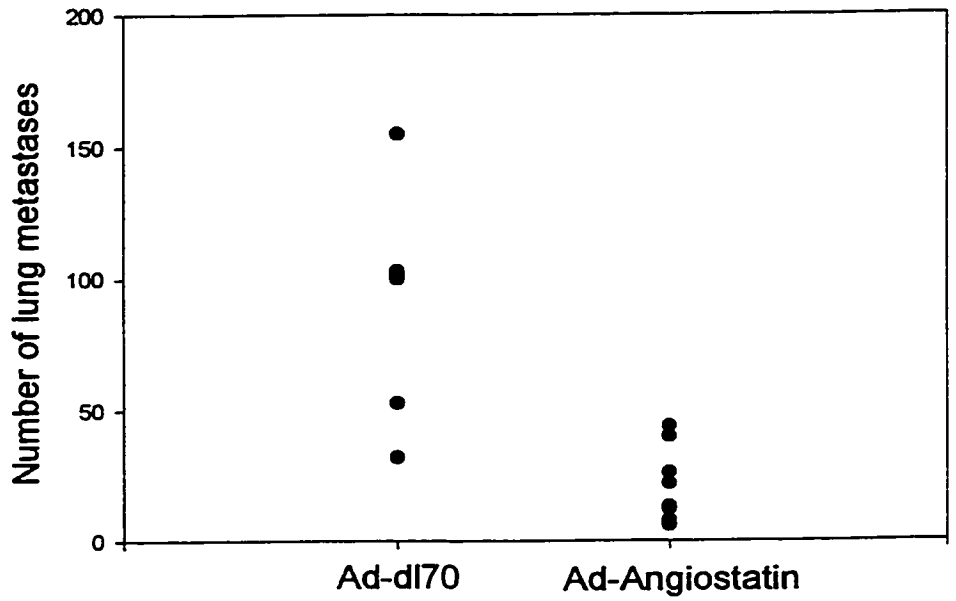

Figure 11. Intranasal administration of Ad-Angiostatin into the lungs of FVB/n mice inhibits the growth of breast tumor metastases. The Ad-Angiostatin treated group (n=10) had an average of 18 (±13) nodules per lung as compared to 98 (±37) nodules for the Ad-dl70 treated group (n=7). Each circle represents the number of nodules counted an individual surface on day 23, seven days post administration of the viruses.

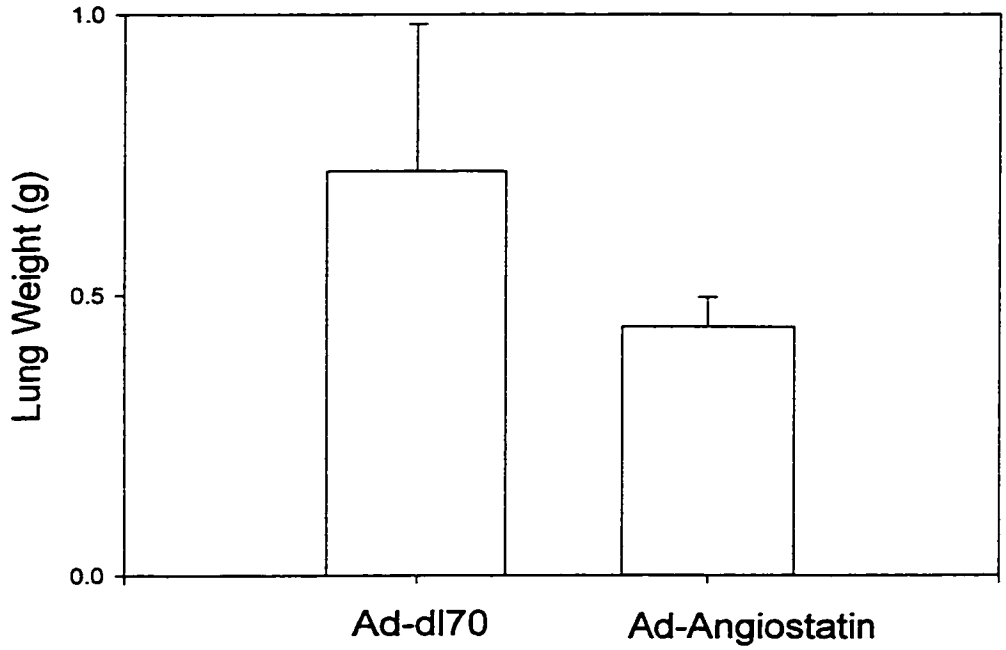

Figure 12. Inhibition of lung metastases by Ad-Angiostatin. Lungs from FVB/n mice bearing breast tumor metastases were removed and weighed seven days after intranasal delivery of Ad-Angiostatin (n=10) or control vector (n=7). Lung weight as a measure of tumor burden was decreased in the Ad-Angiostatin treated animals ($P<0.005$).

of these tumors revealed an extensive network of blood vasculature clearly defined by large amounts of red blood cells (Figure 13, panel 2). In contrast, the Ad-Angiostatin treated lungs contained lesions that were small and isolated but retained most of the normal alveolar architecture of a non-diseased lung (Figure 13, panels 3 and 5). Tumor vasculature and visible red blood cells within these lesions appears to be markedly reduced compared to control treated lungs (Figure 13, panels 4,6).

Figure 13. Photomicrographs of H&E stained sections of metastatic breast cancer in lung tissue. PyMidT cells were injected intravenous into the tail vein of FVB/n mice. Tumor nodules were visible in the lungs on day 14-15. Control virus Ad-dl70-3 or Ad-Angiostatin were administered intranasal on day 16 at a concentration of 1 X 10^9 pfu. Mice were sacrificed one week post viral infection. The lungs were removed, fixed in buffered 10% formalin and embedded.

1-Lung section from a mouse treated with Ad-dl70-3. Extensive tumor growth is evident reducing the alveolar space in the lung. Vascularization is evident in the large tumor nodule in the right corner highlighted by the abundance of red blood cells. Magnification 100X.

2-Enhanced magnification of large tumor nodule described above. Vascular network filled with red blood cells is prominent. Magnification 200X.

3-Lung section from an Ad-Angiostatin treated mouse. Central tumor is surrounded by normal alveolar tissue and does not appear to have extensive vasculature. Magnification 100X.

4-Pre-existing lung vasculature is not effected by the administration of Ad-Angiostatin. Lung morphology appears normal. Magnification 200X .

5-Lung section from an Ad-Angiostatin treated mouse. Magnification 100X.

6-Enhanced magnification of an Ad-Angiostatin treated tumor. Vasculature and red blood cells are not as predominant. Magnification 400X.

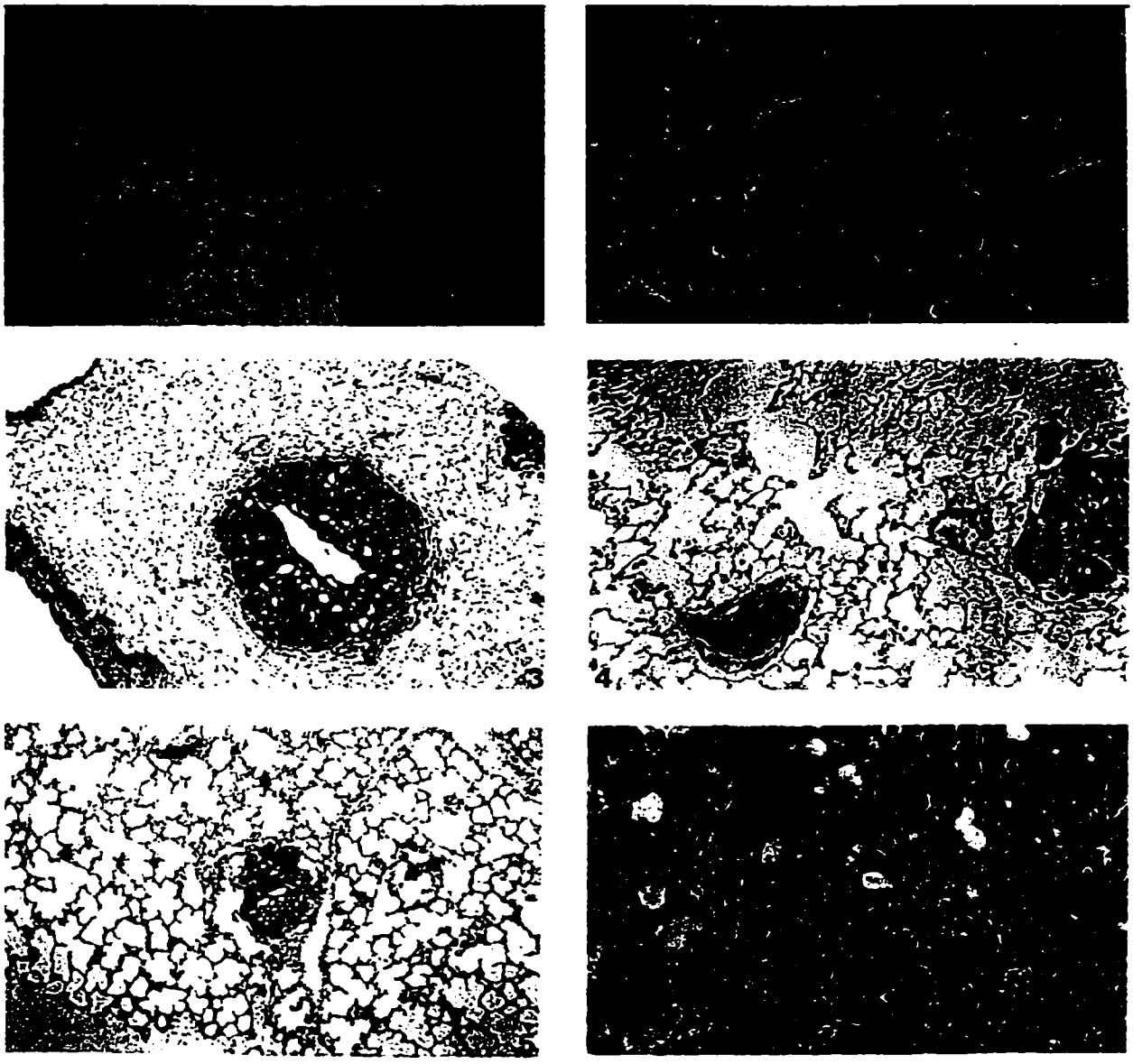
3
4

CHAPTER 4-COMBINATION GENE THERAPY TREATMENT OF A MURINE BREAST CANCER MODEL WITH ADENOVIRUS EXPRESSING ANGIOSTATIN AND INTERLEUKIN-12

4.0 Intratumoral Administration of Adenoviral Vectors

Previous studies have shown that the intratumoral injection of an adenovirus expressing murine IL-12 at 5 X 10^8 pfu can initially cause the regression of the PyMidT tumor in 75% of mice, and that 30% of these treated mice undergo a complete regression and remain tumor free (Bramson et al., 1996). While the regression in our study are lower, the administration of IL-12 induced an initial 20% response and a 13% cure rate in tumor bearing mice. These totally regressed mice were resistant to re-challenge to the PyMidT tumor (Table 2).

Mice bearing tumors which were directly injected with an adenovirus expressing murine angiostatin at 5 X 10^8 pfu responded with a 65% initial tumor regression but none of the treated mice showed total regressions and all mice progressed to tumor growth and death (Table 2). Criteria for initial regression was based on a decrease in tumor volume one week after the administration of a vector as compared to the original tumor volume before treatment.

Administration of the control virus dl70-3, did not delay the growth of the PyMidT tumor in mice. None of the tumors injected with control virus had any

response and none of the mice were cured, a result which has been reported previously (Bramson et al., 1996). Tumor volumes for this group expanded at a near linear rate as determined by weekly measurements and the mice in this group were sacrificed 20 days after virus injection due to excessive tumor size [Figure 14, (data from a representative experiment)]. In contrast, the kinetics of PyMidT tumor growth in Ad-IL-12 and Ad-Angiostatin treated animals was delayed as compared to the control treated animals (Figure 14). This delay extended the survival of the mice in the treatment groups by 14 days on average (Figure 15). The mechanism for this growth delay is a reflection of angiostatin's inhibitory effects on the tumor vasculature, via the apoptosis of endothelial cells. Moreover, the inhibition of tumor growth over this time period may be directly related to the transient expression from the adenovirus.

Table 2. Summary of responses of PyMidT tumors following intratumor injection of Ad-dl70-3, Ad-Angiostatin, Ad- IL-12, and combination Ad-Angiostatin plus Ad-IL-12

Vector injected	Responses/partial regressions	Cures
Ad-dl70-3 ($1X10^9$ pfu)	0/17 (0%)	0/17 (0%)
Ad-Angiostatin ($5X10^8$ pfu)	13/20 (65%)	0/20 (0%)
Ad-IL-12 ($5X10^8$ pfu)	3/15 (20%)	2/15 (13%)
Ad-Angiostatin +IL-12 ($5X10^8$ pfu each)	25/26 (96%)	14/26 (54%)

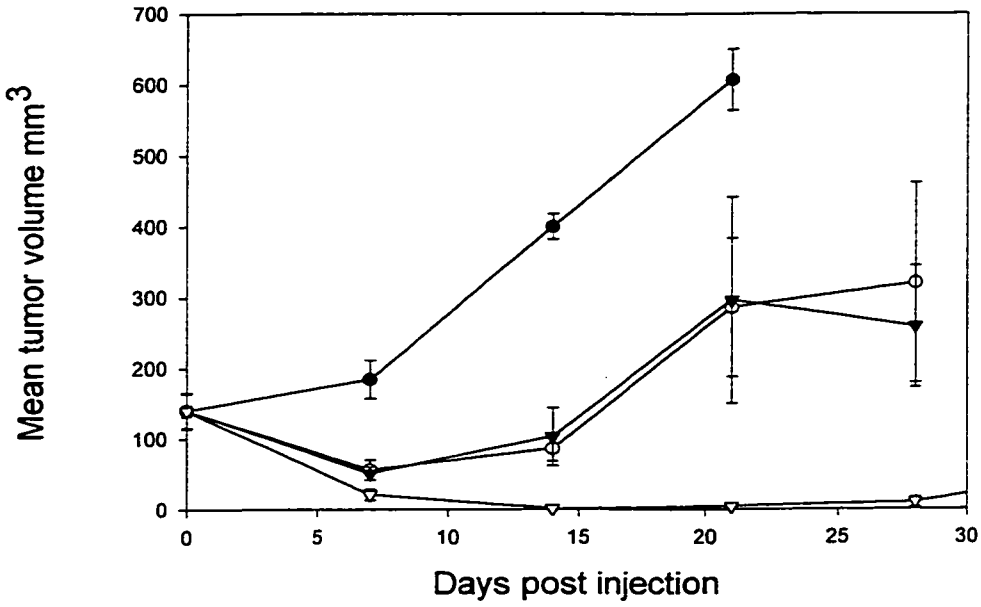

Figure 14. Tumor regression following intratumoral injection of adenovirus. PyMidT tumor cells (5 X 10^5) were injected subcutaneous into the right flank of female FVB mice. Twenty-one days later, palpable tumors were injected with 5 X 10^8 pfu of Ad-Angiostatin (▾, n=5), Ad-IL-12 (◦, n=5) or combination Ad-Angiostatin plus Ad-IL-12 (▽, n=5). Final viral load was adjusted to 1 X 10^9 pfu with control virus, Ad-dl70-3 (•, n=5). Tumors were measured at the time of injection and then weekly using vernier calipers.

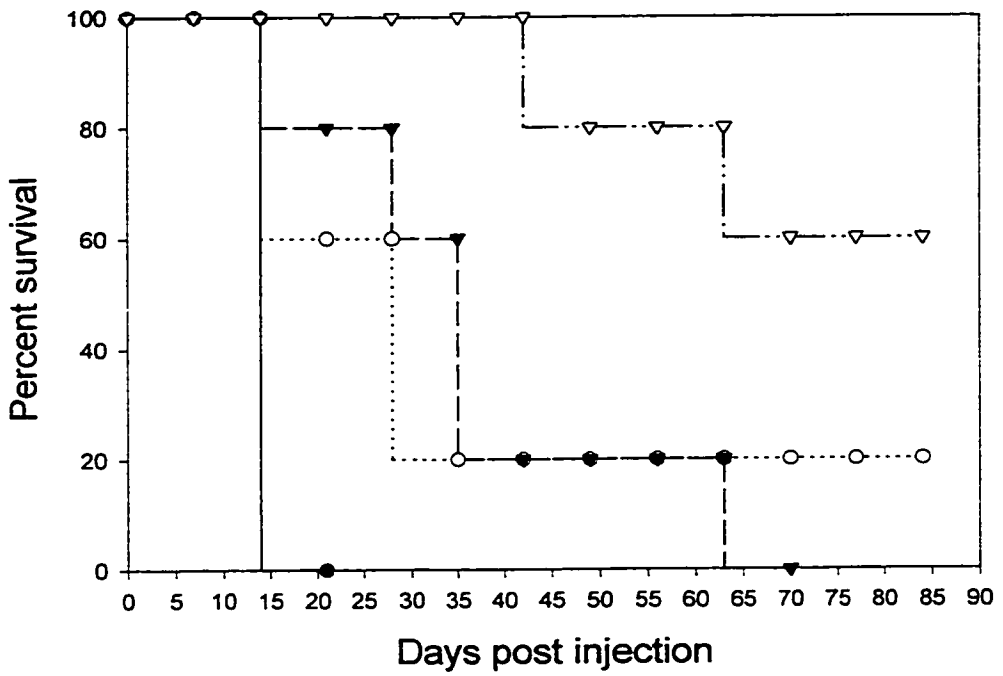

Figure 15. Long-term survival of FVB mice bearing PyMidT tumors following treatment with control virus Ad-dl70-3 (•, n=5), Ad-Angiostatin (▾, n=5), Ad-IL12 (◦, n=5) and combination Ad-Angiostatin plus Ad-IL-12 (▿, n=5).

Unlike Ad-Angiostatin alone, Ad-IL-12 could totally regress tumors in some (13%) mice and vaccinate these mice against re-challenge with PyMidT tumor cells. This illustrates the known role of immune stimulation by IL-12 and the generation of T cell specific responses that have been reported by others (Bramson et al., 1996;Addison et al., 1998). As reported previously, no toxicity was observed with the use of the Ad-IL12 at 5×10^8 pfu. As well, animals that received Ad-Angiostatin as high as 1×10^9 pfu had no noticeable side effects.

The data obtained for the injection of a single virus expressing IL-12 or angiostatin into the tumor model identifies the strengths and weaknesses of both transgene products in producing successful tumor regression. Therefore, it would be expected that a combination of IL-12 and angiostatin would enhance tumor regression following co-injection into the PyMidT tumor.

Co-injection of Ad-Angiostatin with Ad-IL12.1 increased the number of mice that had an initial tumor regression to 96%. Of these mice, 54% went on to develop a total cure and were vaccinated against further challenge with PyMidT tumor cells. In those mice which underwent total tumor regression, tumors were completely absent three weeks after injection of the virus combination. Mice which had a relapse of tumor growth after initial regression had two to three weeks increase in survival time comparable to the kinetics seen with angiostatin alone (Figure15). Interestingly, two mice died of unknown causes in this combined treatment group 13 days after the injection of the viruses. In both cases, the tumors were extremely

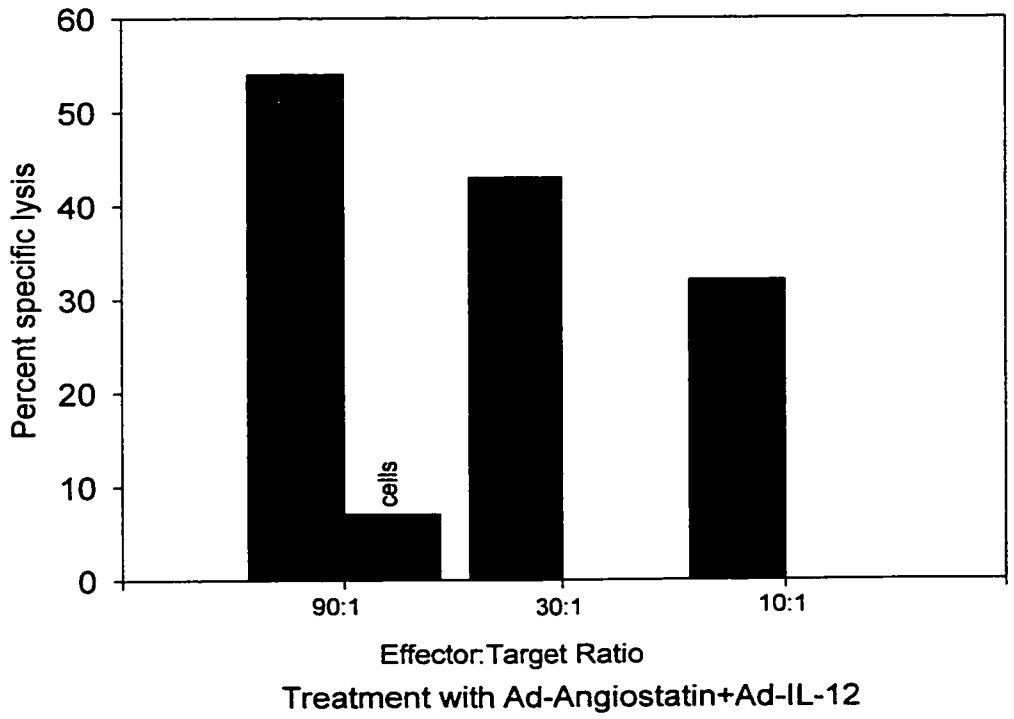

Figure 16. Generation of specific anti-tumor CTL response by combination Ad-Angiostatin plus Ad-IL-12. ^{51}Cr release from 516MT3 target cells (MT3) and PTO 516 non-middle T expressing cells (516) was measured after incubation with *in vitro* stimulated splenocytes from mice that were resistant to tumor rechallenge.

large (383 and 832 mm^3) when injected and had undergone an 80% reduction in tumor volume after one week and were completely absent at the time of death. One can speculate that these mice may have developed some sort of thrombosis or embolism as a result of massive vascular disruption within the tumor. However no pathological examination was possible. Our results demonstrate that the injection of the virus expressing angiostatin, which appears to be benign, to disrupt the tumor endothelium, in combination with the immuno-stimulatory potential of Ad-IL-12 produces a synergistic effect that dramatically reduces tumor size and leads to increased total regressions.

4.1 Anti-tumor Immunity in Mice Injected with Combination Ad-Angiostatin plus Ad-IL-12

Two mice from the cured combination Ad-Angiostatin and Ad-IL12 group were sacrificed and their spleens removed eight weeks after rejecting a re-challenge with 5 X 10^5 PyMidT cells in contra-lateral flank. Splenocytes were co-cultured with irradiated 516MT3 cells, which express the Polyoma middle T antigen (Addison et al., 1998), for five days to activate tumor specific lymphocytes. These activated cells demonstrated a high degree of specific killing against ^{51}Cr labelled 516MT3 cells, but not the PyMidT negative PT516 control cell line (Figure16). CTL killing was 32% at an effector to target ratio of 10:1, and 43% at 30:1, with no

measurable background. These results indicate that the cells of the immune system, specifically cytotoxic T lymphocytes, can recognize a tumor antigen and are capable of reactivation to kill these tumors, thus immunizing or vaccinating the animal from further tumor progression.

4.2 Immunohistochemistry of PyMidT Tumor Vasculature with anti-CD 31 antibody Following Treatments with Ad-dl70-3, Ad-Angiostatin, Ad-IL-12 and Ad-Angiostatin plus Ad-IL-12

The effects of Ad-Angiostatin, Ad-IL-12 and the co-injection of the two adenoviruses on tumor vasculature was analysed by immunohistochemical staining. The vessels within the tumor were stained with an antibody against CD 31, a mouse endothelial cell marker that is involved in endothelial cell-to-cell adhesion and leukocyte transmigration (Blezinger et al., 1999; Gerritsen, 1996).

The photomicrograph of the PyMidT tumor section injected with control Ad-dl70-3 shows extensive CD 31 staining of vessels (Figure 17, panel 1). Examination of the surrounding tumor tissue shows no indication of necrotic or apoptotic regions in the tumor in either the CD 31 or H&E stained sections (Figure 17, panel 1,2).

Sections from tumors injected with adenovirus expressing angiostatin, IL-12, or in combination show a marked decrease in the CD 31 staining pattern compared

Figure 17. Inhibition of tumor vascularization by direct injection of adenoviral vectors. Palpable PyMidT tumors were injected with Ad-dl70, Ad-Angiostatin, Ad-IL12 or combination Ad-Angoistatin and IL-12. One week post injection, the tumors were removed, frozen in OCT compound and cryosectioned at -20°C. Sections were stained with a anti CD31 antibody (left panels) as described in the methods section. Sections were also H&E stained (right panels) to visualize tumor necrosis and apoptosis. All images are at 200X magnification.

Panel

1-2-PyMidT tumor injected with Ad-dl70-3. Extensive CD31 staining (brown) indicating vascularization is evident. H&E staining reveals little tumor necrosis or apoptosis

3-4-Ad-Angiostatin injected tumor show reduced CD31 staining indicating a reduction in tumor vasculature. Tumor necrosis and apoptosis is dramatically increased with the addition of Ad-Angiostatin.

5-6-The injection of Ad-IL-12 also has an angiostatic effect on tumor vasculature. CD31 staining is reduced compared to controls.

7-8-Combination injection of Ad-Angiostatin and Ad-IL-12 shows little CD31 staining, while tumor necrosis and apoptosis is evident in the H&E stained sections.

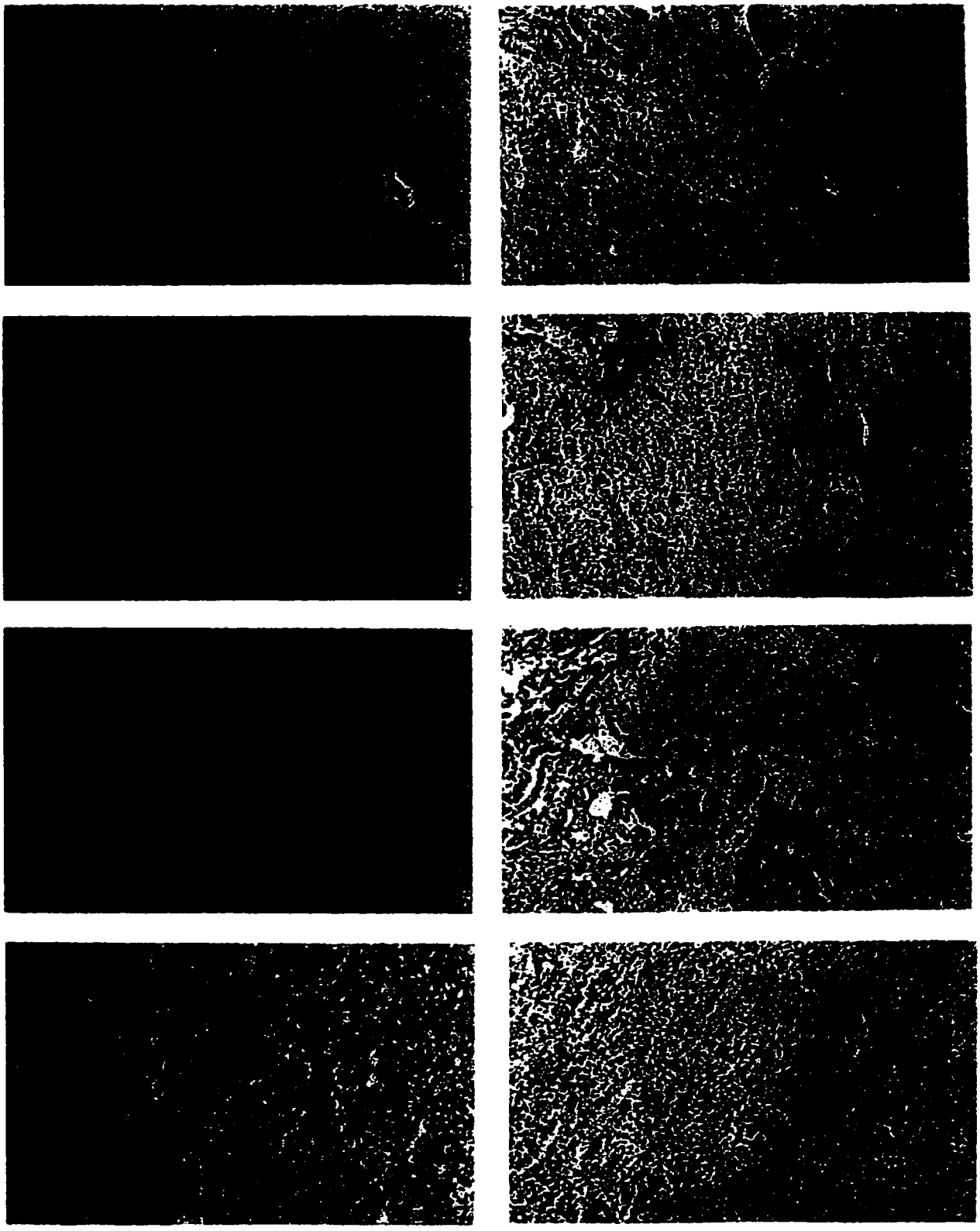

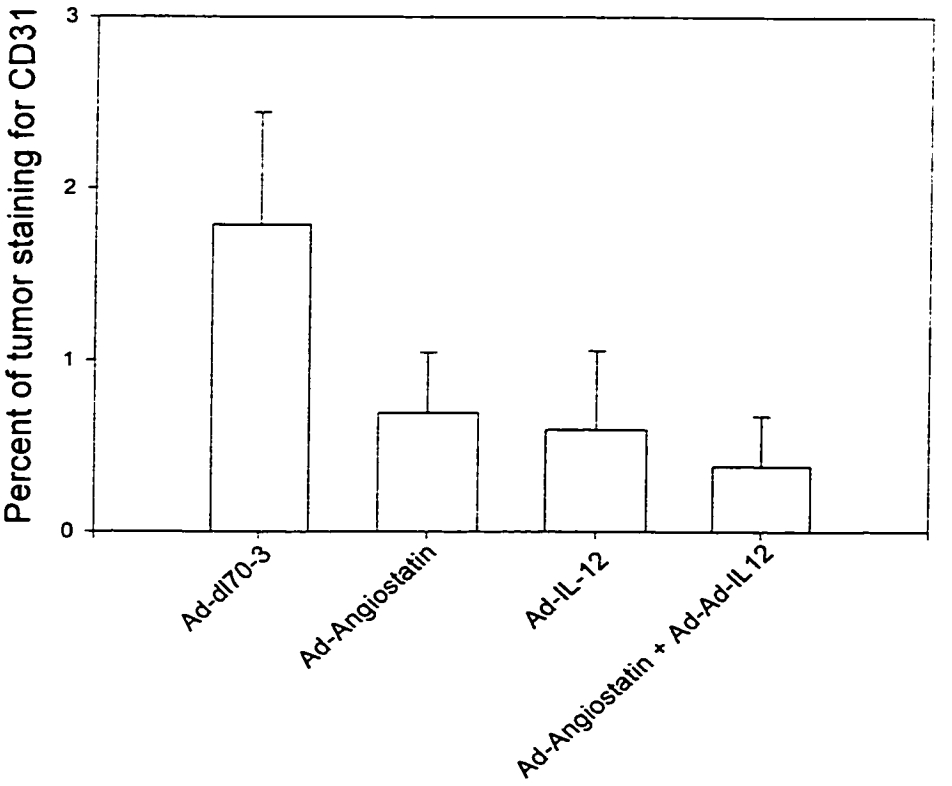

Figure 18. Frozen tumor sections were stained with anti-CD31 antibody, and visualized under 200X magnification. Vessel quantification was calculated by counting five fields in each tumor, with two tumors in each group. Quantification was carried out in a blinded manner using a Leica Laborlux microscope and Northern Exposure V2.9 software. The reduction in vessels counted in the treatment groups as compared to the Ad-dl70-3 was significant ($P<0.005$).

to that seen with control vector. Tumor necrosis and apoptosis are dramatically evident in the tumors treated with angiostatin and IL-12 alone or in combination in both the CD 31 and H&E stained sections (Figure 17, panels 3-8).

Vessel quantification of the CD 31 stained tumor sections is shown in figure 18. In the tumors injected with control virus, 1.8% ($\pm$0.65) of the total surface area within the randomly selected fields stained positive for endothelial cells. In contrast the Ad-Angiostatin, and Ad-IL-12 alone or in combination significantly ($P<0.005$) reduced the tumor vasculature compared to the control as measured by CD 31 staining (Figure 18). Within the treatment groups which can affect angiogenesis, no significant difference was found between the number of CD31 stained regions by treatment with angiostatin or IL-12 alone or in combination.

CHAPTER 5-CHARACTERIZATION OF MURINE AND HUMAN INTERLEUKIN-18

5.0 Cloning and Production of Adenovirus Expressing Murine or Human IL-18

Reverse transcription PCR of total RNA isolated from the livers of normal C57BL/6 mice with primers specific for murine IL-18 (mIL-18) produced a single 662 bp DNA fragment. This fragment was consistent with the expected size based on the murine IL-18 sequence obtained from the NCBI database (accession number D49949). The PCR primers design was based on this sequence data and encompassed nucleotides 130-154 in the 5' untranslated region and nucleotides 768 to 792 in the 3' untranslated region of the mIL-18 cDNA. The cDNA encoding mIL-18 was cloned into the EcoR1 and Xba1 sites of the shuttle plasmid pACCMV downstream of the human CMV promoter.

Homologous recombination between the shuttle plasmid pACCMV carrying the open reading frame for mIL-18, and the rescue plasmid pJM-17 in 293 cells generated the adenovirus, Ad-mIL18. Potential viral plaques were picked and expanded in 293 cells. Northern blot analysis of 293 and A549 cells infected with Ad-mIL18 demonstrated three potential viral clones expressing the appropriate transcript. These clones were designated Ad-mIL-18-1, Ad-mIL-18-2 and Ad-mIL-

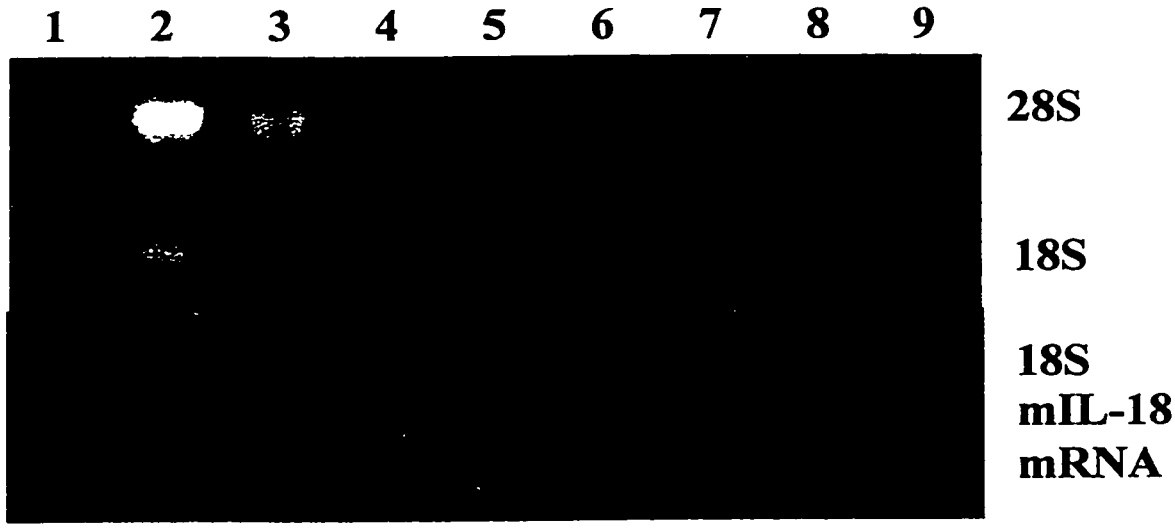

Figure 19. Murine IL-18 mRNA expression from Ad-mIL-18 infected 293 and A549 cells. Total RNA, 20µg per lane was loaded onto a 1% agarose denaturing gel (18S and 28S ribosomal RNA shown), transferred to Nytran membranes and hybridized to ^{32}P labelled murine IL-18 cDNA. No murine IL-18 message could be detected in Ad-dl70-3 infected 293 or A549 cells (Lanes 1,2). Detection of murine IL-18 (mIL-18) mRNA message from A549 cells infected for 36 hours with crude 293 supernatants of Ad-mIL-18-1 and Ad-mIL-18-2 (Lanes 3,4). No mRNA for mIL-18 was detected in A549 cells infected for 36 hours with purified Ad-mIL-18-1 or mIL-18-2 at MOI of 100 (Lanes 5,6). No mIL-18 mRNA message could be detected from 293 cells infected with purified Ad-mIL-18-1 (Lane 7). A single band corresponding to the IL-18 mRNA was detectable following infection of A549 cells with crude and purified preparations of Ad-mIL-18-8 (Lanes 8 and 9, respectively).

18-8. As shown in figure 19, lanes 1 and 2, 293 cells and A549 cells, respectively, do not express mIL-18. Infection of A549 cells for 36 hours with the crude 293 cell culture supernatants containing the replication deficient Ad-mIL-18 clones demonstrated mIL-18 mRNA expression (Lanes 3,4,and 8).

However, following large scale expansion in 293 N3S cells and purification by double density cesium chloride purification, Ad-mIL-18-1 and mIL-18-2 no longer demonstrated any mIL-18 expression from A549 cells. Infection of A549 or 293 cells with purified adenovirus at MOI of 100 for 36 hours did not induce IL-18 mRNA expression seen previously following infection with crude infected 293 cell culture supernatants (Figure 19, Lanes 5-7). Moreover, infection of the A549 cells was not associated with cytopathic events, indicating that the phenomenon was not due to E1 reversions and the development of replication competent adenovirus (RCA). Restriction enzyme digests of the viral DNA revealed the correct DNA ladder pattern that would have been expected for a virus carrying the IL-18 cDNA ruling out the possibility that the IL-18 cDNA had been replaced or excised from the viral genome. The IL-18 sequence was determined to be correct and error free.

The virus designated Ad-mIL-18-8, did retain mRNA expression both before expansion in the 293N3S and after cesium chloride banding. Infection of A549 cells with either crude 293 supernatant or banded Ad-mIL-18-8 virus at MOI of 100 demonstrates mIL-18 message consistent with the expected size of the 662 bp.

A similar cloning strategy was employed in cloning human IL-18 (hIL-18)

from total RNA isolated from the HepG2 liver cell line. Reverse transcription using oligo dT primers was followed by PCR using oligonucleotide primers based on the cDNA sequence obtained from NCBI database (accession number D49950). The forward primer in the 5' untranslated region included nucleotides 139-167 whereas the reverse primer included nucleotides 773-802 in the 3' untranslated region of the hIL-18 cDNA generating a 663 bp DNA fragment. This cDNA was cloned into the shuttle plasmid pACCMV using EcoR1 and Xba1 sites and cotransfected into 293 cells with the rescue plasmid pJM-17. A single adenovirus Ad-hIL-18, was picked and expanded in 293 cells.

Northern blot analysis from infected A549 cells demonstrated that infection at MOI of 100 with purified and banded virus produced a single band consistent with expected mRNA message (Figure 20, top panel, Lane 2). Uninfected A549 cells did not produce any hIL-18 message as seen in lane 1.

Protein expression of mIL-18 and hIL-18 from infected 293 and A549 cell culture supernatants was attempted by Western blotting. Commercially available polyclonal goat anti-mouse IL-18 antibody could not detect any mIL-18 in either the cell culture supernatants or within the cytoplasm of Ad-mIL-18 infected cells. Similarly, a mouse anti human IL-18 monoclonal antibody could not detect any hIL-18 in the conditioned medium of Ad-hIL-18 infected cells. However, hIL-18 was detected in the cytoplasm of infected A549 cells. This single band at 18 kDa corresponds to the expected molecular weight of the biologically active and

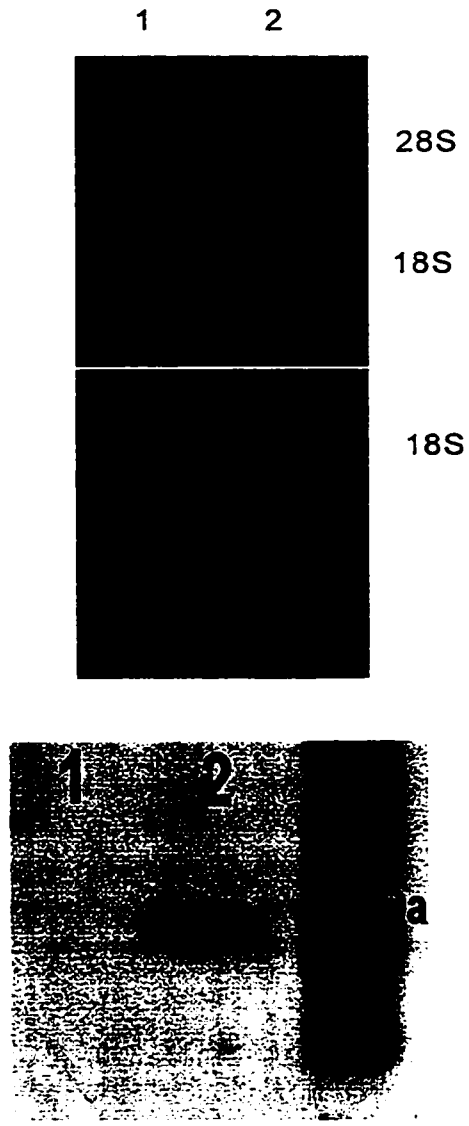

Figure 20. Northern and Western blot analysis of human IL-18 (hIL-18) expression following infection of A549 cells with Ad-hIL-18 at MOI of 100. Top panel, Northern blot of uninfected A549 cells (Lane 1) and infected A549 cells (Lane 2). Bottom panel, Western blot analysis of Ad-hIL-18 infected A549 conditioned medium (Lane 1) and Ad-hIL-18 infected A549 cellular extract (Lane 2).

processed hIL-18 (Figure 20, bottom panel, Lane 2). The biologically inactive pro-IL-18 which has a molecular weight of 24 kDa was not detected indicating that the IL-18 was being processed but could not apparently exit the cell cytoplasm. The correct processing of pro-IL-18 has been reported to required the enzyme Caspase-1 /ICE (Ghayur et al., 1997). Northern blot analysis using a cDNA human ICE probe did not detect any ICE mRNA from uninfected or infected A549, 293 or human adherent PBMC (mainly monocytes and macrophages).

5.1 Production of Recombinant Murine IL-18 from Escherichia coli

Recombinant mIL-18 was expressed using the pET32b expression system in the *E.coli* host BL21 (DE3). The mature mIL-18 cDNA was isolated by designing an oligonucleotide primer which hybridized to the coding sequence for the first eight amino acids in the mature protein at nucleotide 268. The primer included coding sequences for two additional amino acids, a Methionine start signal, and a Glycine residue which was necessary to maintain the DNA sequence in frame. The reverse primer hybridized to a region coding for the final seven amino acids of the protein and included a stop codon. The PCR reaction used the 662 bp mIL-18 cDNA as the initial template, and generated a 493 bp DNA fragment that only encoded for the bioactive mIL-18 protein. The open reading frame coding for the mature, bioactive mIL-18 cDNA was cloned into the pET32b plasmid and was transformed into the *E.coli* host. Expression was induced by the addition of IPTG to growing cultures

and the mIL-18 protein was purified using a nickel chelate column which had affinity for a hexa-Histidine tag on the N-terminal of the protein (Appendix A).

5.2 In vitro IL-18 Bioassay

The biological activity of IL-18 was originally identified by its ability to induce IFNγ from stimulated splenocytes and T cells.(Okamura et al., 1995). An indirect assay based on the initial characterization of IL-18 was modified to measure IFNγ production from ConA stimulated murine splenocytes following the addition of conditioned media from adenoviral infected A549 culture supernatants. Adenoviral derived mIL-12 which also has the ability to stimulate IFNγ production from T cells was included as a positive control, while Ad-dl70-3 infected media was added to rule out the possibility of a viral effect. Recombinant mIL-18 produced from *E.coli* was added directly to the cultured splenocytes.

48 hours after the addition of the conditioned media or the recombinant protein, the cell free splenocyte culture supernatants were analysed by a commercially available murine IFNγ ELISA. As shown in figure 21, the addition 50 and 100 µl of conditioned adenoviral derived mIL-12 induced 7000 and 6000 pg/ml of IFNγ respectively. The decreased amount of IFNγ seen with the increasing amounts of IL-12 could indicate some mechanism whereby the splenocytes become unresponsive to higher levels IL12 and negatively regulate IFNγ levels.

The addition of various volumes of the Ad-mIL-18 conditioned A549 media

Figure 21. Interleukin 18 bioassay. The effects of adenoviral derived murine IL-12, IL-18 and recombinant bacterial murine IL-18 on the production of IFNγ from ConA stimulated splenocytes (top panel). Ad-mIL-12, Ad-mIL-18 and Ad-dl70-3 conditioned A549 culture supernatants were added to 3 X 10^5 Con A stimulated splenocytes in a final volume of 250 µl RPMI for 48 hours. Recombinant mIL-18 was added directly to the splenocytes and also incubated for 48 hours. Following incubation, cell free splenocyte culture supernatants were analysed by ELISA for murine IFNγ production. Lane 1 and 2, IFNγ production from the addition of 50 and 100 µl of Ad-mIL-12 conditioned media. Lanes 3-5, levels of IFNγ induced by 10, 50 and 100 µl of Ad-mIL-18 conditioned media. Lanes 6-8, addition of 100, 200 and 1000 ng of recombinant mIL-18. Lanes 9 and 10, control Ad-dl-70 conditioned media and ConA stimulated splenocytes alone.

Production of IFNγ from Ad-hIL-12 and Ad-hIL-18 stimulated human PBMC (bottom panel). Adenoviral conditioned A549 media was added in an identical manner as described above to Con A stimulated PBMC and incubated for 48 hours. Following incubation, cell free culture supernatants were analysed by ELISA for human IFNγ. Lanes 1-3, IFNγ production from the addition of 10, 50 and 100 µl of Ad-hIL-12 conditioned media. Lanes 4-6, levels of IFNγ induced by 10, 50 and 100 µl of Ad-hIL-18 conditioned media. Lanes 7 and 8, Ad-dl70-3 conditioned media and Con A stimulated PBMC alone.

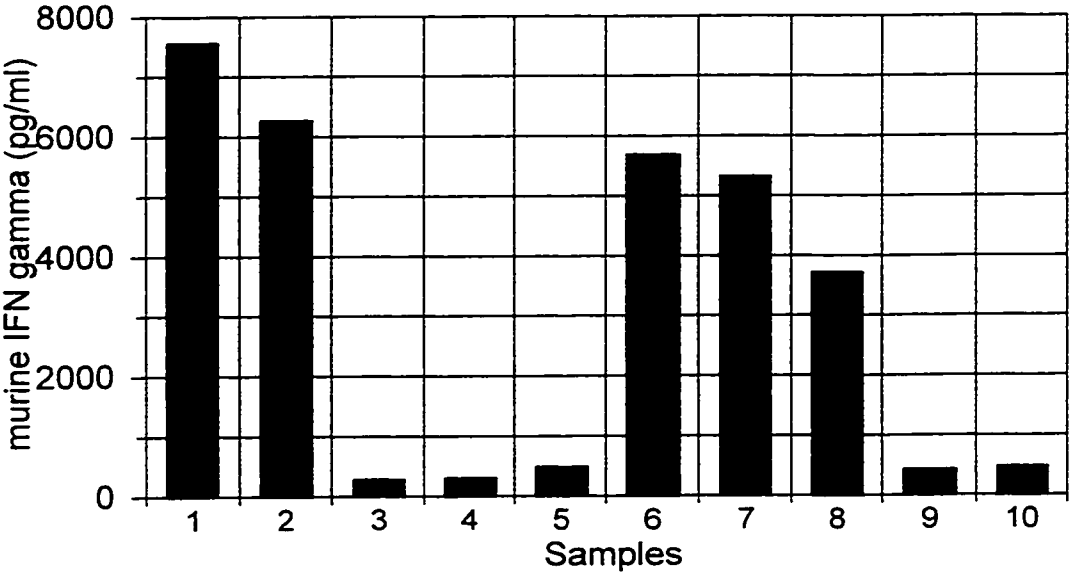
8000
6000
4000
2000
0
murine IFN gamma (pg/ml)
1
2
3
4
5
6
7
8
9
10
Samples

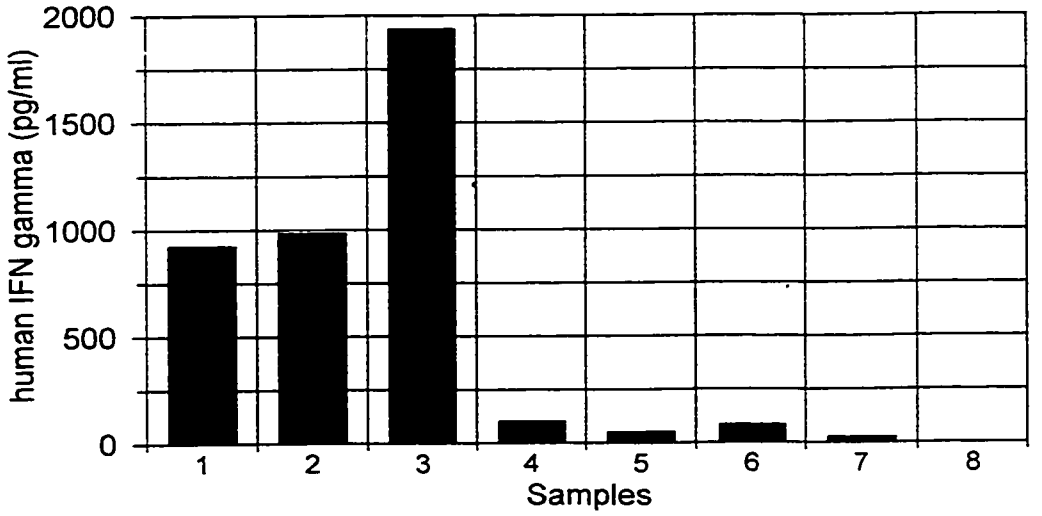
2000
1500
1000
500
0
human IFN gamma (pg/ml)
1
2
3
4
5
6
7
8
Samples

did not induce any IFNγ production. Levels of IFNγ were no higher than the background seen with the control virus or ConA stimulated cells alone (Figure 21, top panel, Lanes 3-5). This confirms the previous result obtained with the Western immunoblot that no IL-18 was being secreted from the cells infected with Ad-mIL-18-8. In contrast, the *E. coli* produced recombinant mIL-18 was bioactive and could induce IFNγ directly from the stimulated splenocytes at levels approaching those seen with Ad-mIL-12 (Lanes 6-8).

A similar strategy was employed for measuring the biological activity of the human IL-18 produced by Ad-hIL-18. Conditioned media from Ad-hIL-18 and Ad-hIL12 infected A549 cells was added to non-adherent ConA stimulated human PBMC, and the production of human IFNγ was measured by ELISA. As with the murine IL-18, no appreciable levels of IFNγ could be produced by the IL-18, whereas IL-12 was shown to be a potent inducer of IFNγ production (Figure 21, bottom panel). This observation reflected the data seen in the Western immunoblot confirming that the IL-18 protein was not being exported out of the cytoplasm of the A549 cell.

5.3 Inhibition of Angiogenesis with Recombinant Murine IL-18

Recombinant mIL-18 was examined for its angiostatic potential using the matrigel assay employed in the study of angoistatin. As in the previous study, 100 ng/ml of pro-angiogenic growth factor bFGF was mixed into the matrigel along with

Figure 22. Photomicrographs of Masson's trichrome stained sections showing inhibition of angiogenesis in a matrigel model, by recombinant murine IL-18. Matrigel was mixed with 100 ng/ml bFGF and 1 µg recombinant murine IL-18 and implanted into C57BL/6 mice for seven days. Top panel. Endothelial cell infiltration is inhibited into the matrigel by the addition of IL-18. Magnification 100X.

Bottom panel. Endothelial cell migration is limited to the edge of the matrigel with the addition of IL-18. Endothelial cells retain elongated phenotype and capillary formation is evident. Magnification 200X.

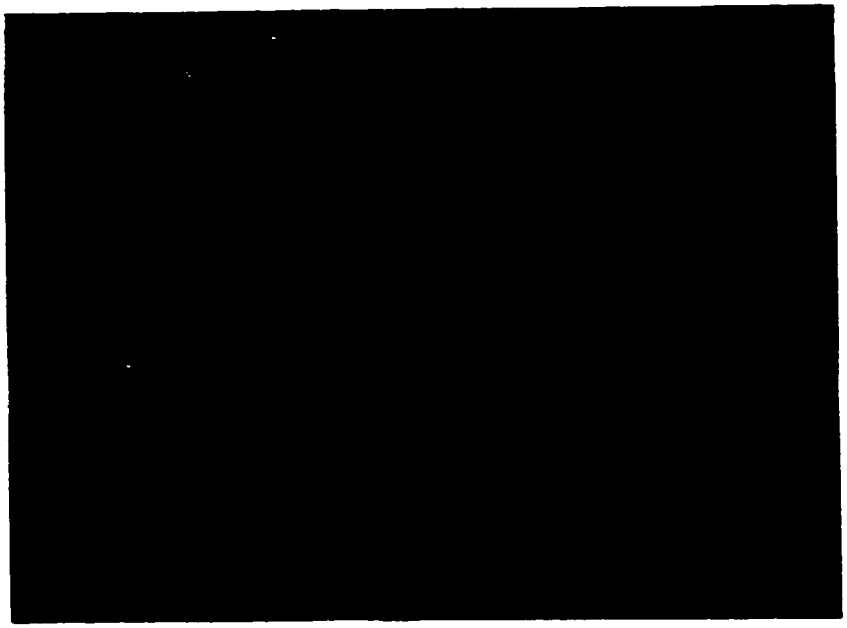

1 μg of the recombinant mIL-18. The mixture was injected into the abdominal midline of C57BL/6 mice for a total of seven days, after which period it was removed and stained with Masson's trichrome.

The results of the Masson's trichrome stained sections revealed inhibition of endothelial cell migration into the matrigel when 1 μg of the recombinant IL-18 was included (Figure 22, top panel). However, unlike the results obtained with Ad-Angiostatin, the endothelial cells within the IL-18 treated matrigel do not possess the rounded phenotype or the picnotic nuclei indicative of apoptosis seen in the angiostatin treatment (Figure 22, lower panel).

5.4 Effects of Recombinant IL-18 on Polyoma Middle T Tumor Regression

Direct comparison between the efficacy of Ad-mIL-12 to Ad-mIL-18 in the PyMidT tumor model was not possible because of the apparent lack of biologically active protein expression from the IL-18 vector. Instead 1 μg of recombinant murine IL-18 was directly injected into the tumor every other day for one week. The IL-18 was co-injected using this treatment regime with a single administration of Ad-Angiostatin at 5 X 10^8 pfu. In addition, tumors were injected with the vectors expressing angiostatin alone or in combination with IL-12. Injections of the recombinant protein did not produce any noticeable side effects.

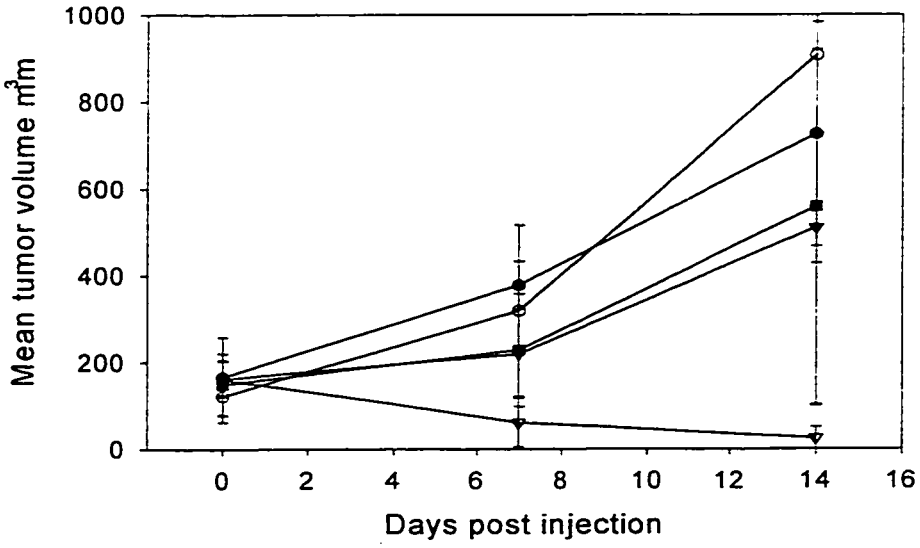

Figure 23. Intratumoral injection of recombinant murine IL-18 does not affect the growth of PyMidT tumor growth in FVB/n mice. Mice were treated every other day for one week intratumorally with 1 µg recombinant IL-18 (◦, n=8) alone or in combination with a single intratumoral injection of 5 X 10^8 pfu Ad-Angiostatin (▪, n=9). Ad-Angiostatin (▾, n=3) alone and in combination with 5 X 10^8 pfu Ad-mIL-12 (▽, n=4). Control virus Ad-dl70-3 (•, n=5) was administered at 1 X 10^9 pfu. Final viral loads were adjusted to 1 X 10^9 pfu with control virus.

As shown in figure 23, this treatment regime of direct injection of the recombinant IL-18 had no effect in delaying or regressing tumor growth. Mice in this treatment group became moribund 14 days after the initial injection as did the control treated Ad-dl70-3 treated group. The combination of IL-18 with angiostatin also did not show any benefits over angiostatin treatment alone. All mice treated with the combination Ad-Angiostatin and Ad-mIL-12 underwent tumor regressions, with 2 of 4 mice having undetectable tumors 14 days after the initial injection. While these results do not reflect favourably on anti-cancer properties of IL-18, factors such as the delivery site, dosage and treatment duration could affect the final outcome.

CHAPTER 6-DISCUSSION

Breast cancer, one of the most frequently diagnosed cancers in women will affect 1 in 10 women in North America (Fornier et al., 1999; Yang and Lippman, 1999). The current therapies for breast cancer rely on surgical techniques, radiation therapy and chemotherapy. However, these therapies often have undesirable side effects and for most patients, especially those with metastatic disease, treatment provides only temporary control of tumor growth (Fornier et al., 1999).

Gene therapy to selectively target and destroy tumors is at the forefront of new biotechnologies which will revolutionize cancer therapy in the new millennium. Potential strategies for cancer gene therapy include: enhancing tumor immunogenicity by introducing genes that encode for immunoregulatory proteins; stimulation of the immune system to increase anti-tumor activity by delivering genes for cytokines; insertion of wild-type tumor suppressor gene and; the insertion of viral vectors engineered to lyse only tumor cells.

Attacking the tumor vasculature by using gene therapy vectors to deliver angiostatic molecules may also be a promising therapeutic approach for cancer. It is hypothesized that a solid tumor may only reach 2 to 3 mm in diameter before requiring a vasculature to perfuse the tumor, thus allowing further growth. This

process of vessel growth from existing vasculature is known as angiogenesis. Recent studies have shown that inhibition of angiogenesis can effectively block the growth of the primary tumor and inhibit dissemination of metastases.

The early tumor immunotherapy trials in the 1980's relied on the systemic administration of cytokines, particularly Interleukin-2, to increase the immune response against tumors. However, the high systemic concentrations required to achieve a clinical response proved to have deleterious toxicity. Genetic modification of tumor cells to secrete cytokines results in localized high concentrations of cytokine within the tumor and reduced systemic toxicity.

The objectives of this thesis were to achieve three main goals: (a) to construct and characterize an adenoviral gene therapy vector expressing the angiogenesis inhibitor angiostatin (Ad-Angiostatin), (b) to combine angiostatic therapy and immunotherapy in a murine breast cancer model by combining Ad-Angiostatin with a vector expressing IL-12 (Ad-IL-12) and, (c) to construct an adenovirus expressing the cytokine IL-18 (Ad-IL-18) and compare its biological properties to that of Ad-IL-12.

Angiostatin is a recently described fragment of the plasma protein plasminogen, and possesses powerful anti-angiogenic properties (O'Reilly et al., 1994). Initially isolated from the urine of mice with primary Lewis lung carcinoma, this 38-45 kDa protein retains four of the five lysine binding kringle domains of the native plasminogen. The biologically active protein is derived from plasminogen by

the enzymatic actions of plasmin reductase, and serine proteases like urokinase (Gately et al., 1996) in the presence of free sulfhydryl donors such as GSH. (Stathakis et al., 1999; Gately et al., 1996).

This study has undertaken an alternative approach to express and deliver murine angiostatin in a tumor model. Whereas other reports have used angiostatin derived from enzymatic digestion, or recombinant protein from Pichia pastoris (Lucas et al., 1998) and baculovirus (Wu et al., 1997), our gene based strategy allows for the *in situ* expression of angiostatin within the tumor. Recombinant angiostatin has been reported to be fragile and can rapidly lose activity (Barinaga, 1999). In addition, recombinant protein may not be correctly glycosylated resulting in a shorter circulating half-life (Sim et al., 1997). In contrast, the angiostatin derived from the adenovirus is produced directly in the infected cell, is properly glycosylated, and is not subject to any physical treatment. Moreover, with this system, cumbersome and time consuming protein purification steps are avoided.

The murine angiostatin cDNA was cloned by reverse transcription PCR of total RNA isolated from the livers of C57BL/6 mice. Oligonucleotide primers were based on the DNA sequence of murine plasminogen,(Degen et al., 1990) to generate the recombinant murine angiostatin. This protocol involved fusing the DNA of the native plasminogen signal sequence, including amino acids 1-32, to the region coding for the four kringle domains at amino acids 98-458. This cDNA was subsequently cloned into the adenovirus shuttle plasmid pACCMV, under the

control of the human cytomegalovirus promotor, and subsequent homologous recombination in 293 cells with the rescue plasmid pJM-17 generated Ad-Angiostatin.

Angiostatin mRNA was measured in 293 and A549 cells 36 hours after infection with Ad-Angiostatin. Angiostatin protein production from infected HUVEC cells was confirmed by Western immunoblotting using a unique chicken polyclonal antibody raised against rabbit plasminogen. Concentrated culture supernatants from infected cells revealed an intense band at approximately 50 kDa in the cultures transduced with Ad-Angiostatin, but not in those transduced with Ad- dl70-3. Migration of this band appeared to be influenced by residual albumin from the culture media that was retained by the lysine-Sepharose bead. This intense band was actually a doublet which was apparent in the unconcentrated culture supernatant, where two distinct bands with approximate molecular weights between 50 and 60 kDa were observed. No bands were visible in the mock infected lane indicating that the results were not an artifact of plasminogen degradation from the culture media.

The binding of the angiostatin to the lysine-sepharose would suggest that the four complex kringle domains, each containing three intra-kringle disulfide bonds have formed correctly. (Degen et al., 1990; Sim et al., 1997). Two protein species of 49 and 51 kDa have been reported in the production of recombinant human angiostatin from *Pichia pastoris* as a result of different glycosylation patterns (Sim

et al., 1997). Human plasminogen exists in two glycosylation forms: type 1, is N-glycosylated at $Asparagine_{289}$ and O-linked at $Threonine_{346}$; type 2 is O-glycosylated at $Threonine_{346}$ only (Miyashita et al., 1988)(Castellino, 1984)(Degen et al., 1990). This glycosylation pattern is retained in all mammals including the mouse which has two putative glycosylation sites at $Asparagine_{288}$ and $Threonine_{345}$ (Degen et al., 1990). The two protein bands in the Western blot may represent differences in the glycosylation patterns of plasminogen, which have been retained by angiostatin.

We then used an unique approach to study the effects of Ad-Angiostatin in a matrigel model of bFGF induced angiogenesis. Matrigel is an extracellular matrix preparation from the Engelbreth-Holm-Swarm (EHS) mouse tumor and is composed primarily of laminin and collagen (Baatout, 1997). Unlike other angiogenesis assays including the chick chorioallantoic membrane (CAM) assay and the corneal pocket assay, matrigel offers distinct advantages which inciude, minimal trauma to the animal, relative ease with which the matrigel can be prepared, and the ability to quantify the vascular invasion (Jain et al., 1997). In the bFGF induced model of angiogenesis, matrigel permitted the study of an almost exclusive population of endothelial cells *in vivo* with minimal interference from adjacent cells or tissue.

Matrigel alone, or in combination with bFGF plus Ad-dl70-3 or Ad-Angiostatin, was injected subcutaneous into the abdominal midline of C57BL/6

mice. A week later the matrigel plugs were removed and processed for histology. Masson's trichrome staining revealed no cellular invasion into the matrigel alone. The addition of an angiogenic factor such as bFGF promoted a large infiltration of endothelial cells, that began to form functional capillaries. Electron microscopy of the matrigel sections demonstrated that the majority of cells within the matrigel were endothelial cells as indicated by the presence of Weibel Palade bodies, which are unique to these cells. Red blood cells were evident in the developing capillaries indicative of anastomoses, connection of the newly formed capillaries to existing vasculature in the mouse. The inclusion of Ad-Angiostatin, but not the control virus, eliminated capillary formation and restricted endothelial cell migration to a small region along the border of the matrigel and normal tissue. Inactive granulocytes, mainly eosinophils with their storage granules intact, were also visible indicating that no inflammatory processes were occurring within the matrigel.

In the bFGF and bFGF plus control virus treated matrigel sections, the endothelial cells maintained the normal spindle shaped morphology, and the cell nuclei were not visible. In contrast, the Ad-Angiostatin treated cells appear rounded with picnotic nuclei indicative of apoptosis (Claesson-Welsh et al., 1998). Electron microscopy of the matrigel sections confirmed that the cells had undergone apoptosis in the Ad-Angiostatin treated group.

The use of matrigel offered an unobstructed view of the processes involved in angiogenesis. The histological staining and electron microscopy revealed that

at day seven, none of the endothelial cells invading the matrigel were observed as being in a mitotic state. This observation is in agreement with the current literature with regards to the initial processes in angiogenesis whereby invading endothelial cells migrate from established capillaries in the tissue in response to the angiogenic stimuli (Jain et al., 1997). It is also possible that angioblasts from the blood, in response to the proper stimulation migrate and differentiate into functioning endothelial cells.

Murine angiostatin expressed from the adenovirus vector not only inhibited endothelial cell migration in the matrigel assay, but it also effectively inhibited the proliferation of HUVEC cells *in vitro*. This effect was specific to Ad-Angiostatin demonstrating that the activity of murine angiostatin is not limited to mouse endothelial cells.

The mechanism by which angiostatin exerts its endothelial cell specific apoptotic effects is not known. Griscelli and co-workers (1998) reported that angiostatin affects only mitotically active endothelial cells by disrupting the G_2/M phase of the cell cycle (Griscelli et al., 1998). However, reports by Lucas and co-workers (1998) as well as Luo et al (1998) observed no effects of angiostatin on cell cycle progression (Lucas et al., 1998;Luo et al., 1998).

A putative receptor for angiostatin has been identified as the α and β subunits of the ATP synthase molecule expressed on the surface of HUVEC cells (Moser et al., 1999). The report by Moser and co-workers (1999) put forth a

hypothesis that included the up regulation of the surface receptor on HUVEC cells in response to the hypoxic conditions of the tumor environment in an attempt by the endothelial cell to maintain high ATP levels. Angiostatin inhibits ATP production by binding to the ATP synthase complex causing endothelial cell death and blood vessel disruption. However, this report did not explain why cultured HUVEC cells under non-hypoxic conditions still expressed a high number of cell surface ATP synthase complexes. The study also did not examine whether angiostatin could inhibit mitochondrial ATP synthase complexes. Moreover, it is not clear why angiostatin is specific only for endothelial cells when ATP synthase is found in all cell types and is often over expressed in tumors. Angiostatin has also been shown to induce the activity of focal adhesion kinases, normally associated with integrin binding (Claesson-Welch et al., 1998). The conclusion of this report was that angiostatin altered normal integrin signalling pathways towards ones that promote apoptosis. However, as with the previously described study, the angiostatin receptor was not identified and no direct binding to any integrin was established.

Angiostatin-based therapy could be applied to all forms of solid tumors to inhibit the growth of both the primary lesion and any metastatic disease. Anti-angiogenesis therapy may represent a universal treatment for cancer because all solid tumors require neovascularization to grow, and the endothelial cell appears to be the same in all tumor types. In addition, the genetically stable endothelial cell is not transformed, and is less likely develop clonal resistance to chemotherapeutic

agents than the tumor cells.

The reduction of metastases in the lung is an example of how an adenovirus expressing angiostatin could be used to reduce the tumor burden. Since adenovirus is naturally tropic for the lung epithelium, the delivery of an Ad-Angiostatin vector could be delivered directly as an inhalant. In the PyMidT metastatic breast cancer model described here, intranasal delivery reduced the number of tumor nodules in the lungs of treated mice, but did not appear to induce any apparent abnormal pathology to the lung tissue. However, Ad-Angiostatin treatment did not totally inhibit the growth of the metastatic nodules, and therefore, angiostatin therapy may need to be combined with traditional therapies like radiation or with gene therapy induced immunotherapy to achieve optimal results.

Mauceri and co-workers (1998), combined systemic angiostatin with radiation therapy in a mouse Lewis lung carcinoma model. Their results indicated that the combination therapy had an additive effect in reducing tumor size in mice. The study also observed enhanced endothelial cell death *in vitro* when HUVEC cells, but not tumor cells, were treated with angiostatin followed by radiated (Mauceri et al., 1998).

The combination of angiostatin and endostatin, a carboxyl-terminal fragment of collagen XVIII which also possesses angiostatic properties, produced enhanced tumor regression in a transgenic RIP1-Tag2 mouse pancreatic carcinoma model (Bergers et al., 1999). The development of tumors in these mice occurs 5 weeks

after birth and progresses in three stages: the angiogenic and transformation stage from weeks 5-10; the small tumor stage at weeks 10-13 and; the invasive tumor stage at week 13 followed by the death of all animals. Angiostatin alone was most effective in reducing tumor burden in the first stage of tumor development, but had limited effects at the later stages of tumor progression. A similar trend was reported for endostatin. However, when these proteins were combined, significant reductions in tumor burden were observed at the angiogenic and invasive tumor stages (Bergers et al., 1999). This study was unique in that it did not involve a xenograft tumor model, but rather the RIP1-Tag2 cancers developed from normal cells, within the native tissue environment and progressed through multiple stages in a manner similar to the development of cancer in humans. The study also demonstrates that the stage at which angiostatin is delivered may be important for obtaining maximum angiostatic benefits.

The potential of a combined anti-angiogenesis and immunotherapy regime for cancer is extremely attractive. The results obtained with angiostatin in the matrigel and lung metastases models suggests that angiostatin is safe with no associated toxicity targeting only endothelial cells. However, a single administration of Ad-Angiostatin can suppress tumor growth but cannot totally regress tumors. Immunotherapy has the advantage of generating a T cell mediated tumor specific response associated with long term memory.

Transgenic PyMidT FVB/n mice develop spontaneous adenocarcinomas of

all the mammary epithelium at 8-10 weeks of age. The tumors were removed and homogenised into single cell suspensions which were reinjected s.q. into the right flank of syngeneic FVB/n female hosts. Palpable tumors with an average size of 150 mm^3 develop 18-21 days later at which time they were injected with adenovirus. Although the PyMidT cells express an antigenic viral protein, no immune rejection of the cells has been reported and all of the injected mice develop tumors (Addison et al., 1995).

Previous studies using an adenovirus expressing IL-12 alone demonstrated a 30% total regression in all PyMidT tumor bearing animals which was associated with long term immunity against re-challenge with levels of IFNγ peaking at days 6-9. IL-12 expression was also shown to stimulate NK cell activity in the spleens and lungs of C57BL/6 mice (Bramson et al., 1996).

In our study, only 20% of mice bearing PyMidT tumors injected with Ad-IL-12 alone underwent initial tumor regression and only 13% developed a total tumor regression. Mice injected with Ad-Angiostatin alone had an initial regression of 65% but none of the mice went on to develop total regressions. The combination Ad-Angiostatin and Ad-IL-12 gene therapy vectors appeared to have synergistic (or additive) benefits in the middle T breast cancer model. This treatment regime produced initial tumor regression in 96% of mice, with 54% of the mice being cured. These mice developed a strong CTL response and were resistant to re-challenge with the tumor.

The combination therapy was well tolerated by all of the mice injected. The relatively benign nature of Ad-Angiostatin allows for the inclusion of Ad-IL-12 at 5 X 10^8 pfu, which has previously been shown to be most efficacious, yet not toxic (Bramson et al., 1996). While Ad-Angiostatin produced no apparent side effects at 1 X 10^9 pfu, the combination therapy utilized 5 X 10^8 pfu of each adenovirus such that the total virus injected did not exceed 1 X 10^9 pfu. It was hoped that the maximum potential of angiogenesis inhibition and immune stimulation would be exploited from both viruses. Unexplained toxicity was associated in the deaths of two mice in the combination treatment group 13 days after injection. Both mice had undergone significant tumor regressions but based on the expression pattern of IL-12 established by Bramson et al (1996) it is unlikely this was related to IL-12 toxicity. It is more probable that the mice succumbed to possible thrombosis or embolisms as a result of apoptotic or necrotic tumor fragments entering the circulatory system.

The use of Ad-Angiostatin in the transgenic PyMidT breast cancer model demonstrates the ability of this vector to limit tumor growth by inhibiting angiogenesis. Tumor growth was reduced in mice treated with Ad-Angiostatin as compared to the control treated mice. This reduction in the rate at which the tumors expanded, increased the survival of the Ad-Angiostatin treated mice by 14 days in most cases. A single mouse underwent a total tumor regression 4 weeks after injection with angiostatin. However by week 8 the tumor had re-emerged. This

mouse survived 42 days longer than the average over the Ad-dl70 treated animal.

This scenario illustrates the short comings of the transient nature of protein expression from the first generation adenoviral vectors. The rapid re-emergence of tumor growth appears to coincide with the clearance of the adenovirus from the animal. Once the adenovirus is gone, and the expression of angiostatin is lost, the tumor can again progress. Similar findings were reported by Griscelli et al (1998), and Tanaka and co-workers (1998), using adenoviruses expressing human and murine angiostatin, respectively, in intracranial glioma models in nude mice.

Mice receiving Ad-Angiostatin did not have any noticeable gross side effects nor was there any mortalilty associated with the administration of this vector at concentrations as high as 1 X 10^9 pfu. One anecdotal observation however is that mice receiving angiostatin alone or in combination with IL-12 had excessive adipose deposition in the abdominal area as compared to mice receiving other treatments. This fat deposition did not appear to depend on the size of the tumor and was also observed in mice which had received intranasal delivery of Ad-Angiostatin to treat the pulmonary breast metastases.

In addition to its ability to generate a potent T1 cytokine profile, IL-12 has also been recognized for its ability to inhibit angiogenesis (Voest et al., 1995). The initial tumor regressions with IL-12 alone may indicate vascular disruption that could precede the development of a tumor specific T cell mediated response. However, this does not eliminate a role for the immune systems role in the delay in tumor

growth. Corneal neovascularization studies in SCID mice deficient in T and B cells demonstrated inhibition of bFGF induced angiogenesis which could be abrogated with anti-IFNγ antibodies (Voest et al., 1995). *In vitro*, neither IL-12 nor IFNγ was shown to affect endothelial cell proliferation. In another study, recombinant IL-12, using a bFGF matrigel model in nude mice, was found to activate NK cells which in turn released IFNγ. IFNγ was found to act on bystander cells, including endothelial cells, to produce IP-10. The locally produced IP-10 feeds back in a paracrine manner to recruit more NK cells that subsequently become activated and exhibit cytolytic activity towards endothelial cells (Dellabona et al., 1999;Yao et al., 1999). If this model of IL-12 inhibition of angiogenesis is correct, then NK cells, IFNγ and IP-10 must all be involved in this anti-angiogenesis phenomenon within the tumor. Therefore, the initial response of the tumor to the administration of Ad-IL-12 may be due to the destruction of the tumor vasculature followed by a T cell-mediated response to tumor associated antigen (TAA). However, the T cell-mediated cytotoxic response is necessary for inducing long-term protection and maybe responsible for the 13% total regressions which were resistant to re-challenge.

The enhanced tumor regressions of the combination Ad-IL-12 and Ad-Angiostatin may be a result of the increased availability of TAA to antigen presenting cells. Conceivably, the necrosis and apoptosis seen in the CD31 stained tumor sections may enhance the number of antigen presenting cells and

may make TAA more accessible. The low level of total regressions seen with IL-12 alone may indicate that the PyMidT tumors could have some immuno-suppressive activity. The PyMidT cell line has been found to secrete significant levels of IL-10, a cytokine which can inhibit T1 cell mediated responses (Emtage, 1998). Other factors including the CD95 or Fas ligand have been reported to be over expressed on the surface of melanoma and liver carcinomas (Strand et al., 1996). The expression of this molecule can lead to apoptosis of T cells expressing Fas, the receptor for the Fas ligand. A mechanism for the enhanced efficacy in the combination therapy may involve an initial reduction of the number of viable tumor cells which could support such immuno-suppressive activities. Disruption of the vasculature by angiostatin, leading to tumor necrosis and apoptosis could break down any immune "privilege" allowing IL-12 to elicit a more successful T cell mediated response. The increased amount of cellular debris from the dead tumor cells, may also enhance the amount of tumor antigen available to infiltrating antigen presenting cells.

Histological examination of PyMidT tumors which underwent initial regression appeared to support the role of IL-12 as an inhibitor of angiogenesis. In these tumors the amount of CD31 staining was significantly less than that seen in the Ad-dl70-3 treated tumors. In addition, massive areas of tumor necrosis and apoptosis were observed within the Ad-IL-12 treated tumor which was not apparent in the control tumors. CD31 staining in the Ad-Angiostatin treated tumor was also

significantly reduced, and large necrotic and apoptotic regions were evident. The combination of Ad-Angiostatin and Ad-IL12 lead to a further decrease of CD31 staining demonstrating the positive benefit of the combination therapy. However, the amount of reduction in the combination treatment was not significantly less than that seen with the vectors used alone.

In conclusion, this study demonstrated that a short term course of anti-angiogenic therapy combined with immunotherapy can effectively shrink a solid tumor and provide an animal with protective immunity. The approach is novel in that it combines the activity the angiogenesis inhibitor angiostatin, with the immune stimulatory cytokine IL-12 via adenoviral gene therapy vectors directly in the tumor environment. The combination Ad-Angiostatin with cytokine expressing vectors is attractive because of the lack of toxicity associated with angiostatin. In addition, the anti-angiogenesis therapy leads to a rapid reduction of tumor mass leading to a possible reduction in the immuno-suppressive environment allowing a CTL response to be generated by the cytokine.

Interleukin-18, is a T1 cytokine with biological properties similar to those of IL-12 (Okamura et al., 1995). A direct comparison to IL12 in the tumor model was therefore undertaken. Both the human and murine versions of IL-18 were cloned, and adenoviral vectors containing these genes were constructed. While Northern blot analysis confirmed the expression of IL-18, Western immunoblotting using commercially available antibodies failed to detect any secreted IL-18 protein in the

culture supernatants from the infected A549 cells. However, A549 cell lysates infected with Ad-hIL-18 but not the murine homologue, were positive by immunoblotting for the mature hIL-18 protein. In addition a biological assay designed to detect IFNγ production from splenocytes or PBMC stimulated with IL-18 conditioned media and Con A failed to detect any biological activity. These results indicated that IL-18 was not being secreted from infected cells. The failure to detect secreted IL-18 was most likely due to its unique activation pathway requiring caspase 1 or ICE. Osaki and co-workers (1999) reported similar difficulties in producing retroviral and adenoviral vectors containing the full length IL-18 cDNA. Their solution to this problem was to add a conventional hydrophobic signal sequence from the parathyroid hormone to the cDNA of the mature IL-18 protein (Osaki et al., 1999).

IL-18 is formed in cytoplasm of LPS activated macrophages where the IL-18 exists in an inactive precursor form (Ghayur et al., 1997). As these cells undergo apoptosis, ICE, a key regulatory protein of the apoptotic pathway, cleaves the initial 35 amino acids from the inactive IL-18 precursor generating mature, biologically active IL-18. Presumably this is followed by release of the mature IL-18 as the cell begins to fragment and break apart. Our observation that mature hIL18 was detected in the cytoplasm of infected A549 cells may indicate an alternate pathway. However, without a hydrophobic export sequence, secretion of the mature protein would still require of membrane breakdown.

Recombinant murine IL-18 was generated by expressing the cDNA for the mature, biologically active protein in bacteria. This recombinant material was purified from the cytoplasm of *Escherichia coli* using a charged Nickel affinity column specific for hexa-Histadine residues added to the N-terminus of the protein. The recombinant mIL-18 retained biological activity in the splenocyte IFNγ assay, and was shown to possess the ability to inhibit angiogenesis in the bFGF induced matrigel model. Interestingly the mechanism of angiogenesis inhibition appears to be different than that seen in the angiostatin studies. In the angiostatin studies, the endothelial cells all had picnotic nuclei indicative of apoptosis. This phenomenon was not visible in the IL-18 treated matrigel. Rather, it appeared that there was a decrease in endothelial cell migration into the matrix. This is consistent with the activities of IP-10 and Mig as inhibitors of angiogenesis (Sgadari et al., 1997). Therefore, IL-18 like IL-12 inhibits angiogenesis through IFNγ dependent mechanisms.

Previous studies have shown that recombinant IL-18 or IL-18 produced *in situ* using viral vectors can cause tumor regressions in mice (Osaki et al., 1999;Micallef et al., 1997). The injection of recombinant IL-18 into the PyMidT tumor model at the concentrations used in previous reports, did not cause any tumor regressions. The combination of IL-18 with Ad-Angiostatin did not significantly delay tumor growth compared to Ad-Angiostatin alone. Due to model differences, our results cannot be compared to the previously published data.

Whereas our model system involves 21 day established tumors, previous reports administered recombinant IL-18 or an adenovirus expressing IL-18 to the mice before or shortly after the injection of tumor cells. Moreover, we delivered the IL-18 protein directly into the tumor and whereas other groups have used alternative routes of administration including intravenous or intraperitoneal, which may be more beneficial.

This thesis has attempted to show the pre-clinical benefits of combination anti-angiogenesis and immunotherapy in a murine breast cancer model. The expression of angiostatin by an adenoviral vector delivered directly into a solid tumor was shown to delay tumor growth, but did not lead to tumor regression. The combination of Ad-Angiostatin with Ad-IL-12, a potent activator of the immune system was shown to be a safe and effective therapy producing regressions in 54% of the treated tumors. The work in this thesis is the first to combine a strictly angiostatic molecule with an immuno-stimulatory cytokine using gene transfer technology. Moreover, it has shown the anti-neoplastic activity of Ad-Angiostatin and supports further studies combining this vector with other cytokine combinations which should prove to be beneficial in the treatment of cancer.

Reference List

Addison, C., Bramson, J.L., Hitt, M., Muller, W.J., Gauldie, J., and Graham, F.L. (1998). Intratumoral coinjection of adenoviral vectors expressing IL-12 and IL-12 results in enhanced frequency of regression of injected and untreated tumors. Gene Ther *5*, 1400-1409.

Addison, C.L., Braciak, T., Ralston, R., Muller, W.J., Gauldie, J., and Graham, F.L. (1995). Intratumoral injection of an adenovirus expressing interleukin 2 induces regression and immunity in a murine breast cancer model. Proc Natl Acad Sci U S A *92*, 8522-8526.

Akita, K., Ohtsuki, T., Nukada, Y., Tanimoto, T., Namba, M., Okura, T., Takakura-Yamamoto, R., Torigoe, K., Gu, Y., Su, M.S.S., Fujii, M., Satoh-Itoh, M., Yamamoto, K., Kohno, K., Ikeda, M., and Kurimoto, M. (1997). Involvement of caspase-1 and caspase-3 in the production and processing of mature human interleukin 18 in monocytic THP.1 cells. J Biol Chem *272*, 26595-26603.

Alberts, B., Bray, D., Lewis, J., Raff, M., Roberts, K., and Watson, J.D. (1994). Molecular Biology of The Cell, New York: Garland Publishing, 1258-1261.

Alon, T., Hemo, I., Itin, A., Pe'er, J., Stone, J., and Keshet, E. (1995). Vascular endothelial growth factor acts as a survival factor for newly formed retinal vessels and has implications for retinopathy of prematurity. Nat Med *1*, 1024-1028.

Angiolollo, A.L., Sgadari, C., Taub, D.D., Liao, F., Farber, J.M., Maheswari, S., Kleinman, H.K., Reaman, G.H., and Tosato, G. (1995). Human Interferon-inducible protein 10 is a potent inhibitor of angiogenesis *in vivo*. J.Exp.Med. *182*, 162

Asahara, T, Murohara, T, Sullivan, A, Silver, M, van der Zee, R, Li, T, Witzenbichler, B, Schatteman, G, and Isner, J. (1997). Isolation of putative endothelial cells for angiogenesis. Science *275*, 964-967.

Baatout, S. (1997). Endothelial differentiation using matrigel. Anticancer Res *17*, 451-456.

Bachmann, F, Egbert, I, and Kruithof, K. O. (1984) Tissue plasminogen activator: Chemical and physiological aspects. Seminars in Thrombosis and Hemostasis *10*, 6-17.

Bargou, R., Jurchott, K., Wagener, C., Bergmann, S., Metzner, S., Bommert, K., Mapara, M., Winzer, K., Dietel, M., Dorken, B., and Royer, H.-D. (1997). Nuclear localization and increased levels of transcription factor YB-1 in

primary human brreast cancers are associated with intrinsic MDR1 gene expression. Nat Med *3*, 447-450.

Barinaga, M. (1997). Designing therapies that target tumor blood vessels. Science *275*, 482-484.

Barinaga, M. (1999). Cancer research. A surprising partner for angiostatin [news]. Science *283*, 1831

Bartek, J, Lukas, J, and Bartkova, J. (1999). Perspective: Defects in cell cycle control and cancer. J.Pathology *187*, 95-99.

Baserga, R. (1993). Principles of molecular cell biology of cancer: The cell cycle. In Cancer: Principles & Practice of Oncology. Vincent T.DeVIta, Samual Hellman, and Steven A.Rosenberg, eds. (Philadelphia: J.B. Lippincott Co), pp. 60-66.

Battista, P. and Soderland, C. (1998). Serum-Free Culture of Human Venous and Artierial Endothelial Cells. In Cell Biology: A Laboratory Handbook. J.E. Celis, ed. (San Diego: Academic Press), pp. 137-141.

Benezra, M., Vlodavsky, I., Ishai-Michaeli, R., Neufeld, G., and Bar-Shavit, R. (1993). Thrombin-induced release of active basic fibroblast growth factor-heparan sulfate complexes from subendothelial extracellular matrix.

Blood *81*, 3324-3331.

Bergers, G., Javaherian, K., Lo, K., Folkman, J., and Hanahan, D. (1999). Effects of angiogenesis inhibitors on multistage carcinogenesis in mice. Science *284*, 808-812.

Bergh, J., Norberg, T., Sjogren, S., Lindgren, A., and Holmberg, L. (1995). Complete sequencing of the p53 gene provides prognostic information in breast cancer patients, particularly in relation to adjuvant systemic therapy and radiotherapy. Nat Med *1*, 1029-1034.

Bett, A.J., Haddara, W., Prevec, L., and Graham, F.L. (1994). An efficient and flexible system for construction of adenovirus vectors with insertions or deletions in early regions 1 and 3. Proc Natl Acad Sci U S A *91*, 8802-8806.

Blezinger, P., Wang, J., Gondo, M., Quezada, A., Mehrens, D., French, M., Singhal, A., Sullivan, S., Rolland, A., Ralston, R., and Min, W. (1999). Systemic inhibition of tumor growth and tumor metastases by intramuscular administration of the endostatin gene. Nat Med *17*, 343-348.

Boehm, U., Klamp, T., Groot, M., and Howard, J. (1997). Cellular responses to interferon-γ. Ann Rev Immunol *15*, 749-795.

Bramson, J., Hitt, M., Gallichan, W.S., Rosenthal, K.L., Gauldie, J., and Graham, F.L. (1996). Construction of a double recombinant adenovirus vector expressing a heterodimeric cytokine: in vitro and in vivo production of biologically active interleukin-12. Hum Gene Ther *7*, 333-342.

Bramson, J.L., Graham, F.L., and Gauldie, J. (1995). The use of adenoviral vectors for gene therapy and gene transfer in vivo. Curr Opin Biotechnol *6*, 590-595.

Bramson, J.L., Hitt, M., Addison, C.L., Muller, W.J., Gauldie, J., and Graham, F.L. (1996). Direct intratumoral injection of an adenovirus expressing interleukin- 12 induces regression and long-lasting immunity that is associated with highly localized expression of interleukin-12. Hum Gene Ther *7*, 1995-2002.

Brooks, P.C., Clark, R.A., and Cheresh, D.A. (1994a). Requirement of vascular integrin αvβ3 for angiogenesis. Science *264*, 569-571.

Brooks, P.C., Montgomery, A.M., Rosenfeld, M., Reisfeld, R.A., Hu, T., Klier, G., and Cheresh, D.A. (1994b). Integrin αvβ3 antagonists promote tumor regression by inducing apoptosis of angiogenis blood vessels. Cell *79*, 1157-1164.

Brooks, P.C., Stromblad, S., Klemke, R., Visscher, D., Sarkar, F., and Cheresh,

D.A. (1995). Antiintegrin αvβ3 blocks human breast cancer growth and angiogenesis in human skin. J Clin Invest *96*, 1815-1822.

Brunda, M.J. and Gately, M.K. (1995). Interleukin-12: Potential role in cancer therapy. In Important Advances in Oncology. V.T. deVita, S. Hellman, and S.A. Rosenberg, eds. (Philadelphia: Lippincott Company), pp. 3-18.

Cantley, L, Auger, K, Carpenter, C, Duckworth, B, Graziani, A, Kapeler, R, and Soltoff, S. (1991) Oncogenes and signal transduction. Cell *64*, 281-302.

Cao, Y., Ji, R.W., Davidson, D., Schaller, J., Marti, D., Sohndel, S., McCance, S.G., O'Reilly, M.S., Llinas, M., and Folkman, J. (1996). Kringle domains of human angiostatin. Characterization of the anti- proliferative activity on endothelial cells. J Biol Chem *271*, 29461-29467.

Castellino, F. J. (1984) Biochemistry of human plasminogen. Seminars in Thrombosis and Hemostasis *10*, 18-23.

Cherwinski, H., Schumacher, J.H., Brown, K., and Mossman, T.R. (1987). Two types of mouse helper T cell clone III. Further differences in lymphokine synthesis between Th1 and Th2 clones revealed by RNA hybridization, functionally monospecific bioassays, and monoclonal antibodies. J Exp Med *166*, 1229-1244.

Cines, D.B., Pollak, E.S., Buck, C.A., Loscalzo, J., Zimmerman, G.A., McEver, R.P., Pober, J.S., Wick, T.M., Konkle, B.A., Schwartz, B.S., Barnathan, E.S., McCrae, K.R., Hug, B.A., Schmidt, A.M., and Stern, D.M. (1998). Endothelial cells in physiology and in the pathophysiology of vascular disorders. Blood *91*, 3527-3561.

Claesson-Welsh, L., Welsh, M., Ito, N., Anand-Apte, B., Soker, S., Zetter, B., O'Reilly, M., and Folkman, J. (1998). Angiostatin induces endothelial cell apoptosis and activation of focal adhesion kinase independently of the integrin-binding motif RGD. Proc Natl Acad Sci U S A *95*, 5579-5583.

Cotran, R., Kumar, A., and Robbins, S.L. (1996). The Breast. In Pathological Basis of Disease. R. Cotran, A. Kumar, and S.L. Robbins, eds. (Toronto: W.B. Saunders), pp. 1089-1111.

Coughlin, C.M., Salhany, K.E., Gee, M.S., LaTemple, D.C., Kotenko, S., Ma, X., Gri, G., Wysocka, M., Kim, J.E., Liu, L., Liao, F., Farber, J., Pestka, S., Trinchieri, G., and Lee, W.M.F. (1998). Tumor cell responses to IFNγ affect tumorigenicity and response to IL12 therapy and antiangiogenesis. Immunity *9*, 34

Coughlin, C.M., Salhany, K.E., Wysocka, M., Aruga, E., Kurzawa, H., Chang, A.E., Hunter, C.A., Fox, J.C., Trinchieri, G., and Lee, W.M.F. (1998).

Interleukin-12 and interleukin-18 synergistically induce murine tumor regression which involves inhibition of angiogenesis. J Clin Invest *101*, 1441-1452.

Dameron, K.M., Volpert, O.V., Tainsky, M.A., and Bouck, N. (1994). Control of angiogenesis in fibroblasts by p53 regulation of thrombospondin-1. Science *265*, 1582-1584.

Davis, S., Aldrich, T.H., Jones P.F, Acheson, A., Compton, D.L., Jain, V., Ryan, T.E., Bruno, J., Radziejewski, C., Maisonpierre, P.C., and Yancopoulos, G.D. (1996). Isolation of angiopoietin-1 a ligand for the TIE2 receptor, by secretion trap expression cloning. Cell *87*, 1161-1169.

Degen, S.J., Bell, S.M., Schaeffer, L., and Elliott, R.W.(1990). Characterization of the cDNA coding for mouse plasminogen and localization of the gene to mouse chromosome 17. Genomics *8*, 49-61.

Dellabona, P., Moro, M., Crosti, M.C., Casorati, G., and Corti, A. (1999). Vascular attack and immunotherapy: a 'two hits' approach to improve biological treatment of cancer. Gene Therapy *6*, 153-154.

deVries, T.J., vanMuijen, G.N., and Ruiter, D.J. (1996). The plasminogen activator system in tumor invasion and metatasis. Path Res Prac *192*, 718-733.

Dinarello, C.A., Novick, D., Puren, A.J., Fantuzzi, G., Shapiro, L., Muhl, H., Yoon, D.Y., Reznikov, L.L., Kim, S.H., and Rubinstein, M. (1998). Overview of interleukin-18: more than an interferon-gamma inducing factor. J Leukoc Biol *63*, 658-664.

Dong, Z., Kumar, R., Yang, X., and Fidler, I.J. (1997). Macrophage-derived metalloelastase is responsible for the generation of angiostatin in Lewis lung carcinoma. Cell *88*, 801-810.

Douglas, J.T. and Curiel, D.T. (1997). Adenoviruses as vectors for gene therapy. Science and Medicine *4*, 44-53.

Elledge, R. and Allred, D.C. (1998). Prognostic and predictive value of p53 and p21 in breast cancer. Breast Cancer Res Treat *52*, 79-98.

Emtage, P. (1998).Cytokine therapy of cancer by gene therapy transfer. 234-234. Ph.D thesis, McMaster University.

Emtage, P.C., Wan, Y., Bramson, J.L., Graham, F.L., and Gauldie, J. (1998). A double recombinant adenovirus expressing the costimulatory molecule B7-1 (murine) and human IL-2 induces complete tumor regression in a murine breast adenocarcinoma model. J Immunol *160*, 2531-2538.

Fearon, D.T. and Locksley, R.M. (1996). The instructive role of innate immunity

in the aquired immune response. Science *272* , 50-54.

Fearon, E.R. (1997). Human cancer syndromes: clues to the origin and nature of cancer. Science *278*, 1043-1050.

Flamme, I and Risau, W.(1992) Induction of vasculogenesis and hematopoiesis. Development *116*, 435-439.

Folkman, J. (1995). Clinical applications of research on angiogenesis. New England Journal of Medicine *333*, 1757-1763.

Folkman, J. and D'Amore, P.A. (1996). Blood Vessel Formation: What is its molecular basis? Cell *87*, 1153-1155.

Folkman, J. and Shing, Y. (1992). Angiogenesis. J Biol Chem *267*, 10931-10934.

Fornier, M., Munster, P., and Seidman, A. (1999). Update on the management of advanced breast cancer. Oncology *13*, 647-658.

Friedmann, T. (1997). Overcoming the obstacles to gene therapy. Sci Am *276*, 96-101.

Gately, S., Twardowski, P., Stack, M.S., Cundiff, D.L., Grella, D., Castellino, F.J., Enghild, J., Kwaan, H.C., Lee, F., Kramer, R.A., Volpert, O., Bouck, N.,

and Soff, G.A. (1997). The mechanism of cancer-mediated conversion of plasminogen to the angiogenesis inhibitor angiostatin. Proc Natl Acad Sci U S A *94*, 10868-10872.

Gately, S., Twardowski, P., Stack, M.S., Patrick, M., Boggio, L., Cundiff, D.L., Schnaper, H.W., Madison, L., Volpert, O., Bouck, N., Enghild, J., Kwaan, H.C., and Soff, G.A. (1996). Human prostate carcinoma cells express enzymatic activity that converts human plasminogen to the angiogenesis inhibitor, angiostatin. Cancer Res *56*, 4887-4890.

Germann, T., Gately, M.K., Schoenhaut, D., Lohoff, M., Mattner, F., Fischer, S., Jin, S.-C., Schmitt, E., and Rude, E. (1993). Interleukin-12/T cell stimulating factor, a cytokine with multiple effects on T helper type 1(Th1) but not on Th2 cells. Eur J Immunol *23*, 1762-1770.

Gerritsen, M.E. (1996). Physiological functions of normal endothelial cells. In Vascular Medicine. J. Loscalzo, M.A. Creager, and V.J. Drar, eds. (New York: Little Brown and Co.), pp. 3-38.

Ghayur, T., Banerjee, S., Hugunin, M., Butler, D., Herzog, L., Carter, A., Quintal, L., Sekut, L., Talanian, R., Paskind, M., Wong, W., Kamen, R., Tracey, D., and Allen, H. (1997). Caspase-1 processes IFN-gamma-inducing factor and regulates LPS-induced IFN-gamma production. Nature *386*, 619-

623.

Ghosh-Choudhury, G., Haj-Ahmad, Y., Brinkley, P., Rudy, J., and Graham, F.L. (1986). Human adenovirus cloning vectors based on infectious bacterial plasmids. Gene *50*, 161-171.

Graham, F.L., Smiley, J.R., Russell, W.C., and Nairn, R. (1977). Characteristics of a human cell line transformed by DNA from human adenovirus type 5. J.Gen.Virol *36*, 59

Griscelli, F., Li, H., Bennaceur-Griscelli, A., Soria, J., Opolon, P., Soria, C., Perricaudet, M., Yeh, P., and Lu, H. (1998). Angiostatin gene transfer: inhibition of tumor growth in vivo by blockage of endothelial cell proliferation associated with a mitosis arrest. Proc Natl Acad Sci U S A *95*, 6367-6372.

Gu, Y., Kuida, K., Tsutsui, H., Ku, G., Hsiao, K., Fleming, M.A., Hayashi, N., Higashino, K., Okamura, H., Nakanishi, K., Kurimoto, M., Tanimoto, T., Flavell, R.A., Sato, V., Harding, M.W., Livingston, D.J., and Su, M.S. (1997). Activation of interferon-gamma inducing factor mediated by interleukin- 1beta converting enzyme. Science *275*, 206-209.

Guinan, E., Bribben, J., Boussiotis, V., Freeman, G., and Nadler, L. (1994). Pivotal role of the B7:CD28 pathway in transplantation tolerance and

tumor immunity. Blood *84*, 3261-3282.

Guy, C.T., Cardiff, R.D., and Muller, W.J. (1992). Induction of mammary tumors by expression of polyomavirus Middle T oncogene: A transgenic model for metastatic disease. Mol Cell Bio *12*, 954-961.

Guy, C.T., Cardiff, R.D., and Muller, W.J. (1996). Activated neu induces rapid tumor progression. J Biol Chem *271*, 7673-7678.

Guy, C.T., Muthuswamy, S.K., Cardiff, R.D., Soriano, P., and Muller, W.J. (1994). Activation of the c-Src tyrosine kinase is required for the induction of mammary tumors in transgenic mice. Genes Dev *8*, 23-32.

Hanahan, D. (1997). Signaling vascular morphogenesis and maintenance. Science *277*, 48-50.

Hanahan, D and Folkman, J. (1996) Patterns and emerging mechanisms of the angiogenic switch during tumorgenesis. Cell *86*, 353-364.

Harris, J.R., Morrow, M., and Bonadonna, G. (1993). Cancer of the breast. In Cancer: Principles and Practice of Oncology. V.T. deVita, S. Hellman, and S.A. Rosenberg, eds. (Philadelphia: J.B. Lippincott Co.), pp. 1264-1332.

Hartmann, W.H. (1984). Minimal breast cancer. An update. Cancer *53*, 681-684.

Hayes, D. F. (1994) Angiogenesis and breast cancer. Hematology/Oncology clinics of North America 8, 51-71.

Helmlinger, G., Yuan, F., Dellian, M., and Jain, R.K. (1997). Interstitial pH and pO_2 gradients in solid tumors *in vivo*: High -resolution measurements reveal a lack of correlation. Nat Med *3*, 177-182.

Hendrzak, J.A. and Brunda, M.J. (1995). Interleukin-12: Biological activity, therapeutic utility and role in disease. Laboratory Investigation *72*, 619-637.

Hitt, M., Bett, A., Prevec, L., and Graham, F.L. (1998). Construction and propagation of human adenovirus vectors. In Cell Biology: A Laboratory Handbook. J.E. Celis, ed. (San Deigo: Academic Press), pp. 500-512.

Holash, J., Maisonpierre, P.C., Compton, D., Boland, P., Alexander, C., Zagzag, D., Yancopoulos, G.D., and Wiegand, S. (1999). Vessel cooption, regression and growth in tumors mediated by angiopoitins and VEGF. Science *284*, 1994-1998.

Huang, X., Molema, G., King, S., Watkins, L., Edgington, T., and Thorpe, P. (1997). Tumor infarction in mice by antibody directed targeting of tissue factor to tumor vasculature. Science *275*, 547-550.

Hulett, M., Freeman, C., Hamdorf, B., Baker, R., Harris, M., and Parish, C. (1999). Cloning of mammalian heparanase, an important enzyme intumor invasion and metastasis. Nat Med *5*, 803-809.

Hunter, T and Pines, J. (1994) Cyclins and Cancer II: Cyclin D and CDK inhibitors come of age. Cell *79*, 573-582.

Jain, R.K. (1994). Barriers to drug delivery in solid tumors. Sci Am *271*, 58-65.

Jain, R.K., Schlenger, K., Hockel, M., and Yuan, F. (1997). Quantitative angiogenesis assays: Progress and problems. Nat Med *3*, 1203-1208.

Ji, W.R., Castellino, F.J., Chang, Y., DeFord, M.E., Gray, H., Villarreal, X., Kondri, M.E., Marti, D., Llinas, M., Schaller, J., Kramer, R.A., and Trail, P.A. (1998). Characterization of kringle domains of angiostatin as antagonists of endothelial cell migration, an important process in angiogenesis. FASEB *12*, 1731-1738.

Kerbel, R.S. (1997). A cancer therapy resistant to resistance [news]. Nature *390*, 335-336.

Klein, G and Klein, E. (1985) Evolution of tumors and the impact of molecular oncology. Nature *315*, 190-195.

Kohno, K., Kataoka, J., Ohtsuki, T., Suemoto, Y., Okamoto, I., Usui, M., Ikeda,

M., and Kurimoto, M. (1997). IFN-gamma-inducing factor (IGIF) is a costimulatory factor on the activation of Th1 but not Th2 cells and exerts its effect independently of IL-12. J Immunol *158*, 1541-1550.

Kohno, K. and Kurimoto, M. (1998). Interleukin 18, a cytokine which resembles IL-1 structurally and IL-12 functionally but exerts its effect independently of both. Clin Immunol Immunopathol *86*, 11-15.

Kojima, H., Takeuchi, M., Ohta, T., Nishida, Y., Arai, N., Ikeda, M., Ikegami, H., and Kurimoto, M. (1998). Interleukin-18 activates the IRAK-TRAF6 pathway in mouse EL-4 cells. Biochem Biophys Res Commun *244*, 183-186.

Laemmli, K. (1970). Cleavage of structural proteins during the assembly of the head of bacteriophage T4. Nature *227*, 680-685.

Lamont, A.G. and Adorini, L. (1996). IL-12: a key cytokine in immune regulation. Immunology Today *17*, 214-216.

Leek, R.D., Harris, A.L., and Lewis, C.E. (1994). Cytokine networks in solid human tumors: regulation of angiogenesis. J Leukoc Biol *56*, 423-435.

Levine, A.J. (1997). p53, the cellular gatekeeper for growth and division. Cell *88*, 323-331.

Low, K.B., Ittensohn, M., Le, T., Platt, J., Sodi, S., Amoss, M., Ash, O., Carmichael, E., Chakraborty, A., Fisher, S., Luo, X., Miller, S.,King, I., Pawelek, J.M., and Bermudes, D. (1999). Lipid A mutant *Salmonella* with suppressed virulence and TNFα induction retain tumor-targeting *in vivo*. Nat Biotech *17*, 37-41.

Lucas, L., Holmgren, L., Jimenez, G.B., Mandriota, S.J., Borlat, F., Sim, B.K.L., Wu, Z., Grau, Y., Shing, Y., Soff, G.A., Bouck, N., and Pepper, M.S. (1998). Multiple forms of angiostatin induce apoptosis in endothelial cells. Blood *92*, 4730-4741.

Luo, J., Lin, J., Paranya, G., and Bischoff, J. (1998). Angiostatin upregulates E-selectin in proliferating endothelial cells. Biochem Biophys Res Commun *245*, 906-911.

Maisonpierre, P.C., Suri, C., Jones P.F, Bartunkova, S., Wiegand, S., Radziejewski, C., Compton, D.L., McClain, J., Aldrich, T.H., Papadopoulos, N., Daly, T., Davis, S., Sato, T., and Yancopoulos, G.D. (1997). Angiopoietin-2, a natural antagonist for Tie2 that disrupts *in vivo* angiogenesis. Science *277*, 55-60.

Matsumoto, S., Tsuji-Takayama, K., Aizawa, Y., Koide, K., Takeuchi, M., Ohta, T., and Kurimoto, M. (1997). Interleukin-18 activates NF-kappaB in

murine T helper type 1 cells. Biochem Biophys Res Commun *234*, 454-457.

Mauceri, H.J., Hanna, N.N., Beckett, M.A., Gorski, D.H., Staba, M.J., Stellato, K.A., Bigelow, K., Heimann, R., Gately, S., Dhanabal, M., Soff, G.A., Sukhatme, V.P., Kufe, D.W., and Weichselbaum, R.R. (1998). Combined effects of angiostatin and ionizing radiation in antitumour therapy. Nature *394*, 287-291.

Micallef, M.J., Yoshida, K., Kawai, S., Hanaya, T., Kohno, K., Arai, S., Tanimoto, T., Torigoe, K., Fujii, M., Ikeda, M., and Kurimoto, M. (1997). In vivo antitumor effects of murine interferon-gamma-inducing factor/interleukin-18 in mice bearing syngeneic Meth A sarcoma malignant ascites. Cancer Immunol Immunother *43*, 361-367.

Miyashita, C, Wenzel, E, and Heiden, M. (1988) Plasminogen: A brief introduction into its biochemistry and function. Haemostasis *18* (supplement), 7-14.

Morrison, B. W. (1994) The genetics of breast cancer. Hematology/Oncology clinics of North America *8*, 15-27.

Moser, T. L, Stack, M. S., Asplin, I, Enghild, J., Hojrup, P, Everitt, L, Hubchak, S, Schnaper, H. W., and Pizzo, S. V. (1999). Angiostatin binds ATP

synthase on the surface of endothelial cells. Proc Natl Acad Sci U S A *96*, 2811-2816.

Mossman, T.R., Cherwinski, H., Bond, M.W., Giedlin, M., and Coffman, R. (1986). Two types of murine helper T cell clone I.Definition according to profiles of lymphokine activities and secreted proteins. J Immunol *136*, 2348-2357.

Norton, L. (1999). Kinetic concepts in the systemic drug therapy of breast cancer. Semin Oncol *26*, 11-20.

O'Connell, J., Bennett, M., O'Sullivan, G., Collins, J., and Shanahan, F. (1999). The FAS counterattack: cancer as a site of immune privilege. Immunology Today *20*, 46-51.

O'Reilly, M.S., Boehm, T., Shing, Y., Fukai, N., Vasios, G., Lane, W.S., Flynn, E., Birkhead, J.R., Olsen, B.R., and Folkman, J. (1997). Endostatin: an endogenous inhibitor of angiogenesis and tumor growth. Cell *88*, 277-285.

O'Reilly, M.S., Holmgren, L., Shing, Y., Chen, C., Rosenthal, R.A., Cao, Y., Moses, M., Lane, W.S., Sage, E.H., and Folkman, J. (1994a). Angiostatin: a circulating endothelial cell inhibitor that suppresses angiogenesis and tumor growth. Cold Spring Harb Symp Quant Biol *59*, 471-482.

O'Reilly, M.S., Holmgren, L., Shing, Y., Chen, C., Rosenthal, R.A., Moses, M., Lane, W.S., Cao, Y., Sage, E.H., and Folkman, J. (1994b). Angiostatin: a novel angiogenesis inhibitor that mediates the suppression of metastases by a Lewis lung carcinoma. Cell *79*, 315-328.

Okamura, H., Nagata, K., Komatsu, T., Tanimoto, T., Nukata, Y., Tanabe, F., Akita, K., Torigoe, K., Okura, T., Fukuda, S., and Kurimoto, M. (1998). A novel costimulatory factor for gamma interferon induction found in the livers of mice causes endotoxic shock. Infect Immun *63*, 3966-3972.

Okamura, H., Tsutsi, H., Komatsu, T., Yutsudo, M., Hakura, A., Tanimoto, T., Torigoe, K., Okura, T., Nukada, Y., and Hattori, K. (1995). Cloning of a new cytokine that induces IFN-gamma production by T cells. Nature *378*, 88-91.

Oppenheim, M. and Lotze, M.T. (1994). Interleukin-2: Solid tumor therapy. Oncology *51*, 154-169.

Oren, M. (1997). Lonely no more: p53 finds its kin in a tumor suppressor haven. Cell *90*, 829-832.

Osaki, T., Hashimoto, W, Okamura, H, Gambotto, A, Robbins, P. D., Kurimoto, M, Lotze, M. T., and Tahara, H. (1999). Potent antitumor effects mediated by local expression of the mature form of interferon gamma inducing

factor , interleulin-18 (IL-18). Gene Ther *6*, 808-815.

Osaki, T., Peron, J.M., Cai, Q., Okamura, H., Robbins, P.D., Kurimoto, M., Lotze, M.T., and Tahara, H. (1998). IFN-gamma-inducing factor/IL-18 administration mediates IFN-gamma- and IL-12-independent antitumor effects. J Immunol *160*, 1742-1749.

Pan, Z.-K., Ikonomidis, G., Lazenby, A., Pardoll, D., and Paterson, Y. (1995). A recombinant *Listeria monocytogenes* vaccine expressing a model tumor antigen protects mice against lethal tumor cell challenge and causes regression of established tumors. Nat Med *1*, 471-477.

Paulovich, A.G., Toczyski, D.P., and Hartwell, L.H. (1997). When checkpoints fail. Cell *88*, 315-321.

Pegram, M., Pauletti, G., and Slamon, D. (1998). HER-2/*neu* as a protective marker of reponse to breastcancer therapy. Breast Cancer Res Treat *52*, 65-77.

Plow, E.F., Herren, T., Redlitz, A., Miles, L., and Hoover-Plow, J. (1995). The cell biology of the plasminogen system. FASEB *9*, 939-945.

Porter, P., Malone, K., Heagerty, P., Alexander, G., Gatti, L., Firpo, E., Daling, J., and Roberts, J. (1997). Expression of cell-cycle regulators p27 and cyclin

E, alone and in combination, correlate with survival in young breast cancer patients. Nat Med *3*, 222-225.

Prives, C and Hall, P. A. (1999). The p53 pathway. J.Pathology 187, 112-126.

Puisieux, I., Odin, L., Poujol, D., Moingeon, P., Tartaglia, J., Cox, W., and Favrot, M. (1998). Canarypox virus-mediated interleukin-12 gene transfer into murine mammary adenocarcinoma induces tumor suppression and long-term immunity. Hum Gene Ther *9*, 2481-2492.

Putzer, B.M., Hitt, M., Muller, W.J., Emtage, P., Gauldie, J., and Graham, F.L. (1997). Interleukin 12 and B7-1 costimulatory molecule expressed by an adenovirus vector act synergistically to facilitate tumor regression. Proc Natl Acad Sci U S A *94*, 10889-10894.

Robertson, M., Cameron, C., Atkins, M., Gordon, M., Lotze, M.T., ShermanM.L, and Ritz, J. (1999). Immunological effects of interleukin-12 administration by bolus intravenous injection to patients with cancer. Clin Cancer Res *5*, 9-16.

Robinson, D., Shibuya, K., Mui, A., Zonin, F., Murphy, E., Sana, T., Hartley, S.B., Menon, S., Kastelein, R., Bazan, F., and O'Garra, A. (1997). IGIF does not drive Th1 development but synergizes with IL-12 for interferon-gamma production and activates IRAK and NFkappaB. Immunity *7*, 571-581.

Romer, J, Bugge, T. H., Pyke, C, Lund, L. R, Flick, M. J., Degen, J. L., and Dano, K. (1996). Imparied wound healing in mice with a disrupted plasminogen gene. Nat Med 2, 287-292.

Rosenberg, S.A. (1997). Cancer vaccines based on the identification of genes encoding regression antigens. Immunology Today *18*, 175-182.

Rosenberg, S.A., Aebersold, P., Cornetta, K., Kasid, A., Morgan, R., Meon, R., Karson, E., Lotze, M.T., Yang, J., Topalian, S., Merino, M., Culver, K., Miller, D., Blaise, R.M., and Anderson, W.F. (1990). Gene transfer into humans-immunotherapy of patients with advanced melanoma, using tumor infiltrating lymphoctyes modified by retroviral gene therapy. New England Journal of Medicine *323*, 570-602.

Ruetz, S. and Gros, P. (1994). Phosphatidylcholine translocase: a physiological role for the mdr2 gene. Cell *77*, 1071-1081.

Ruoslahti, E. and Reed, J. (1994). Anchorage dependence, integrins, and apoptosis. Cell *77*, 478

Sambrook, J., Fritsch, E.F., and Maniatis, T. (1989). Molecular cloning, a laboratory manual (Cold Spring Harbour, New York: Cold Spring Harbour Laboratory Press).

Schultz, J., Pavolivic, J., Strack, B., Nawrath, M., and Moen, R. (1999). Long lasting anti-metastatic efficiency of Interleukin 12 encoding plasmid DNA. Human Gene Therapy *10*, 407-417.

Seder, R.A. and Paul, W.E. (1994). Acquistion of lymphokine producing phenotype by CD4+ T cells. Annu Rev Immunol *12*, 635-673.

Seljelid, R. and Busund, L. (1994). The biology of macrophages: II Inflamation and tumors. Eur J Haematol *52*, 1-12.

Sethi, T., Rintoul, R., Moore, S., MacKinnon, A., Salter, D., Choo, C., Chilvers, E., Dransfield, I., Donnelly, S., Strieter, R., and Haslett, C. (1999). Extracellular matrix proteins protect small lung cancer cells against apoptosis: A mechanism for small cell lung cancer growth and drug resistance *in vivo*. Nat Med *5*, 662-668.

Sgadari, C., Faber, J., Angiolillo, A.L., Liao, F., Teruya-Feldstein, J., Burd, P., Yao, L., Gupta, G., Hanegane, C., and Tosato, G. (1997). Mig, the monokine induced by Interferon-γ, promotes tumor necrosis *in vivo* . Blood *89*, 2635-2643.

Sherr, C. J. (1996). Cancer Cell Cycles. Science 274(1672), 1677.

Shu, S., Plautz, G., Krauss, J., and Chang, A.E. (1997). Tumor Immunology.

JAMA *278*, 1972-1980.

Siegel, P.M., Dankort, D.L., Hardy, W.R., and Muller, W.J. (1994). Novel activating mutations in the *neu* proto-oncogene involved in induction of mammary tumors. Mol Cell Bio *14*, 7068-7077.

Sim, B.K., O'Reilly, M.S., Liang, H., Fortier, A.H., He, W., Madsen, J.W., Lapcevich, R., and Nacy, C.A. (1997). A recombinant human angiostatin protein inhibits experimental primary and metastatic cancer. Cancer Res *57*, 1329-1334.

Skobe, M, Rockwell, P, Goldstein, N, Vosseler, S, and Fusenig, N. (1997). Halting angiogenesis suppresses carcinoma cell invasion. Nat Med *3*, 1222-1227.

Stathakis, P., Fitzgerald, M., Matthias, L.J., Chesterman, C.N., and Hogg, P.J. (1997). Generation of Angiostatin by reduction and proteolysis of plasmin. J.Biol.Chem. *272*, 29641-20645.

Stathakis, P., Lay, A.J., Fitzgerald, M., Schlieker, C., Matthias, L.J., and Hogg, P.J. (1999). Angiostatin formation involves disulfide bond reduction and proteolysis in kringle 5 of plasmin. J Biol Chem *274*, 8910-8916.

Steele, R. J., Thompson, A. M, Hall, P. A, and Lane, D. P. (1998) The p53

tumor suppressor gene. Br J Surg 85, 1460-1467.

Stephens, R., Brunner, N., Janicke, F., and Schmitt, M. (1998). The urokinase plasminogen activator system as a target for prognostic studies in breast cancer. Breast Cancer Res Treat *52*, 99-111.

Storgard, C.M., Stupack, D.G., Jonczyk, A., Goodman, S.L., Fox, R.I., and Cheresh, D.A. (1999). Decreased angiogenesis and arthritic disease in rabbits treated with an αvβ3 antagonist. J.Clin.Invest. *103*, 47-54.

Storkus, W., Tahara, H., and Lotze, M.T. (1998). Interleukin-12. In The Cytokine Handbook. A.W. Thomson, ed. (New York: Academic Press), pp. 391-425.

Strand, S., Hofmann, W., Hug, H., Muller, M., Otto, G., Strand, D., Mariani, M., Stremmel, W., Krammer, P., and Galle, P. (1996). Lymphocyte apoptosis induced by CD95 (APO-1/Fas) ligand-expressing tumor cells--A mechanism of immune invasion? Nat Med 2, 1361-1366.

Suri, C., Jones P.F, Patan, S., Bartunkova, S., Maisonpierre, P.C., Davis, S., Sato, T., and Yancopoulos, G.D. (1996). Requisite role of angiopoietin-1,a ligand for the TIE2 receptor during embryonic angiogenesis. Cell *87*, 1171-1180.

Sussman, J.J., Shu, S., Sondak, V.K., and Chang, A.E. (1994). Activation of T lymphocytes for the adoptive immunotherapy of cancer. Ann Surg Oncol *1*, 296-306.

Tanaka, T., Cao, Y., Folkman, J., and Fine, H.A. (1998). Viral vector-targeted antiangiogenic gene therapy utilizing an angiostatin complementary DNA . Cancer Res *58*, 3362-3369.

Thierfelder, W.E. (1996). Requirement for Stat4 in interleukin-12 mediated responses of natural killer cells. Nature *382*, 171-174.

Timmerman, J.M. and Levy, R. (1999). Dendritic cell vaccines for cancer immunotherapy. Annu Rev Med. *50*, 507-529.

Tomura, M., Zhou, X.Y., Maruo, S., Ahn, H.J., Hamaoka, T., Okamura, H., Nakanishi, K., Tanimoto, T., Kurimoto, M., and Fujiwara, H. (1998). A critical role for IL-18 in the proliferation and activation of NK1.1+ CD3- cells. J Immunol *160*, 4738-4746.

Torry, R.J. and Rongish, B.J. (1992). Angiogenesis in the uterus: potential regulation and relation to tumor angiogenesis. Am J Reprod Immunol *27*, 171-179.

Trinchieri, G. and Scott, P. (1994). The role of interleukin 12 in the immune

response, disease and therapy. Immunology Today *15*, 460-463.

Ushio, S., Namba, M., Okura, T., Hattori, K., Nukada, Y., Akita, K., Tanabe, F., Konishi, K., Micallef, M., Fujii, M., Torigoe, K., Tanimoto, T., Fukuda, S., Ikeda, M., Okamura, H., and Kurimoto, M. (1996). Cloning of the cDNA for human IFN-gamma-inducing factor, expression in Escherichia coli, and studies on the biologic activities of the protein. J Immunol *156*, 4274-4279.

van Diest, P.J. (1999). Ductal carcinoma in situ in breast carcinogenesis. J Pathol *187*, 383-384.

Vassalli, J.-M. and Pepper, M.S. (1994). Membrane proteases in focus. Nature *370*, 14-15.

Vassalli, J.-M., Sappino, A.-P., and Belin, D. (1991). The plasminogen activator/plasmin system. J Clin Invest *88*, 1067-1072.

Vernon, R.B. and Sage, E.H. (1995). Extracellular matrix and creation of vascular form. Am.J.Pathol *147*, 873-883.

Vlodavsky, I., Friedman, Y., Elkin, M., Aingorn, H., Atzmon, R., Ishai-Michaeli, R., Bitan, M., Pappo, O., Peretz, T., Michal, I., Spector, L., and Pecker, I. (1999). Mammalian heparanase; Gene cloning,expression and function in

tumor progression and metastasis. Nat Med *5*, 793-802.

Voest, E.E., Kenyon, B.M., O'Reilly, M.S., Truitt, G., D'Amato, R.J., and Folkman, J. (1995). Inhibition of angiogenesis in vivo by interleukin 12. J Natl Cancer Inst *87*, 581-586.

Wan, Y., Bramson, J., Carter, R., Graham, F.L., and Gauldie, J. (1997). Dendritic cells transduced with an adenoviral vector encoding a model tumor-associated antigen for tumor vaccination. Human Gene Therapy *8*, 1355-1363.

Webster, M. and Muller, W.J. (1994). Mammary tumorigenesis and metastasis in transgenic mice. Cancer Biology *5*, 69-76.

Weidner, N. (1995a). Current pathologic methods for measuring intratumoral microvessel density within breast carcinoma and other solid tumors. Breast Cancer Res Treat *36*, 169-180.

Weidner, N. (1995b). Intratumor microvessel density as a prognostic factor in cancer. Am.J.Pathol *147*, 9-19.

Winslow-Saslow, D., Merino, M.J., Manrow, R.E., Lawrence, J.A., Bluth, R.F., Wittenbal, K., Simpson, J.F., Page, D.L., and Steeg, P.S. (1995). Overexpression of cyclin D mRNA distinguishes invasive and *in situ*

breast carcinomas from non-malignant lesions. Nat Med *1*, 1257-1260.

Wu, Z., O'Reilly, M.S., Folkman, J., and Shing, Y. (1997). Suppression of tumor growth with recombinant murine angiostatin. Biochem Biophys Res Commun *236*, 651-654.

Wyllie, A. H., Kerr, J. F., and Currie, A. R. (1980) Cell Death: The Significance of Apoptosis. International Review of Cytology 68, 251-305.

Xie, B., Dong, Z., and Fidler, I.J. (1994). Regulatry mechanisms for the expression of type IV collagenases/gelatinases in murine macrophages. J Immunol *152*, 3637-3643.

Yancopoulos, G. D, Klagsburn, M, and Folkman, J. (1998). Vasculogenesis, angiogenesis, and growth factors: Ephrins enter the fray at the border. Cell *93,* 661-664.

Yang, X. and Lippman, M. E. (1999). BRCA1 and BRCA2 in breast cancer. Breast Cancer Res Treat *54*, 1-10.

Yao, L., Sgadari, C., Furuke, K., Bloom, E.T., Teruya-Feldstein, J., and Tosato, G. (1999). Contribution of natural killer cells to inhibition of angiogenesis by interleukin-12. Blood *93*, 1612-1621.

Yurchenco, P.D. and Schittny, J.C. (1990). Molecular architecture of basement

membranes. FASEB *4*, 1577-1590.

Zhang, H, Tombline, G, and Weber, B. (1998) BRCA1, BRCA2 and DNA damage response: Collision or Collusion? Cell *92*, 433-436. 1998.

Zitvogel, L., Tahara, H., Cai, Q., Storkus, W., Muller, G., Wolf, S.F., Gately, M.K., Robbins, P.D., and Lotze, M.T. (1994). Construction and characterization of retroviral vectors expressing biologically active human interleukin-12. Hum Gene Ther *5*, 1493-1506.

Zitvogel, L., Tahara, H., Robbins, P.D., Storkus, W., Clarke, M., Nalesnik, M., and Lotze, M.T. (1995). Cancer immunotherapy of established tumors with IL-12: Effective delivery by engineered fibroblasts. J Immunol *155*, 1393-1403.

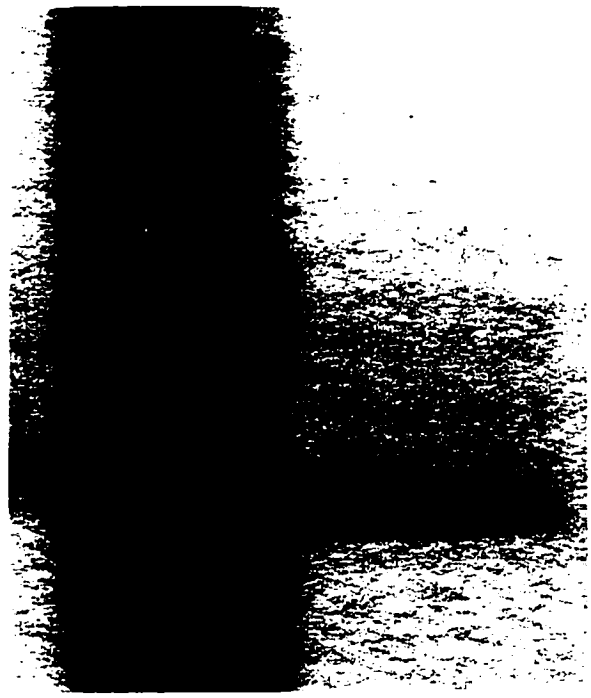

Appendix A. Purification of recombinant murine IL-18. Coomassie stained SDS -Page gel showing a single protein band (1 µg) expressed from *Escherichia coli*. IL-18 was purified from a Nickel chelate affinity column which bound hexa-histadine residues. Molecular weight marker in kDa (Gibco).